

PROBABILISTIC OPTIMAL OPERATION OF BIPOLAR DC MICROGRID  
CONSIDERING EV INTEGRATION



GUNTINAN SAKULPHAISAN

A Thesis Submitted in Partial Fulfillment of the Requirements for the  
Degree of Doctor of Philosophy in Electrical Engineering  
Suranaree University of Technology  
Academic Year 2022

การดำเนินการเหมาะสมที่สุดสำหรับไมโครกริดกระแสตรงแบบสองขั้ว  
โดยคำนึงถึงการบูรณาการรถยนต์ไฟฟ้าสู่กริด



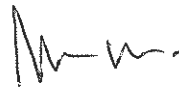
นายกันตินันท์ สกุลไพศาล

วิทยานิพนธ์นี้เป็นส่วนหนึ่งของการศึกษาตามหลักสูตรปริญญาปรัชญาดุษฎีบัณฑิต  
สาขาวิชาวิศวกรรมไฟฟ้า  
มหาวิทยาลัยเทคโนโลยีสุรนารี  
ปีการศึกษา 2565

PROBABILISTIC OPTIMAL OPERATION OF BIPOLAR DC MICROGRID  
CONSIDERING EV INTEGRATION

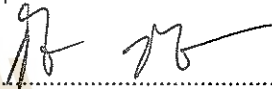
Suranaree University of Technology has approved this thesis submitted in partial fulfillment of the requirements for The Degree of Doctor of Philosophy.

Thesis Examining Committee



.....  
(Assoc. Prof. Dr. Naebboon Hoonchareon)

Chairperson



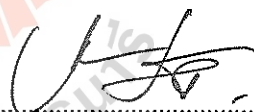
.....  
(Assoc. Prof. Dr. Keerati Chayakulkheeree)

Member (Thesis Advisor)



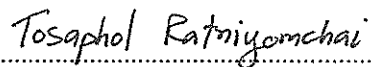
.....  
(Prof. Dr. Thanatchai Kulworawanichpong)

Member



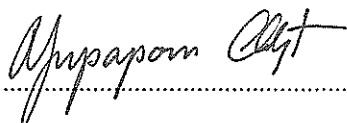
.....  
(Asst. Prof. Dr. Uthen Leeton)

Member



.....  
(Asst. Prof. Dr. Tosaphol Ratniyomchai)

Member



.....  
(Assoc. Prof. Dr. Yupaporn Ruksakulpiwat)

Vice Rector for Academic Affairs  
and Quality Assurance



.....  
(Assoc. Prof. Dr. Pornsiri Jongkol)

Dean of Institute of Engineering

กัณตินันท์ สกุลไพศาล: การดำเนินการที่เหมาะสมที่สุดสำหรับไมโครกริดกระแสตรงแบบสองขั้ว  
โดยคำนึงถึงการบูรณาการรถยนต์ไฟฟ้าสู่กริด (PROBABILISTIC OPTIMAL OPERATION  
OF BIPOLAR DC MICROGRID CONSIDERING EV INTEGRATION)  
อาจารย์ที่ปรึกษา : รองศาสตราจารย์ ดร.กิริติ ชยะกุลศิริ, 152 หน้า

คำสำคัญ: การจำลองการไหลของกำลังไฟฟ้าในระบบจำหน่ายกระแสตรง, การประเมินความต้องการ  
อัดประจุของรถยนต์ไฟฟ้า

วิทยานิพนธ์ฉบับนี้นำเสนอ กระบวนการสำหรับจำลองการทำงานของระบบจำหน่าย  
กระแสตรงแบบสองขั้วที่ประยุกต์พร้อมทั้งนำเสนอผลกระทบของปัญหาที่จะเกิดขึ้นในระบบจำหน่าย  
ในกรณีที่เกิดความไม่สมดุลในระบบและผลกระทบของการอัดประจุของรถยนต์ไฟฟ้า โดยผลกระทบ  
ของความไม่สมดุลของโหลดและระบบจำหน่ายจะถูกนำเสนอในรูปแบบของกำลังไฟฟ้าสูญเสียและ  
ดัชนีชี้วัดความไม่สมดุลของแรงดันไฟฟ้า (Voltage Unbalance Factor, VUF) ในการจำลองการ  
ทำงานของระบบจำหน่ายอาศัยวิธีการจำลองการไหลของกำลังไฟฟ้าร่วมกับการคำนวณแบบวนรอบ  
ของเกาส์ (Gauss's iteration method) เพื่อคำนวณหาแรงดันไฟฟ้าแต่ละบัสภายในระบบพร้อมทั้ง  
กำลังไฟฟ้าสูญเสียของกรณีฐาน ในส่วนการลดผลกระทบของความไม่สมดุลของโหลด วิทยานิพนธ์  
ฉบับนี้อาศัยวิธีการหาค่าที่เหมาะสมแบบฝูงอนุภาค (Particle Swarm Optimization ,PSO) ในการ  
คำนวณหารูปแบบการเชื่อมต่อของโหลดแต่ละบัสลดความไม่สมดุลที่ส่งผลกระทบต่อกำลังไฟฟ้า  
สูญเสียของระบบและความไม่สมดุลของแรงดันไฟฟ้าแต่ละบัส ในส่วนสุดท้ายเป็นการจำลอง  
ผลกระทบของรถยนต์ไฟฟ้าต่อระบบจำหน่ายกระแสตรงแบบสองขั้ว โดยที่โหลดที่เกิดขึ้นจากรถยนต์  
ไฟฟ้าถูกจำลองโดยใช้วิธีการมอนติคาโรล์ (Monte Carlo Simulation ,MCS) ร่วมกับวิธีการการ  
คำนวณแบบวนรอบของเกาส์ ซึ่งการจำลองโหลดรถยนต์ไฟฟ้าจะจำลองเป็นระยะเวลา 48 ชั่วโมง  
เพื่อให้เห็นถึงผลกระทบของการอัดประจุ

การนำเสนอผลลัพธ์การศึกษาของวิทยานิพนธ์ฉบับนี้ได้แบ่งหัวข้อนำเสนอผลลัพธ์  
ออกเป็น 7 ส่วน เริ่มต้นที่การจำลองเพื่อวัดความผิดพลาดของชุดโปรแกรมที่สร้างขึ้นกับ  
เอกสารอ้างอิง โดยการจำลองอาศัยระบบจำหน่ายกระแสตรงแบบ 4 บัส แบบสมดุล และ 21 บัส  
แบบไม่สมดุล โดยพบว่ามีความคลาดเคลื่อนอยู่ที่ 0.31 % และ <0.01% ตามลำดับ ต่อมาชุด  
โปรแกรมดังกล่าวจะถูกนำมาจำลองกรณีฐาน โดยใช้ระบบจำหน่ายกระแสตรงแบบ 21 บัสจำลอง  
ร่วมกับโหลดที่มีระยะเวลา 48 ชั่วโมง เป็นกรณีฐาน ซึ่งผลการจำลองแสดงให้เห็นถึงความไม่สมดุล

ของแรงดันไฟฟ้าที่สูงถึง 3.34 % ที่ตำแหน่งบัส 18 ณ เวลา 15.30 น. และพลังงานไฟฟ้าสูญเสียทั้งระบบสูงถึง 958.10 kWh เพื่อแก้ไขปัญหาความไม่สมดุลของแรงดันไฟฟ้า กระบวนการหาค่าที่เหมาะสมถึงถูกนำมาประยุกต์ใช้ โดยผลการจำลองพบว่าการหารูปแบบการเชื่อมต่อที่เหมาะสมสามารถกำลังไฟฟ้าสูญเสียได้ถึง 50.82 % พร้อมทั้งลดความไม่สมดุลของแรงดันเหลือ -0.006% ณ บัสที่ 18

เพื่อจำลองผลของการอัดประจุของรถยนต์ไฟฟ้า เส้นโค้งโหลดของการอัดประจุถูกสร้างขึ้นเป็นระยะเวลา 48 ชั่วโมงด้วยวิธีการจำลองแบบมอนติคาโร หลังจากนั้นเส้นโค้งดังกล่าวจะถูกนำไปจำลองร่วมกับระบบจำหน่ายไฟฟ้ากระแสตรงที่ถูกปรับรูปแบบการเชื่อมต่อด้วยวิธีการหาค่าที่เหมาะสมด้วยฝูงอนุภาค โดยผลการจำลองพบว่าผลกระทบของรถยนต์ไฟฟ้าสามารถทำให้พลังงานไฟฟ้าสูญเสียเพิ่มขึ้นสูงถึง 1.132 MWh และค่าของดัชนีชี้วัดความไม่สมดุลของแรงดันสูงถึง 1.326 % ที่บัส 17 เพื่อลดผลกระทบที่เกิดขึ้น ระบบดังกล่าวถูกนำไปแก้ไขปัญหาที่เหมาะสมด้วยกระบวนการหาค่าที่เหมาะสมที่สุดแบบฝูงอนุภาค โดยผลการจำลองพบว่าการปรับเปลี่ยนรูปแบบการเชื่อมต่อของโหลดอัดประจุของรถยนต์ไฟฟ้าสามารถลดกำลังสูญเสียสูงถึง 57.72 % และค่าดัชนีความไม่สมดุลของแรงดันไฟฟ้าของกรณีดังกล่าวมีค่า 1.766 % ณ บัสที่ 17

มหาวิทยาลัยเทคโนโลยีสุรนารี

สาขาวิชา วิศวกรรมไฟฟ้า  
ปีการศึกษา 2565

ลายมือชื่อนักศึกษา .....  
ลายมือชื่ออาจารย์ที่ปรึกษา .....

GUNTINAN SAKULPHAISAN: PROBABILISTIC OPTIMAL OPERATION OF BIPOLAR DC  
MICROGRID CONSIDERING EV INTEGRATION

THESIS ADVISOR: ASSOC. PROF. DR. KEERATI CHAYAKULKHEEREE, D.Eng., 152 PP.

Keyword: DC power flow simulation, EV charging demand evaluation

This thesis presents a DC bipolar distribution system with EV integration simulation to present an impact of load unbalance and EV charging load impact which the impact is proposed in form of energy loss and voltage unbalance factor. A simulation method of DC bipolar distribution system uses a Gauss's matrix method (GMM) to compute bus voltage profile and calculate total daily loss of the study system. In case of load unbalance problem reduction, this thesis uses a particle swarm optimization to search a suitable connection type of load at each bus. In case of EV load demand, the load demand is simulated by Monte Carlo Simulation (MCS) with 48 hours duration to present an impact of EV charging.

The simulation result of the thesis comprises of 7 sections that starts with validation simulation to compare a base case with reference paper. The validation result uses balanced 4-bus DC bipolar distribution grid and unbalanced 21-bus DC bipolar distribution grid with the errors of 0.31 % and < 0.01 %, respectively. then, the source code is used to simulate a base case with 21-bus DC bipolar distribution system to use as a base case of study for 48 hours. The result shows a 958.10 kWh of energy loss and 3.34 % of VUF at bus 18 on 15.30 p.m. To reduce an unbalance problem of base case, the PSO is used to solve the problem. The proposed method can reduce energy loss up to 50.82% with -0.006% of VUF at bus 18.

To simulate an EV charging demand, 48 hours charging load profile is built by MCS. After that, the profile is simulated with balanced 21 bus DC bipolar distribution system that can be increased energy loss up to 1.12 MWh and increased VUF up to 1.326 % at bus 17. To reduce an effect of EV charging load demand, the PSO is used to search a suitable of EV charging demand connection type in simulation system which

the simulation result shows a 57.72% of energy loss reduction and 1.766 % of VUF at bus 17.



School of Electrical Engineering  
Academic Year 2022

Student's Signature ..... *Cauntinan Sen* .....  
Advisor's Signature ..... *RB* .....  
.....

## ACKNOWLEDGEMENT

Writing a Ph.D. thesis has been a challenging and fulfilling journey, and it would not have been possible without the support and guidance of numerous people. I would like to express my heartfelt gratitude to all those who have contributed to my research and my personal growth.

Firstly, I would like to thank my supervisor, Assoc. Prof. Dr. Keerati Chayakulkheeree, for their continuous support, guidance, and encouragement throughout my research journey. Their vast knowledge, expertise, and constructive criticism have been instrumental in shaping my ideas and approach toward research. I am grateful for their patience, understanding, and belief in me.

I am also deeply indebted to Assoc. Prof. Dr. Naebboon Hoonchareon, Prof. Dr. Thanatchai Kulworawanichpong, Asst. Prof. Dr. Uthen Leeton and Asst. Prof. Dr. Tosaphol Ratniyomchai for their valuable insights, encouragement, and assistance throughout my research. Their enthusiasm and motivation have been a constant source of inspiration for me, and I am grateful for their guidance and support.

I would like to acknowledge the financial support provided by Suranaree University of Technology for my research. Without their support, this research would not have been possible.

Lastly, I would like to thank my family for their support and encouragement throughout my Ph.D. journey.

In conclusion, I am grateful to all those who have contributed to my research, my personal growth, and my overall success. Thank you all for your support and encouragement.

GUNTINAN SAKULPHAISAN



## TABLE OF CONTENTS

|  | Page      |
|--|-----------|
| ABSTRACT (THAI).....                         | I         |
| ABSTRACT (ENGLISH).....                      | III       |
| ACKNOWLEDGEMENT.....                         | V         |
| TABLE OF CONTENTS.....                       | VI        |
| LIST OF TABLES.....                          | IX        |
| LIST OF FIGURES.....                         | XI        |
| <b>CHAPTER</b>                               |           |
| <b>I INTRODUCTION.....</b>                   | <b>1</b>  |
| 1.1 Background.....                          | 1         |
| 1.2 Problem statement.....                   | 2         |
| 1.3 Research objective.....                  | 4         |
| 1.4 Limitation.....                          | 5         |
| 1.5 Structure of thesis.....                 | 5         |
| 1.6 Thesis overview.....                     | 7         |
| 1.7 References.....                          | 8         |
| <b>II LITERATURE REVIEWS.....</b>            | <b>10</b> |
| 2.1 Overview of DCDG and application.....    | 10        |
| 2.1.1 DCDG topology.....                     | 13        |
| 2.1.2 Voltage level standard of DCDG.....    | 19        |
| 2.1.3 Impact of load unbalance on DCDG.....  | 21        |
| 2.2 Electric vehicle technology.....         | 21        |
| 2.2.1 Fuel cell electric vehicle (FCEV)..... | 21        |
| 2.2.2 Hybrid electric vehicle (HEV).....     | 23        |

## TABLE OF CONTENTS (Continued)

|  | Page      |
|--|-----------|
| 2.2.3 Plug-in hybrid electric vehicle (PHEV) .....                                       | 27        |
| 2.2.4 Battery electric vehicle (BEV) .....   | 28        |
| 2.2.5 Comparative of different electric vehicle technology .....                         | 29        |
| 2.3 Battery charger and architecture .....   | 30        |
| 2.3.1 EV's charging method .....   | 30        |
| 2.3.2 EV's charging classification strategy .....  | 39        |
| 2.4 Impact of EV charging demand .....   | 50        |
| 2.4.1 The impact of EV charging station on distribution grid .....                       | 50        |
| 2.5 Literature review .....  | 54        |
| 2.6 Reference .....  | 58        |
| <b>III Methodology</b> .....   | <b>70</b> |
| 3.1 Introduction .....   | 70        |
| 3.2 Bipolar DC power flow calculation with Gauss's iteration method .....                | 72        |
| 3.3 Particle swarm optimization-based load balancing method .....                        | 78        |
| 3.4 Conclusion .....   | 86        |
| 3.5 Reference .....  | 86        |
| <b>IV Simulation result</b> .....  | <b>87</b> |
| 4.1 Introduction .....   | 87        |
| 4.2 Validation simulation .....  | 88        |
| 4.3 Case I: Base Case Simulation .....   | 93        |
| 4.4 Case II Load Balancing Case Simulation .....   | 97        |
| 4.5 Probabilistic EV load demand simulation .....  | 101       |
| 4.6 Case III: Load Balancing Case with Unbalancing Probabilistic EV Load<br>Demand ..... | 107       |

## TABLE OF CONTENTS (Continued)

|  | Page |
|--|------|
| 4.7 Case IV: Load Balancing Case with Balancing Probabilistic EV Load<br>Demand..... | 112  |
| 4.8 Conclusion .....   | 117  |
| <b>V Conclusion</b> .....  | 119  |
| 5.1 Future work .....  | 121  |
| <b>APPEXDIX</b>  |      |
| A Simulation data and result.....  | 124  |
| B PUBLICATIONS .....   | 129  |
| <b>BIOGRAPHY</b> .....   | 152  |

## LIST OF TABLES

| Table |   | Page |
|-------|---|------|
| 2.1   | Application of MVDC.....  | 12   |
| 2.2   | DC voltage standard and application.....  | 20   |
| 2.3   | Several aspects of FCEV .....   | 22   |
| 2.4   | HEV topology and application.....   | 25   |
| 2.5   | Feature of HEV.....   | 26   |
| 2.6   | Comprehensive summary of PHEV.....  | 28   |
| 2.7   | Comprehensive summary of BEV.....   | 29   |
| 2.8   | Comprehensive study of all EV technology .....                                      | 31   |
| 2.9   | Specification of charging level.....  | 35   |
| 2.10  | Advantage and disadvantage of each charging method.....                             | 38   |
| 2.11  | Comparison of centralize and decentralize charging control.....                     | 44   |
| 2.12  | Literature review of various objective function simulation.....                     | 46   |
| 4.1   | 4-bus bipolar DC distribution grid simulation result.....                           | 89   |
| 4.2   | Load data of 21-bus bipolar DC distribution grid .....                              | 91   |
| 4.3   | Bus data of 21-bus bipolar DC distribution grid.....                                | 102  |
| 4.4   | Amount of EV at each bus based on charging time interval .....                      | 104  |
| 4.5   | Quantity of EV based on daily travel mileage .....                                  | 105  |
| 4.6   | Amount of EV at each bus.....   | 107  |
| 4.7   | Simulation result comparison.....   | 112  |
| 4.8   | The Highest VUF and Total Daily Loss Comparison of Cases III and IV ....            | 117  |
| A.1   | 4-bus simulation result .....   | 124  |
| A.2   | Load data of 21-bus bipolar DC distribution grid for validation<br>simulation ..... | 125  |

## LIST OF TABLES (Continued)

| Table | Page  |
|-------|---|
| A.3   | Bus data of 21-bus bipolar DC distribution grid..... 126          |
| A.4   | Validation result of 21-bus bipolar DC distribution grid..... 126 |
| A.5   | Load connection type of base case system ..... 128                |



## LIST OF FIGURES

| Figure |  | Page |
|--------|--|------|
| 1.1    | Thesis overview .....                              | 7    |
| 2.1    | DCDG systematic based on AC main grid .....        | 14   |
| 2.2    | Network topology.....                              | 16   |
| 2.3    | Unipolar topology .....                            | 18   |
| 2.4    | Bipolar topology .....                             | 19   |
| 2.5    | FCEV configuration of powertrain .....             | 22   |
| 2.6    | HEV powertrain configuration .....                 | 25   |
| 2.7    | PHEV basic layout .....                            | 27   |
| 2.8    | BEV powertrain configuration.....                  | 29   |
| 2.9    | Charging topology .....                            | 31   |
| 2.10   | On-board EV charger component.....                 | 33   |
| 2.11   | Off-board EV charger component.....                | 33   |
| 2.12   | Charging port.....                                 | 36   |
| 2.13   | Charging connector .....                           | 36   |
| 2.14   | Simplified diagram of inductive charging.....      | 37   |
| 2.15   | EV charging method classification.....             | 40   |
| 2.16   | Centralize charging method configuration .....     | 42   |
| 2.17   | Decentralize charging method configuration.....    | 43   |
| 2.18   | Unidirectional and bidirectional energy flow ..... | 45   |
| 2.19   | Impact of EV fleet on distribution system .....    | 50   |
| 3.1    | Overall calculation program .....                  | 71   |
| 3.2    | Gauss's iteration procedure .....                  | 74   |
| 3.3    | Components of DC power system .....                | 74   |

## LIST OF FIGURES (Continued)

| Figure |  | Page |
|--------|--|------|
| 3.4    | Unipolar load connection .....                               | 75   |
| 3.5    | Bipolar load connection .....                                | 75   |
| 3.6    | Power flow calculation procedure .....                       | 78   |
| 3.7    | Neutral current characteristic .....                         | 79   |
| 3.8    | PSO based load balancing method.....                         | 82   |
| 3.9    | EV charging demand based on Monte Carlo.....                 | 83   |
| 4.1    | Simulation case .....  | 87   |
| 4.2    | 4-bus bipolar DC distribution grid .....                     | 89   |
| 4.3    | 4-bus bipolar DC distribution grid validation result .....   | 89   |
| 4.4    | 21-bus bipolar DC distribution grid.....                     | 90   |
| 4.5    | 21-bus bipolar DC distribution grid validation result .....  | 91   |
| 4.6    | 21-bus bipolar DC distribution grid simulation result.....   | 92   |
| 4.7    | 48-hrs. load profile.....                                    | 92   |
| 4.8    | Base case load connection type.....                          | 93   |
| 4.9    | Base case positive voltage profile .....                     | 94   |
| 4.10   | Base case negative voltage profile.....                      | 95   |
| 4.11   | 48 hours VUF of base case.....                               | 96   |
| 4.12   | PSO convergence characteristic .....                         | 98   |
| 4.13   | Load connection type comparisons of case I and case II ..... | 98   |
| 4.14   | Positive voltage profile of case II.....                     | 99   |
| 4.15   | Negative voltage profile of case II .....                    | 100  |
| 4.16   | Voltage unbalance factor of case II.....                     | 101  |
| 4.17   | Plug-in time of home charger.....                            | 103  |
| 4.18   | EV charging behavior of home charger .....                   | 103  |
| 4.19   | Probabilistic of EV daily distance travel .....              | 104  |

## LIST OF FIGURES (Continued)

| Figure |   | Page |
|--------|---|------|
| 4.20   | Sampling of EV based on daily travel distance probability ..... | 105  |
| 4.21   | EV 's SOC remaining and daily distance travel .....             | 106  |
| 4.22   | EV charging demand of home charging pattern .....               | 107  |
| 4.23   | Load connection type of case III .....                          | 108  |
| 4.24   | Positive voltage profile of case III .....                      | 109  |
| 4.25   | Negative profile of case III .....                              | 110  |
| 4.26   | Voltage unbalance factor of case III .....                      | 111  |
| 4.27   | Load connection type of case IV .....                           | 113  |
| 4.28   | Positive voltage profile of case IV .....                       | 114  |
| 4.29   | Negative voltage profile of case IV .....                       | 115  |
| 4.30   | Voltage unbalance factor of case IV .....                       | 116  |



# CHAPTER I

## INTRODUCTION

### 1.1 Background

In A.D. 1883, The DC distribution system was proposed by Edison for service lighting system (Edison, 1883). At the moment, DC distribution grid (DCDG) attention is piqued by the increasing penetration of distribution energy resources (DERs) and some kind of load have to use DC voltage such as Data center and communications systems, which require 48 Vdc, are instances of DCDG. (Prabhala, Baddipadiga, & Ferdowsi, 2014). As is well known, DCDG distribution systems have several benefits over AC systems. However, DCDG has several drawbacks, including challenges with varying high-range voltage levels and producing significant amounts of DC power. An increase in load demand in DCDG will result in voltage drop and significant power loss; thus, systems with higher voltage levels often have higher reliability and efficiency levels. A voltage level changing of AC distribution system uses transformer which a transformer has high voltage changing ratio. To adjust a voltage level in the AC distribution system, a transformer with a high voltage changing ratio is used. Because of this, advances in AC distribution system technology have gained more traction than advancements in the evolution of DC distribution technology. Home DC power systems have the following three main advantages over AC systems: three main features: 1. great power quality, 2. great efficiency, and 3. no synchronization required. The internal circuits of the majority of appliances in homes nowadays are powered by DC. As a result, an AC-DC converter is not needed for household appliances that are connected to DC power. When electric vehicles (EVs) are charged, the power converter stage's power loss may be minimized. Most power quality issues that are common in AC power systems may be more easily avoided in DC systems. Voltage sag and swell are seldom, and frequency fluctuation is not experienced by DC-powered home appliances.

Additionally unlike AC microgrids, which require a synchronization component for distributed generation, the DC power system allows cooperative control of PV, wind turbines, and ESS. (Nasirian, Moayedi, Davoudi, & Lewis, 2015).

Additionally, a distribution system is dealing with the rapidly increasing electric vehicles (EVs) penetration, which can significantly increase load demand and security and stability impact the system. (Anastasiadis, Kondylis, Polyzakis, & Vokas, 2019). As previously indicated, by transferring load demand from peak to off-peak hours, load management techniques like load leveling, load filling, or load shifting can lessen the impact of load charging demand. However, an electric vehicle's battery may function as a mobile energy storage device that charges power from the grid during off-peak hours and discharges it back to the grid during peak hours. (Putrus, Suwanapingkarl, Johnston, Bentley, & Narayana, 2009). In general, EV charging load is lowest in the morning and peaks in the evening. A charging load demand evaluation was proposed in (Tiantian, 2018) based on Monte Carlo to model a large scale of EV charging demand. The load demand evaluation may be used to control the charging power level of a smart charging station to manage load charging demand based on charger connecting and disconnecting times, or it can be used to restrict charging power at the charging station via the operator. (Camus, Silva, Farias, & Esteves, 2009) (Schey, Smart, & Scoffield, 2012) (Morrissey, Weldon, & O'Mahony, 2016).

## 1.2 Problem statement

The DC grid is one of alternative in future power system because source, load and energy storage can be easy to integrate in the system through power electronic interface. DC grid has a better efficiency of interface with several renewable source such as photovoltaic based energy source and suitable with domestic and commercial appliances. There are two aspects of DC grid including urban point as well as rural point. in the urban point of view, a various appliance in commercial and residential such as laptop, computer, smart phone charger and so on require DC power which obtain from AC to DC converter or storage device. Hence, this circumstance can be

overcome by a DC grid system which can ensure stable and efficient supply of DC power directly serving for the appliances. In the rural point of view, many homes in rural areas of various developing countries are far from the main utility grid which grid extension is a serious concern. A grid transmission and distribution system building may have high cost and may not guarantee power supply reliable due to load shedding and poor power quality. So, A renewable energy resource-based generation such as photovoltaic become a popular as a solution for energy generation in rural area.

Beside the increment of distributed energy resource (DERs), the number of EV significantly increase which can be made environmental benefit and economic benefit. The IEA predict a number of EV will reach 250 million in 2030. The main barrier of EV penetration is charging rate limitation which limitation causes long charging period from traditional charger such as level 1 and level 2 charger that have charging time around four to six hours. Normally, level 1 and level 2 charger are only used for overnight or charging at work. A level 3 DC fast charging have the charging capability less than 30 minutes. However, the high charging power of level 3 charger brings additional burden of power grid which a large portion of energy requirement of charging station and a non-characteristic of charging station can be caused voltage fluctuation and power loss.

To decrease impact of EV charging demand in form of high transmission energy loss and voltage fluctuation due to huge charging current flow which the reasons of impact are depended on connection type of load at each bus in DCDG, behavior of EV owner that effects to EV charging demand and building load profile.

The author studies a DC distribution grid, impact of EV integration on distribution system and load balancing method to solve the problem of distribution grid and EV integration. To support various load voltage, the study led to bipolar DC distribution grid. The main problem of the distribution grid is unbalancing problem which increases a neutral current flow and lead to neutral power loss. The reason of the problem is unipolar load demand which can connect on positive pole or negative pole of the system. A different load demand at each pole can be unequal and led to unbalance problem. In case of impact of EV integration, an EV load demand integration is simulated in form of charging load demand which can impact on distribution grid

like unipolar load. A charging load demand have to evaluate based on EV owner behavior. Which charging load demand can improve unbalance problem on DC bipolar distribution grid. So, an unbalance problem of distribution grid and EV charging load demand can be solved by using load balancing method to search a optimal connection of load at each bus to reduce a total energy loss and VUF.

So, the thesis presents a solution to impact of EV penetration in DC grid which research can be separated into 4 phrases as follow: phase 1 are validation simulation and base case simulation which simulate an IEEE system as a DC bipolar system to study an unbalance problem of bipolar system to reduce power loss and manage load connection type to have lowest power loss during 48-hours. The other part of phase 1 is to balance load of base case to find an optimal connection type by using Particle Swarm Optimization (PSO). Phase 2 is a probability simulation of EV daily distance pattern by using Monte Carlo Simulation (MCS) to evaluate charging load demand, charging duration, plug-in duration and total duration of charging operation of EV fleet. Phase 3 is EV load demand integration on DCDG. The phase uses balanced DCDG integrating with EV charging demand based on MCS to study an impact of EV charging demand on DCDG in case of non-control a charging load at each bus. Lastly, Phase 4 is to find an optimal connection type of EV load demand at each bus to reduce energy loss and voltage fluctuation by using PSO.

### 1.3 Research objective

The objectives of load balancing method of DC bipolar distribution system are to reduce effect of unbalance problem of DCDG due to non-equal load capacity of positive pole and negative pole at each node. The unbalance problem of DCDG can be measured by using Voltage Unbalance Factor (VUF) which the reasons of unbalance load of DCDG are unplanned load, renewable energy resource integration and EV charging demand.

The primary goal of this study comprises of the following objectives:

1.3.1 To study unbalance problem of DCDG and reduce unbalance problem by using load balancing method based on Particle Swarm Optimization (PSO).

1.3.2 To evaluate probabilistic of EV charging demand by using Monte Carlo Simulation (MCS).

1.3.3 To reduce impact of EV charging demand on DCDG by using load balancing method based on PSO.

## 1.4 Limitation

1.4.1 A 48-hours of power flow simulation period is separated into 196 timeslots with 15 minutes per timeslot.

1.4.2 Static switch power consumption is neglected.

## 1.5 Structure of thesis

The present thesis is composed of six chapters, and the subsequent section provides concise overviews of each chapter.

**Chapter I** serves as the introductory section of this thesis, wherein the background information, problem statement, objectives, and overall structure of the thesis are outlined.

**Chapter II** provides an overview of DCDG that discusses a detail of DCDG topology. This includes an overview of impact of load unbalance on DCDG and load balancing method to solve the problem. The EV charging demand was discussed to evaluate load demand on DCDG based on probability distribution function (PDF) of plug-in time and unplug time by using Monte Carlo simulation. Lastly, this section discusses a V2G application on DCDG to solve the unbalance problem.

**Chapter III** presents a methodology of this research which comprises of bipolar DC power flow with Gauss's iteration method, load balancing method based on particle swarm optimization and Probability of EV charging demand based on Monte Carlo simulation.

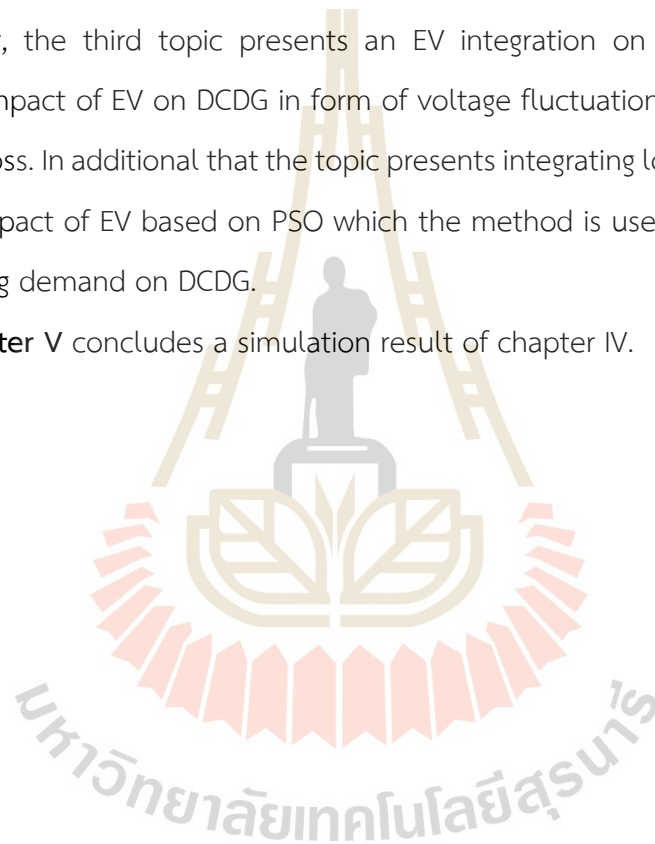
**Chapter IV** presents a simulation result that can be separated into 3 main topics. The first topic is a preliminary study of a DC bipolar distribution system. It includes Particle swarm optimization (PSO) is used to solve with a load balancing

technique for reduce power loss from neutral current and voltage unbalance factor (VUF) from unbalanced loads at each bus., as well as a power flow model of bipolar DC distribution grid. The goal function is load transferring at each bus to balance a load at each pole by taking into account different conditions, which results in a reduction in neutral current.

The second topic presents an EV charging demand evaluation based on MCS which discusses a several behavior factor of EV owner on EV load demand.

Lastly, the third topic presents an EV integration on balanced DCDG that present an impact of EV on DCDG in form of voltage fluctuation, neutral current flow and energy loss. In additional that the topic presents integrating load balancing method to reduce impact of EV based on PSO which the method is used to search a optimal of EV charging demand on DCDG.

**Chapter V** concludes a simulation result of chapter IV.



## 1.6 Thesis overview

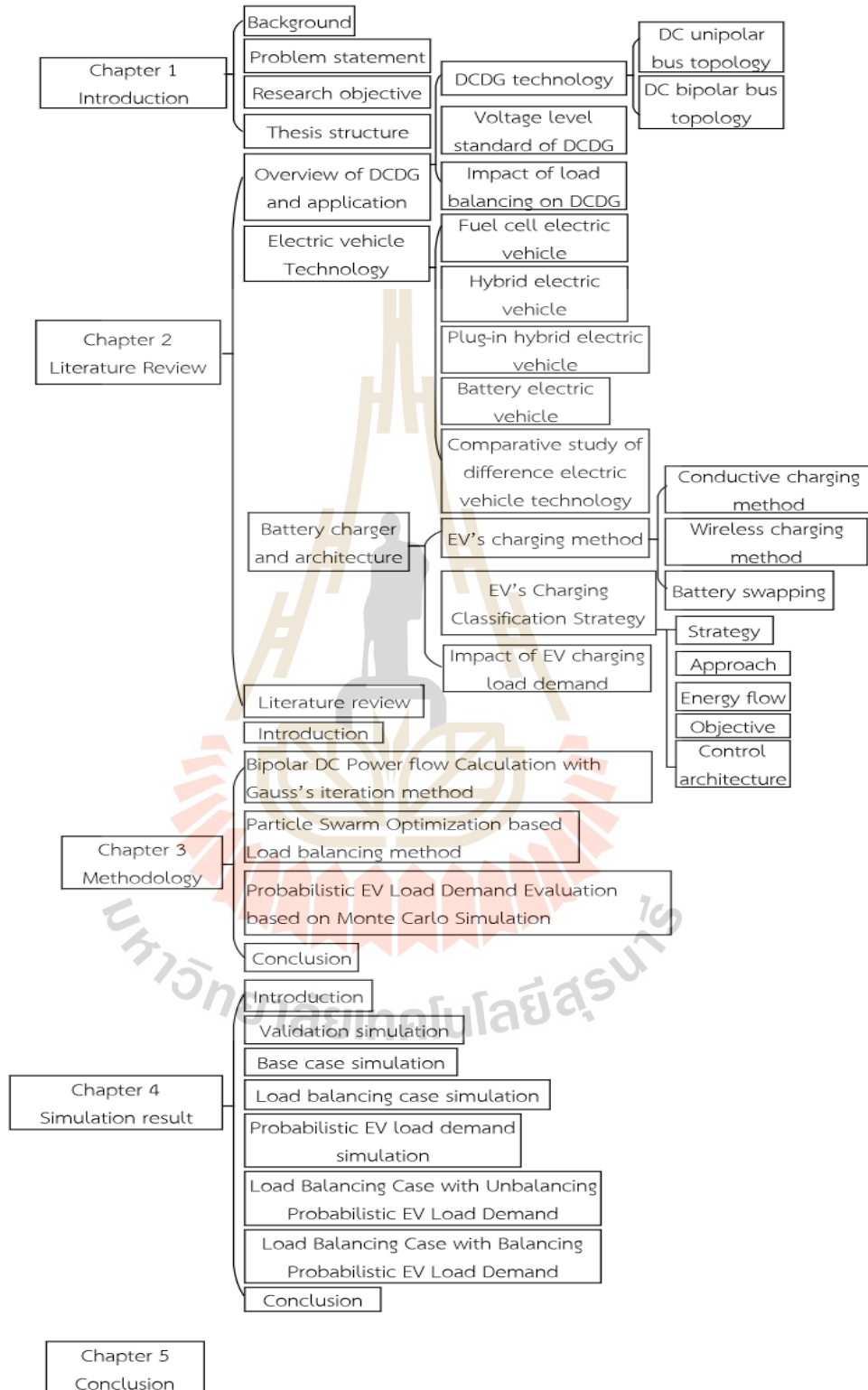


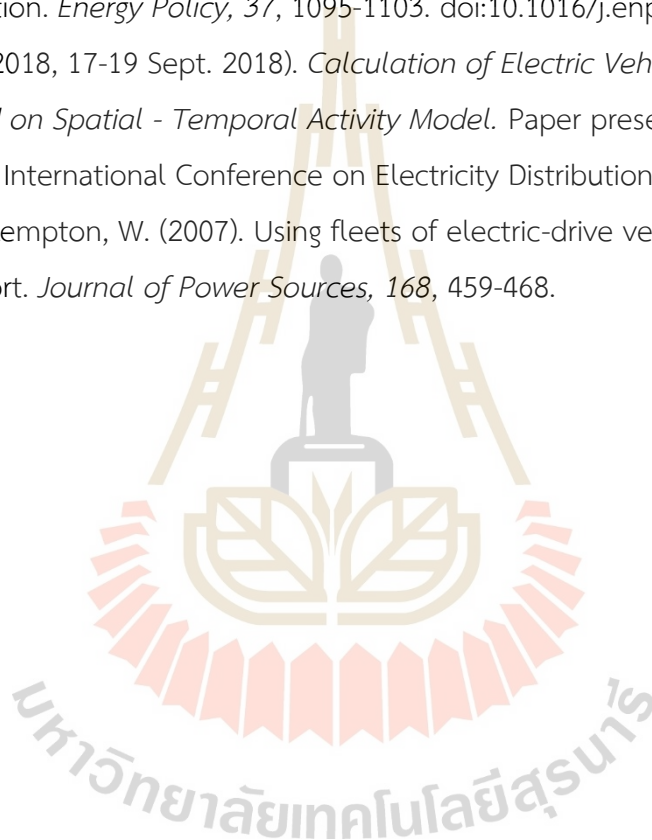
Figure 1.1 Thesis overview

## 1.7 References

- Anastasiadis, A. G., Kondylis, G. P., Polyzakis, A., & Vokas, G. (2019). Effects of Increased Electric Vehicles into a Distribution Network. *Energy Procedia*, 157, 586-593. doi:<https://doi.org/10.1016/j.egypro.2018.11.223>
- Antonanzas, J., Osorio, N., Escobar, R., Urraca, R., Martinez-de-Pison, F. J., & Antonanzas-Torres, F. (2016). Review of photovoltaic power forecasting. *Solar Energy*, 136, 78-111. doi:<https://doi.org/10.1016/j.solener.2016.06.069>
- Camus, C., Silva, C. M., Farias, T. L., & Esteves, J. (2009, 18-20 March 2009). *Impact of Plug-in Hybrid Electric Vehicles in the Portuguese electric utility system*. Paper presented at the 2009 International Conference on Power Engineering, Energy and Electrical Drives.
- Edison, T. A. (1883). United State of America Patent No.
- Kim, T., Ko, W., & Kim, J. (2019). Analysis and Impact Evaluation of Missing Data Imputation in Day-ahead PV Generation Forecasting. *Applied Sciences*, 9(1). doi:10.3390/app9010204
- Liu, J., Fang, W., Zhang, X., & Yang, C. (2015). An Improved Photovoltaic Power Forecasting Model With the Assistance of Aerosol Index Data. *IEEE Transactions on Sustainable Energy*, 6(2), 434-442. doi:10.1109/TSTE.2014.2381224
- Mayer, M. J., & Gróf, G. (2021). Extensive comparison of physical models for photovoltaic power forecasting. *Applied Energy*, 283, 116239. doi:<https://doi.org/10.1016/j.apenergy.2020.116239>
- Morrissey, P., Weldon, P., & O'Mahony, M. (2016). Future standard and fast charging infrastructure planning: An analysis of electric vehicle charging behaviour. *Energy Policy*, 89, 257-270. doi:<https://doi.org/10.1016/j.enpol.2015.12.001>
- Nasirian, V., Moayedi, S., Davoudi, A., & Lewis, F. L. (2015). Distributed Cooperative Control of DC Microgrids. *IEEE Transactions on Power Electronics*, 30(4), 2288-2303. doi:10.1109/TPEL.2014.2324579
- Prabhala, V. A., Baddipadiga, B. P., & Ferdowsi, M. (2014). *DC Distribution Systems – An Overview*.



- Putrus, G., Suwanapingkarl, P., Johnston, D., Bentley, E. C., & Narayana, M. (2009). *Impact of electric vehicles on power distribution networks*.
- Schey, S., Smart, J., & Scoffield, D. (2012). A First Look at the Impact of Electric Vehicle Charging on the Electric Grid in The EV Project. *World Electric Vehicle Journal*, 5. doi:10.3390/wevj5030667
- Sovacool, B., & Hirsh, R. (2009). Beyond batteries: An examination of the benefits and barriers to plug-in hybrid electric vehicles (PHEVs) and a vehicle-to-grid (V2G) transition. *Energy Policy*, 37, 1095-1103. doi:10.1016/j.enpol.2008.10.005
- Tiantian, Q. (2018, 17-19 Sept. 2018). *Calculation of Electric Vehicle Charging Power Based on Spatial - Temporal Activity Model*. Paper presented at the 2018 China International Conference on Electricity Distribution (CICED).
- Tomic, J., & Kempton, W. (2007). Using fleets of electric-drive vehicles for grid support. *Journal of Power Sources*, 168, 459-468.



## CHAPTER II

### LITERATURE REVIEWS

In order to identify and determine the appropriate methodology, a thorough review of related research and methods is necessary. Chapter 2 addresses this need by providing an overview of recent research in several key areas, including the background of DCDG, impact of load unbalance in DCDG, Impact of EV charging demand and EV integration on DCDG.

#### 2.1 Overview of DCDG and application

Since the "Current War" between Nikola Tesla and Thomas Edison, AC has been the foundation of electrical systems worldwide for the past century. (D. Kumar, Zare, & Ghosh, 2017). AC technology is utilized because AC voltage level can be changed by using transformer which at high AC voltage level can reduce power losses. Protection and semiconductor device developments that brought in the DC voltage era, including MVDC distribution systems and HVDC transmission. Due to increasing of populations is affect to distribution grid strain and extra capacity is required to serve all load in distribution grid. The power reliability and quality in urban areas is important.

High-Voltage DC is suitable for transmission (Ryndzionek & Sienkiewicz, 2020) meanwhile MVDC is suggested for distribution in power system for rail system of urban or suburban traction system (Morris, Federica, & Dario, 2018) which MVDC is suggested for application for many reasons such as a limitation of transfer capacity increasing with the AC infrastructure. When compares a same size of DC conductor and AC conductor, a transfer capacity of DC is higher than AC at 1.5 to 1.8 times (L. Zhang et al., 2016). It improves power transmission efficiency due to DC uses a peak-voltage capability and doesn't suffer from skin effect (Bathurst, Hwang, & Tejwani, 2015). So, MVDC can increase voltage and capacity in utilization areas by replace MVAC to MVDC.

A other main advantage of DC system is not need reactive power compensation which in AC system needed (Zhou & Yuan, 2009). A distribution renewable energy source connection to AC grid has to use conversion equipment and the unreliable problem of DGs that require BESS to storage excess power. In case of DC system, MVDC doesn't required a conversion stage for support distribution renewable energy source and BESS. A goal of DG connection is voltage disturbance controlling and MVDC system with power converter can provide DG voltage control (Hrishikesan et al., 2021).

MVDC is suitable for highly populated small metropolitan region such as where a high voltage transmission network could not be easily installed or the area without transmission network. After this, high voltage transmission system has a visual impact from power tower and power line which have an electromagnetic field impact along the cable pass way. Additionally, at low voltage level, MVDC capability can reduce a cost and sizing of converter (Stieneker & Doncker, 2016).

However, MVDC have many challenges to reach the objective such as lack of protection system and circuit breaker development, lack of standardization and high DC installation cost due to power converter at high voltage level and a life span and efficient of power converter is lower when compared with AC transformer (Giannakis & Peftitsis, 2018). A main applications of DC system are railway, MVDC distribution system, offshore energy collection system and shipboard systems which are overviewed and summarized in TABLE 2.1. For railway systems, a low DC voltage technology is used for metro, tram and subway systems that at long distance service route is recommended to use medium voltage around 750 to 10 kV and 20-30 kV for high-speed railway system. On shipboard, MVDC power system is alternative to AC system due to reduce a weight of ship due to heavy transformer. In the other hand, the benefit of MVDC is not require a large onboard substation which the substation is replaced by MVDC power electronic with 5 to 35 kV of DC buses (Soman, Steurer, Toshon, Faruque, & Cuzner, 2017). The technology of DC distribution grid presents in form of MVDC system which have a reliability and flexibility with unipolar and bipolar bus topology. A distribution grid voltage range suggestion operation varies several

levels such as 1.5 kV to 100 kV, 5 kV to 50kV (Simiyu, Xin, Wang, Adwek, & Salman, 2020) or 10-27 kV. From a voltage range can be concluded that a voltage level depends on range for distribution but some voltage range such as 50 kV or 100 kV is used for connecting to distribution renewable resource at far from main grid. Offshore collection is a renewable energy resource that installed on the ocean such as offshore wind collection. At present, MVDC is no active on offshore systems but a MVDC offshore advantage is lower weight of substation when compared with AC collection which can be reduce an investment cost of the system (Abeynayake, Li, Joseph, Liang, & Ming, 2021).

Table 2.1 Application of MVDC

|               | Application  |  |                           |   |
|---------------|--|--|---------------------------|---|
|               | Railways   | MVDC Distribution                                | Offshore Collection       | Shipboard   |
| Voltage level | - 600V-3kV for trams and suburb trains<br>- 9 kV to 10.5 kV for long distance<br>- 20 kV to 30 kV for High-speed train | - 5 kV to 100 kV<br>- $\pm 10$ kV to $\pm 70$ kV | - $\pm 25$ to $\pm 50$ kV | 1 kV to 35 kV   |
| Power         | - 3 MW to 5 MW for suburban<br>- 12 MW for higher speed  | 3 MW to 200 MW                                   | 160 MW to 1200 MW         | - 2 MW to 7 MW for smaller ship<br>- 10 MW to 20 MW for cruise ship |

Table 2.1 Application of MVDC (Continued)

|       | Application  |   |                     |                                  |
|-------|--|---|---------------------|----------------------------------|
|       | Railways   | MVDC Distribution   | Offshore Collection | Shipboard                        |
| Cases | -London underground<br>-Paris-Strasbourg high speed line | -Zhuhai distribution project<br>- Shenzhen MVDC demonstration project | None Implemented    | Forsea Ferries<br>Yara Birkeland |

Due to lack of standardize, a MVDC voltage ranges are required for several application have not been standardized. A rail system is a trend that uses various voltage range beginning at 600 to 1500 in 2010s and from 2010 to present the voltage can be reached to 24kV. In case of distribution system, a demonstrate project voltage range can be reach 27 kV. A MVDC is most implemented for shipboard system that the voltage was also 10kV. Finally, the suggested voltage of wind offshore collection is in the higher than other application that can be up to 20-35 kV.

### 2.1.1 DCDG topology

There is a lack point of standardization on the technology. Therefore, A several difference configuration and voltage level can be implemented. The DCDG is widely used in data center, residential application and telecommunication system.

A DCDG component comprises of 1.) DC bus 2.) AC/DC converter 3.) energy storage and 4.) distributed generation. Typically, an AC/DC converter is used to link a DC bus to the main grid, converting AC voltage to DC voltage and powering the system's whole load. The simple DCDG is illustrated in FIGURE 2.1

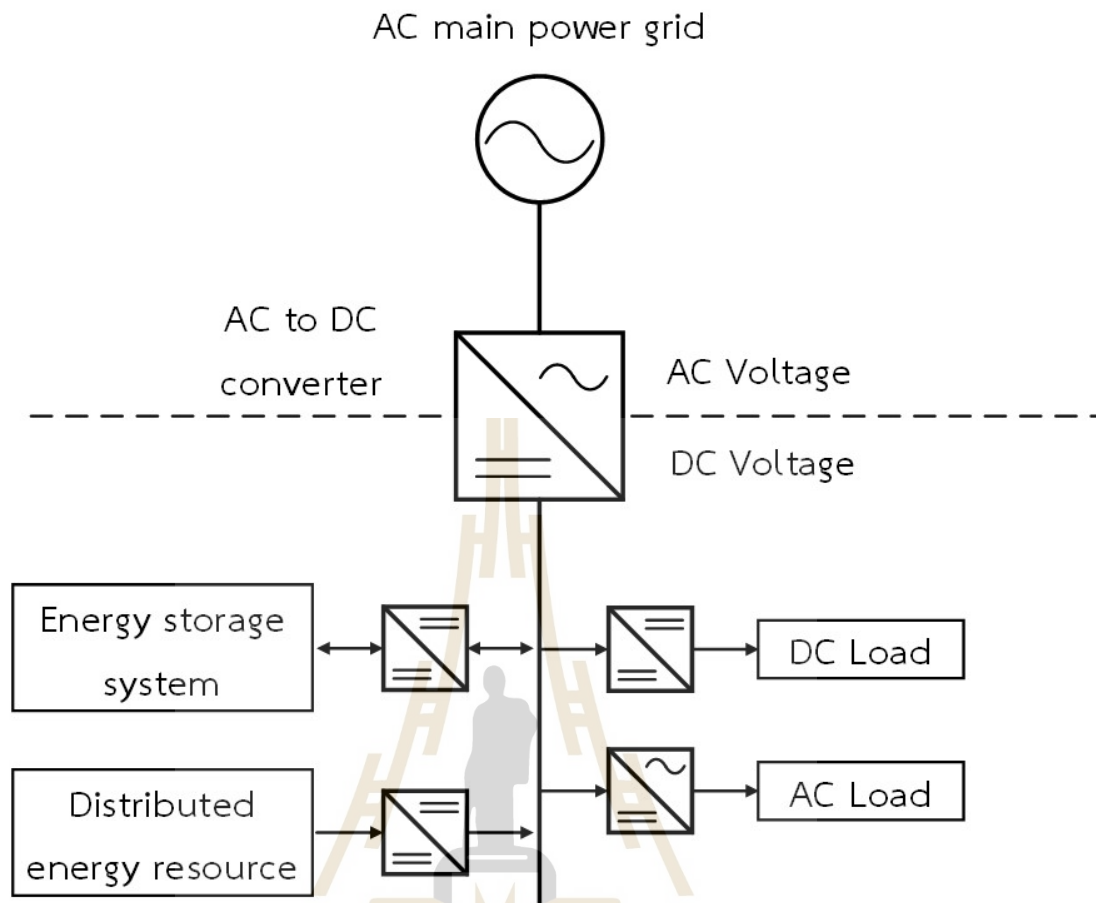


Figure 2.1 DCDG systematic based on AC main grid

In figure 1, AC to DC converter acts as an interface of DCDG which the converter function is used to convert AC voltage to DC voltage. In a DC side of converter is connected to transmission line which there are many loads type as follow: AC load type and DC load type. In case of DC load type, a voltage level of application is lower than transmission voltage level in distribution system. So, the DC-to-DC converter is used to reduce voltage level from transmission level to household level. In case of AC load type, the DC to AC converter is used to convert from DC voltage to AC voltage.

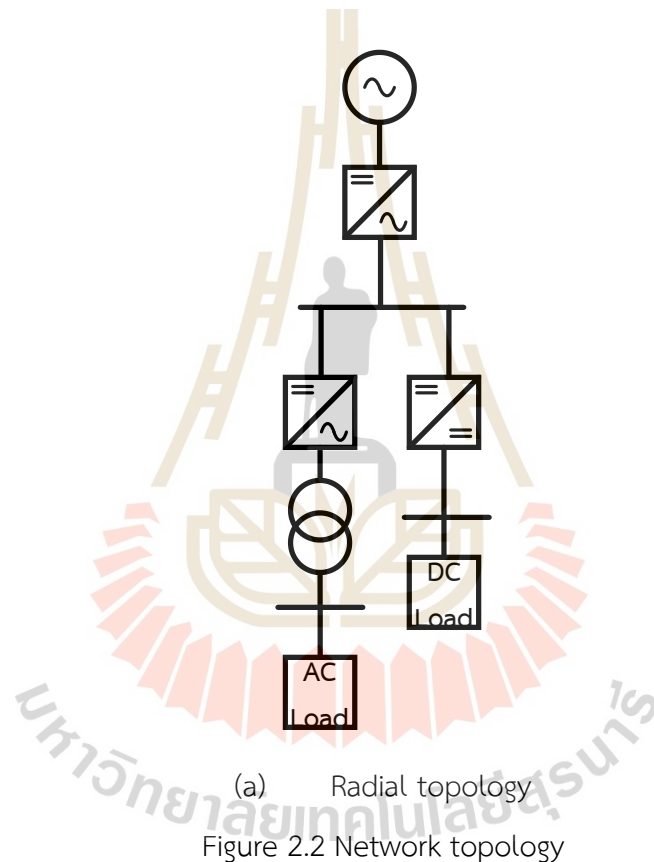
The DCDG supports an energy storage system (ESS) and distributed energy resource (DER) which ESS is based on DC voltage same as voltage system. So, the DC-to-DC converter function is to increase from storage level to transmission level. In case of DER, the converter can be separated into 2 type that depends on voltage

type of DER. An AC to DC converter is used to convert AC voltage of DER to DC voltage of transmission system. In the other hand, DER based-on DC voltage uses a DC-to-DC converter to change voltage level from DER voltage level to transmission level. a loss characteristic comparison of ACDG and DCDG is an effective way to lower power loss by minimizing power conversion because DCDG need at least one converter to connect to DC bus. The system efficiency, cost, and system size are all great for DCDG. Additionally, DCDG has high stability owing to the absence of reactive power and is more suitable with the integration of DERs (Yoldaş, Önen, Muyeen, Vasilakos, & Alan, 2017). A DCDG can transmit power with two configuration that consists of unipolar and bipolar system. The difference of those configuration offer difference system ability such as available voltage level, reliability and power quality.

MVDC distribution system have several topologies such as radial, meshed, multi-terminal hand in hand, ring or combination as shown in Figure 2.2 (M. Yang, Xie, Zhu, & Lou, 2015) which the selected topology is depended on design requirements. When a conductor is placed farther down the feeder and has a lower diameter, radial topologies are more cost-effective (Jovcic, Taherbaneh, Taisne, & Nguefeu, 2015). However, the topologies are not reliable because a fault at beginning feeder can be cause of supply failure and lead to power outage. The topology is a unidirectional power flow which have a flexibility limit on distributed generation integration (Prakash, Lallu, Islam, & Mamun, 2016).

Ring structures provide a reliability system which load can be fed by two feeders. The structures comprise of two substructure that are open-ring loop structure and closed-loop structure. The open-ring loop structure in normal operation has a normally open point between two feeder that can be separated the ring structure to two radial feeders. In case of failure operation, the switch is closed and a failure section can be energized from other source in other side of system. The structure provides a reliability and flexibility because of multiple paths of power flow. In additional to that, a normally open point can balance load between feeding which improves a power supply reliability.

Multi-terminal MVDC network is connected with multiple MVAC grid that provides many benefits such as power quality, flexibility and voltage support (Musa, Rehan, Sabug, Ponci, & Monti, 2017). Compared to ring networks, multi-terminal systems are easier to extend and have the capacity to connect several networks at once. Because the network with VSC-based systems are inherently unstable, further research and development is necessary to provide the safety and management of multiterminal MVDC networks (Pinto, Rodrigues, Bauer, & Pierik, 2013).





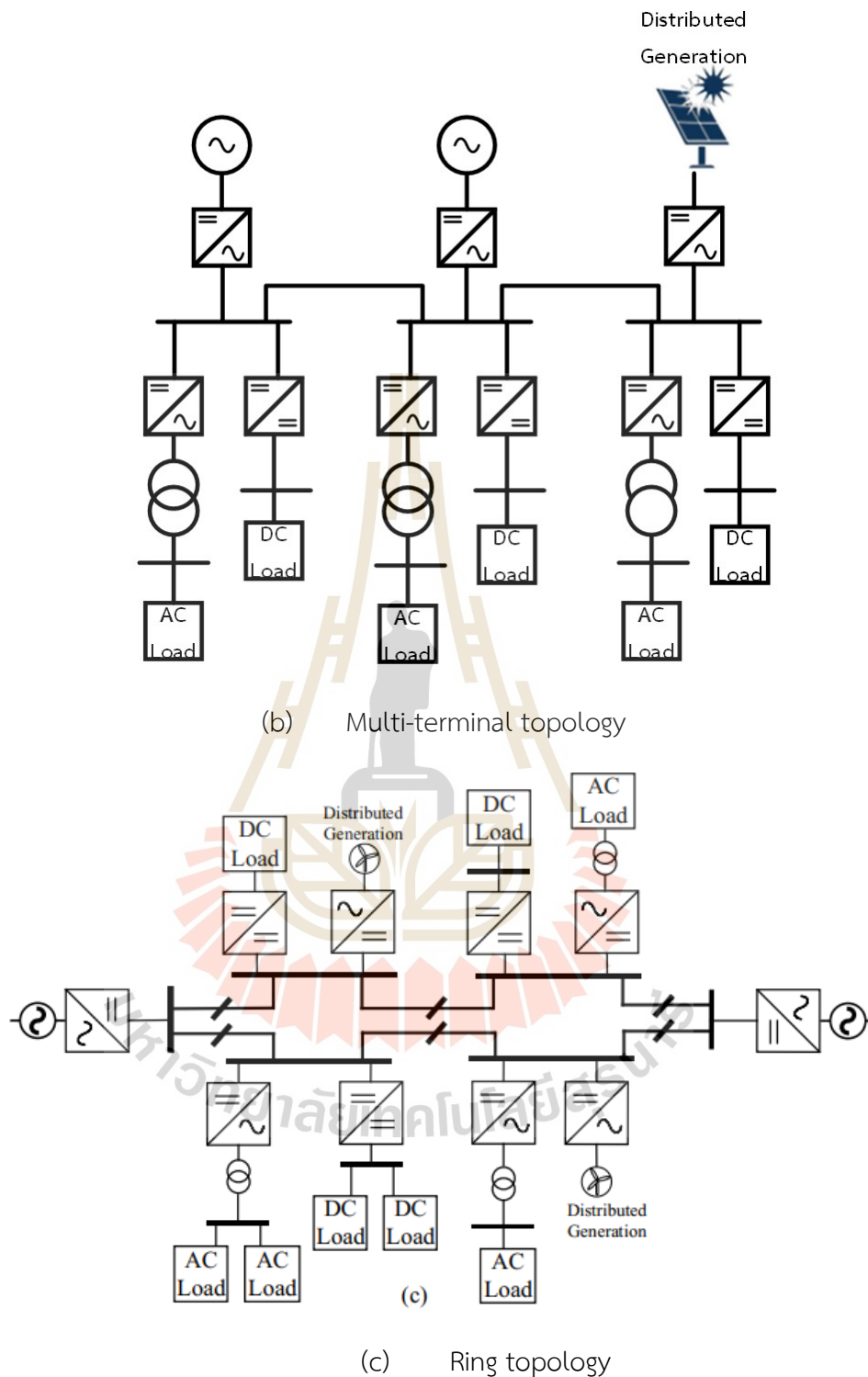


Figure 2.2 Network topology (cont.)

Which each topology can be separated into two main bus structure there are unipolar bus topology and bipolar bus topology.

### DC UNIPOLAR BUS TOPOLOGY

A DC unipolar bus topology likes a single-phase AC power system that have only two wires for distribute power to load. In case of DC unipolar bus, the wires are called positive wire and neutral wire which a one conductor is used for feed current to load and other conductor act as a current return path of load. a source and loads are connected between the wires as shown in FIGURE 2.3 The energy is transferred through the DC bus at a single voltage level, so the DC bus voltage level choosing is important in this system. the system capability depends on voltage level which the high voltage level can increase power transmission system capability but the system demands DC-DC converter to match user voltage level and increase safety risks. In the other hand, low voltage level has a transmission distance limitation. So, the suitable voltage level selection can avoid a large number of DC – DC converter deployment. The topology is practical for off-grid homes in isolated rural locations without utility grid infrastructure. The topology is a simple to implement and have symmetry between the pole. In the other hand, a single fault can be led to shut down the system and doesn't offer different voltage level option to user (Jhunhunwala, Lolla, & Kaur, 2016) (Karppanen et al., 2015).

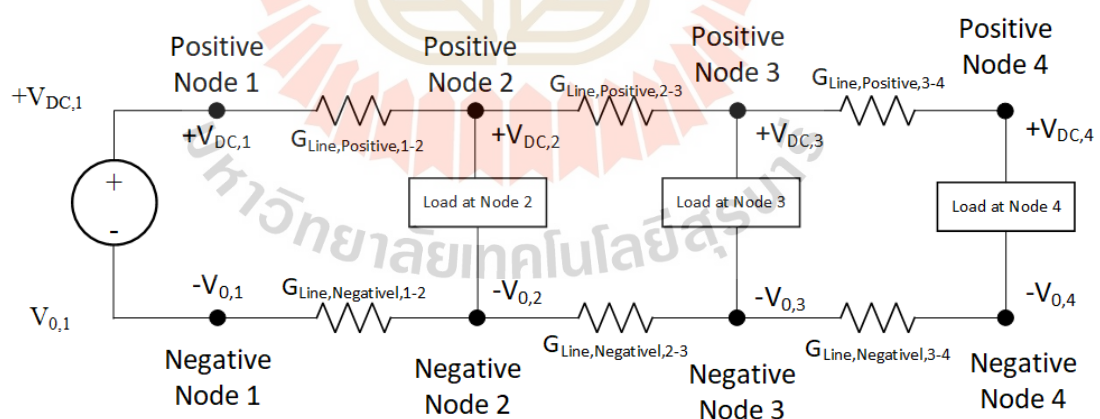


Figure 2.3 DC unipolar bus topology

## DC BIPOLAR BUS TOPOLOGY

A DC bipolar bus topology is a combination of two unipolar distribution systems which have a superior advantage over DC unipolar bus topology. The topology structure likes a three-phase AC power system with three wires for distribute an energy to load which the wires are called positive line, negative line and neutral line respectively as shown in FIGURE 2.4. The topology offers three voltage levels option which consists of +VDC, -VDC and 2VDC. Under a fault condition, when the system have a fault at one bus of DC pole. The load at fault bus can be transfer to other pole at same bus by using converter to switch load to another DC pole. Therefore, the reliability power quality and availability of the system during fault condition is higher than unipolar DC bus topology. A difference voltage level option offers a flexibility to consumer but the ability can be led the system to unbalance condition. The unbalance condition can increase neutral current flow that is a cause of neutral power loss and increase overall system power loss. So, the system demands a voltage balancer or load balance strategy to prevent unbalance condition (Kakigano, Miura, Ise, & Uchida, 2007).

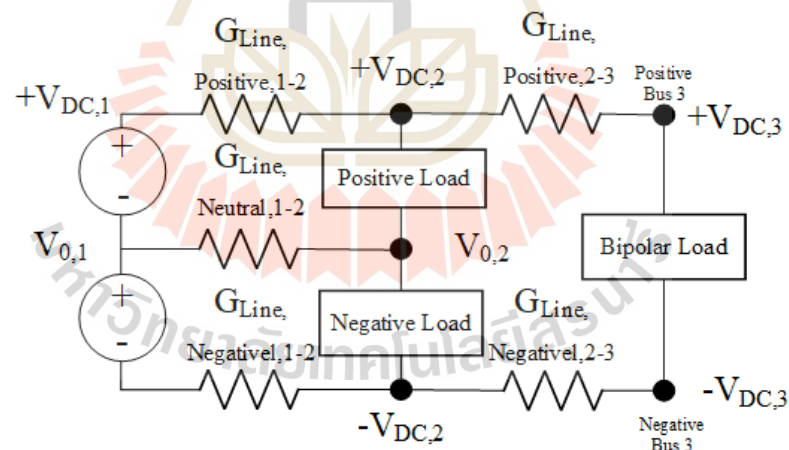


Figure 2.4 DC bipolar bus topology

### 2.1.2 Voltage level standard of DCDG

The main barrier of adoption of LVDC is lack of standardization which the LVDC products are already available on the market with their specification. The result of the barrier is additional cost of interface converter and complicated design process. The DC voltage level standard can be concluded in TABLE 2.2

Table 2.2 DC voltage standard and application

| Standard     | Voltage range  | Application   | reference                  |
|--------------|--|---|----------------------------|
| IEC          | <48V   | Household appliance   | (Jang et al., 2021)        |
| SEG4         | 400 V-1500 V   | Electronic component<br>EV charger<br>EV fast charger<br>Data center<br>Aerospace project |                            |
| IEC TR 63282 | 320 V-380 V<br>640 V-760 V   | Commercial building<br>Rail transit<br>Distribution system                                | (Ma, Li, Sun, & Sun, 2023) |
| GB/T 35727   | 110 V to 1500 V  |   | (Ma et al., 2023)          |
| CIGRE SC6.31 | 1500 V, ( $\pm 750$ V)<br>750 V ( $\pm 375$ V)<br>220 V ( $\pm 110$ V) | DC distribution grid  | (F. Wang et al., 2021)     |

A low and medium voltage standard of DC distribution system specifies 110 to 1500 V, ( $\pm 750$  V) as the low voltage range which is used such as communication, rail transportation, distributed power supply, etc. the range can be classified in two type depends on user's point of view. The application of low- voltage can be divided into two category there are civilian and professional field. case of civil field is closely related to user's lives such as office and residential. In such situations, safety and economy should come first in point of personal safety. So, the DC distribution network voltage level shouldn't be excessive. For professional field such as ship power supply, rail transportation, distribution system. the Practicality and flexibility are prioritized above everything else and relatively high voltage values can be selected.

### 2.1.3 Impact of load unbalance on DCDG

In a bipolar DC distribution grid, a neutral current flowing depends on load demand at each pole which can be considered as 2 cases as follows: 1) load demand balancing case and 2) load demand unbalancing case.

In case of load demand balancing case, a power demand at positive pole and negative pole is same which the load current of those pole will be equal. So, the both load current will flow to neutral bus with same current magnitude which the summation of those current at neutral bus will be equal zero and a neutral voltage at neutral bus will be equal zero, respectively. In case of load unbalancing, A magnitude of load demand of positive pole and negative pole is unequal. So, the summation of those current flow at neutral bus is unequal zero and the total current flow will flow to other bus for return to substation. So, this condition will be increasing neutral voltage bus and increase a power loss at neutral conductor which the problem can be increase neutral current on nearby balance load demand bus.

## 2.2 Electric Vehicle Technology

A CO<sub>2</sub> emission and fossil fuels dependence are a primary problem of internal combustion engine vehicle (ICE). The problem leads to energy security concern and rises of CO<sub>2</sub> releasing in section of transportation system. A Figure .... presents an Electric vehicle technology which usually has four categories. Each type of EV, an electrification increases from left to right which fuel cell electric vehicle, hybrid electric vehicle and plug-in hybrid electric vehicle consume gasoline or diesel fuel together with electric energy to reduce carbon dioxide production and improve efficiency of vehicle. The first and fourth categories are not generated emission during operation vehicle which uses hydrogen fuel and battery to generate energy and storage energy during operation (Sanguesa, Torres-Sanz, Garrido, Martinez, & Marquez-Barja, 2021).

### 2.2.1 Fuel Cell Electric Vehicle (FCEV)

FCEV is a space travel technology which developed in 1960 and become a commercial concept in 2000. FCEV uses hydrogen as a fuel instead of

electricity or fossil fuel. The exhaust of FCEV doesn't generate harmful emissions which is a cause of greenhouse effect phenomena. The FCEV can be categorized as follow: fuel cell electric vehicle and fuel cell hybrid electric vehicle which a configuration of powertrain displays in Figure 2.5 (Muthukumar et al., 2021).

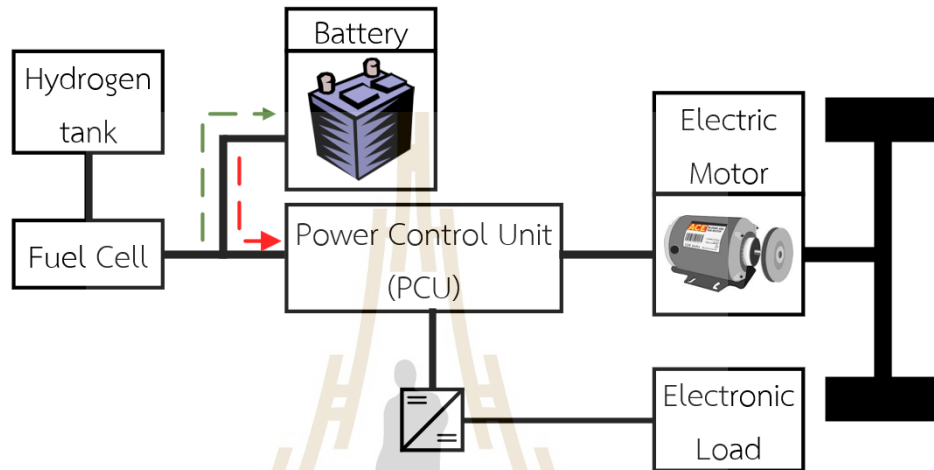


Figure 2.5. FCEV configuration of powertrain

The FCEV suitable in application that requires a constant power at constant speed such as buses, forklifts, tram and etc. nowadays many manufacturers such as Toyota, Honda and Hyundai develop a prototype of FCEV with high efficiency in term of fuel economy and performance by implement with energy management strategy which a several aspects of FCEV is summarized in TABLE 2.3

Table 2.3 several aspects of FCEV

| FCEV       |   |
|------------|---|
| Drivetrain | FCEV uses a fuel cell or hydrogen fuel to generate electricity by using cell membrane to drive a traction motor   |
| Efficiency | Due to use electrical motor as a powertrain, FCEV offers a good acceleration and excellent performance, but a main drawback is availability of hydrogen fuel. |

Table 2.3 several aspects of FCEV (Continued)

| FCEV                    |  |
|-------------------------|--|
| Cost                    | A cost of FCEV is higher than BEV due to Fuel cell is high and complex technology.   |
| Range                   | FCEV have more traveling range than BEVs because fuel cell technology can be generated electricity to serve traction system, but a main drawback is availability of hydrogen fuel. |
| Environmental Influence | little influence on the environment  |
| Important Issue         | Fuel price<br>Lifecycle of fuel cell technology in FCEV<br>Lack of hydrogen refueling station  |

### 2.2.2 Hybrid Electric Vehicle (HEV)

HEV is a combination of internal combustion engines (ICE) with an electric power train system which HEV can be operated in both fossil fuel and electricity. HEV is optimal for daily usage in urban areas than driving in the city because an urban area can recharge the battery during braking operations in regenerative braking operation. While driving in the city, HEV is operated in an idling stop which HEV must frequent starting and stopping ICE of the car.

The ICE and electric motor of HEV are optimized to reduce release pollution and convert inertia energy to electric energy for improving fuel efficiency and performance (K. V. Singh, Bansal, & Singh, 2019). The design of HEV is illustrated in Figure 2.6. The HEV's drivetrain converts vehicle's power source such battery or ICE to wheel which HEV can be categorized into 3 types depending on connecting of ICE and electric motor as follow: series-HEV, parallel-HEV and series-parallel HEV. A series HEV topology

is the best performance for stop-and-go driving pattern which ICE and wheels does not connected with mechanical part. Generally, ICE is used to driving a generator to generate electrical power which the output power is stored in battery and transmits to electric motor via DC bus and converter to drive the wheel (Tran et al., 2020). The engine runs with various speed to reach the high efficiency. Series-hybrids HEV is suitable for infrastructure service such as bus with high traffic route. A parallel HEV topology has directly mechanical connection of ICE and wheel which electric motor is used at low speed. The topology combines a torque to transfer to wheel via transmission system and gear. The topology reduces energy loss but less suitable for stop-and-go traffic when compared with series-hybrid HEV (Emadi, Rajashekar, Williamson, & Lukic, 2005).

With the gearbox, series-parallel HEV have an extra mechanical link between the generator and motor which give a benefit of series HEV and parallel HEV. Power flow management of splitting power is one of the primary issues with series-parallel HEVs as it incorporates operational parts from both series and parallel systems, adding to the complexity of the system. The summary of HEV topology and application is presented in Table 2.4 -2.5



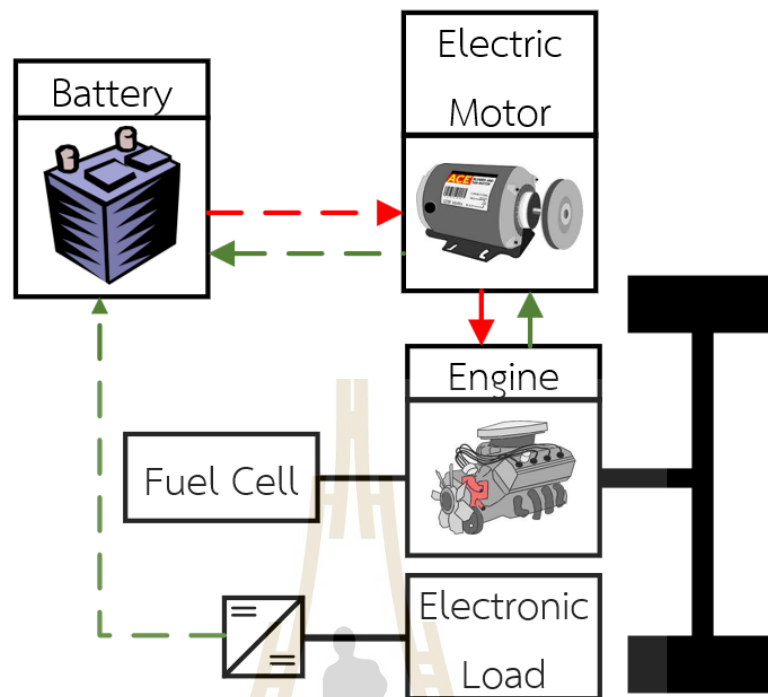


Figure 2.6 design powertrain of HEV

Table 2.4 HEV topology and application

| HEV topology | Efficiency | Advantage  | Drawback   | Application/Example   |
|--------------|------------|--|--|---|
| Serie        | Low        | Traction powertrain efficiency improvement<br>Flexibility improvement<br>Operate with low emission | Large capacity of traction powertrain system<br>Several level of energy transformation | Heavy vehicle such buses, truck and locomotive<br>Example<br>- Renault Kangoo |

Table 2.4 HEV topology and application (Continued)

| HEV topology    | Efficiency | Advantage  | Drawback                                      | Application/Example   |
|-----------------|------------|--|---|---|
| Parallel        | Medium     | Possible to operate with zero emission                     | Require high voltage for improve efficiency   | Household car for inner city<br>Example<br>- Honda Civic<br>- BMW 7 Serie |
| Series-Parallel | high       | Possible to operate with zero emission<br>High flexibility | High-cost system<br>Complexity control system | Light commercial vehicle<br>Example<br>- Volvo C30<br>- Toyota Prius      |

Table 2.5 A feature of HEV

| Hybrid Electric Vehicle (HEV) |  |
|-------------------------------|--|
| Powertrain                    | Internal combustion engine and electric motor with battery   |
| Performance                   | A good performance for EV with a good accelerating rate  |
| Cost                          | A HEV cost is the lowest when compares with other EV technology  |
| Range                         | Due to hybrid engine can provide additional range which have a moderate range.   |
| Environmental Impact          | an electric motor can reduce environment emission releasing. So, HEV releases emission more than FCEV bus less than ICE. |
| Important Issue               | Overall price and complexity<br>Battery maintenance cost   |

### 2.2.3 Plug-in Hybrid Electric Vehicle (PHEV)

PHEV is a combination of ICE with electric motor and battery same as HEV but PHEV have larger battery pack than HEV with onboard charging system which can be recharged battery during parking at parking lot. The vehicle can operate on electricity for a short trip. In case of long distance, PHEV have to operate with ICE. The on-board computer of the car will determine when and how much gasoline to utilize based on the driving style selected (X. Wang, He, Sun, Sun, & Tang, 2013). which the basic layout of PHEV is illustrated in Figure 2.7 and a TABLE 2.6 presents a comprehensive summary of PHEV.

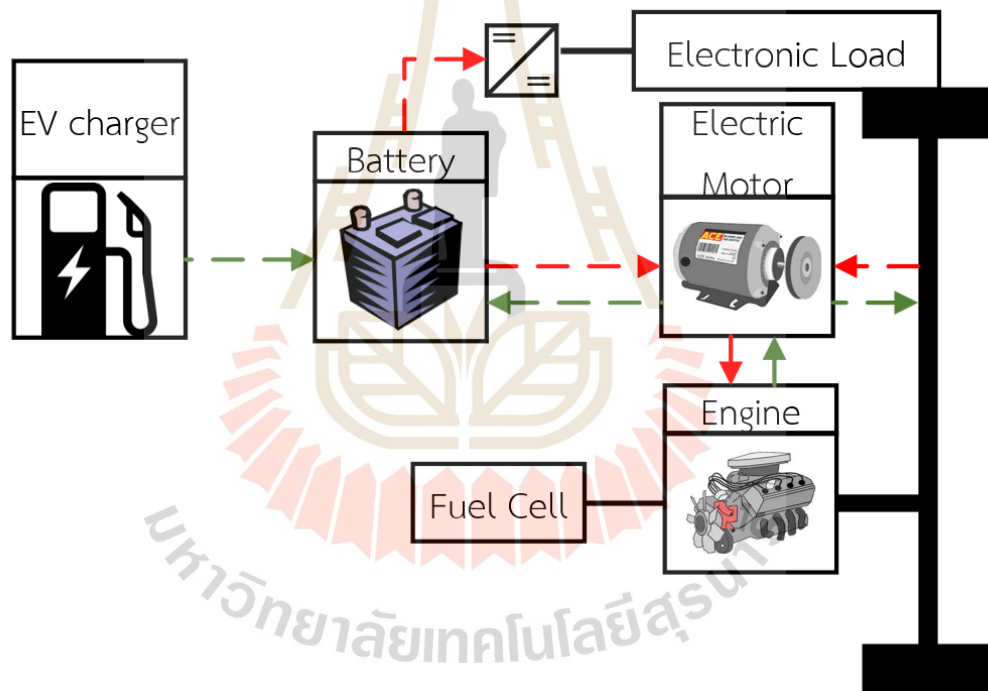


Figure 2.7 PHEV basic layout

Table 2.6 comprehensive summary of PHEV

| Plug-in Hybrid Electric Vehicle (PHEV) |   |
|--|---|
| Powertrain                             | Combine of ICE with electric motor and large capacity of battery which can use external power source to charge the battery. |
| Performance                            | Good performance and acceleration but lower top speed   |
| Cost                                   | Due to large capacity of battery, it has higher cost than HEV.  |
| Range                                  | Due to larger capacity of battery than HEV, PHEV has a extended range.  |
| Environmental Impact                   | Low environment impact  |
| Important Issue                        | High weight and dimension of battery pack<br>Impact on distribution grid due to charging ability<br>Battery management      |

#### 2.2.4 Battery Electric Vehicle (BEV)

BEV is a fully electric vehicle which operate with full source of electricity and battery pack. An efficiency of EV is higher than HEV in term of greenhouse effect gas releasing and energy conversion. EV have a regenerative braking to convert wheel kinetics energy to electrical energy via generator that was converted from electric motor to store in battery. So, EVs are suitable for city driving cycle because EVs can frequent stop and starts application during heavy traffic jam in a city(Nicoletti, Mayer, Brönnner, Schockenhoff, & Lienkamp, 2020). A basic layout of EV is presented in Figure 2.8 and comprehensive summary is presented in TABLE 2.7

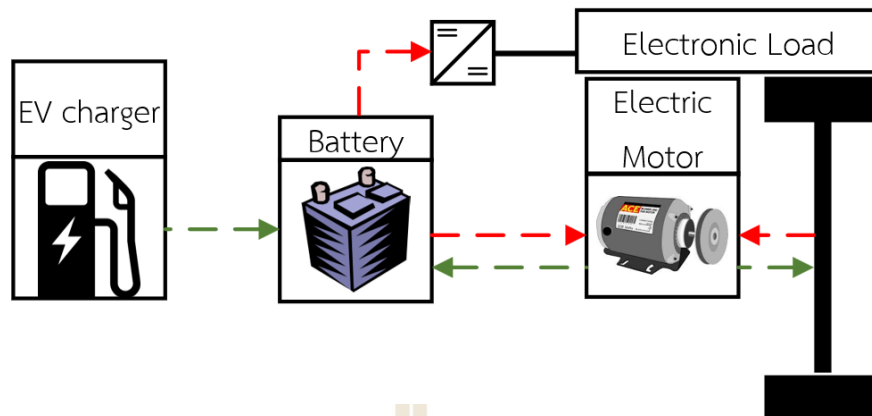


Figure 2.8 BEV powertrain configuration

Table 2.7 comprehensive summary of BEV

| Battery Electric Vehicle (BEV) |   |
|--------------------------------|---|
| Powertrain                     | High accelerating rate and top speed  |
| Performance                    | The efficiency of EV is limited by capacity of battery and converter unit   |
| Cost                           | Highest cost due to large of battery and EV technology  |
| Range                          | The range is limit by capacity of battery and distance between charging infrastructure  |
| Environmental Impact           | Low impact due to no emission from electric motor but it has an environment emission from electricity generation of power plant |
| Important Issue                | Stationary battery-charging infrastructure<br>Battery pack replacement cost   |

### 2.2.5 Comparative of Different Electric Vehicle Technology

Since the late 19th century, when EV technology was first developed, it has advanced quickly. There are many different technologies available on the market today, ranging from conventional internal combustion engines to more contemporary hybrid electric, plug-in hybrid electric, battery electric, and fuel cell electric cars. The

consumer must determine which kind of EV technology best meets their demands, as each has pros and downsides of its own. In the end, each user's money, objectives, and lifestyle will determine which EV is ideal for them in any specific circumstance. Table 2.8 presents a comprehensive comparative study of all EV types, along with their respective advantages and disadvantages.

## **2.3 Battery charger and architecture**

A one of important components of electric vehicle are battery and charging topology that likes a fuel tank and refueling method of internal combustion engine vehicle. which are two main categories of EV charging facilities as follow :1) on-board charging and 2) off-board charging. Each category can be categorized based on their power flow designs, which might be unidirectional or bidirectional. EV battery chargers can be further classified. The bidirectional charging system ability can deliver power from grid to vehicle and discharge energy back to grid with a high power which can't be supported by on-board charger due to restriction of several factor. EV charger can be categorized many types such as energy source, charger installation, cable type and charging level which the detail is presented in next subsection

### **2.3.1 EV's Charging method**

Normally, an EV's battery energy is consumed by traction motor and auxiliary service such as air condition, front and rear lighting system, multimedia system and driving support system. So, the battery requires to recharge for refill the energy to reach a suitable level for daily usage via charging infrastructure which have mainly three charging method as shown in Figure 2.9

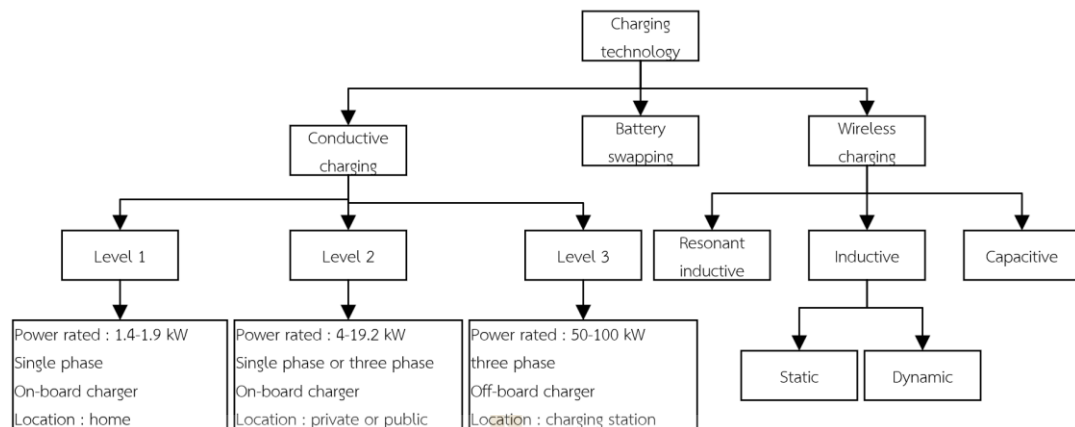


Figure 2.9 Charging topology

Table 2.8 Comprehensive study of all EV technology (M. Kumar, Panda, Naayagi, Thakur, &amp; Panda, 2023)

| Technology                             | Description  | Advantage   | Disadvantage   |
|--|--|---|--|
| Hybrid Electric Vehicle (HEV)          | An internal combustion engine and electric motor combination that the vehicle consumes gasoline fuel integrating with traction motor and battery | - The efficient is higher<br>- conventional ICE vehicle<br>- low emission<br>- fuel cost saving             | -High manufacturing cost<br>- short of battery range                               |
| Plug-in Hybrid Electric Vehicle (PHEV) | An internal combustion engine, electric motor and battery combination with an ability to charge a battery from external power source.            | -Longer battery range<br>- low emission<br>- low fuel cost<br>- support plug-in charge from external source | - high manufacturing cost<br>-limited charging infrastructure<br>-battery lifetime |

Table 2.8 Comprehensive study of all EV technology (Continued)

| Technology                        | Description  | Advantage  | Disadvantage   |
|-----------------------------------|--|--|--|
| Battery Electric Vehicle (BEV)    | A fully powered by electricity with rechargeable batteries                         | <ul style="list-style-type: none"> <li>- Zero emission</li> <li>- Low fuel cost</li> <li>- Long battery range</li> </ul> | <ul style="list-style-type: none"> <li>- high manufacturing cost</li> <li>-limited charging infrastructure</li> <li>-battery lifetime</li> </ul> |
| Fuel Cell Electric Vehicle (FCEV) | A combination of electric motor and fuel with reaction between oxygen and hydrogen | <ul style="list-style-type: none"> <li>-High efficiency</li> <li>-No emission</li> </ul>                                 | <ul style="list-style-type: none"> <li>- High cost</li> <li>- Limited fueling station</li> </ul>   |

### Conductive charging method

The charging method is conventional method that uses a conductor wire to directly connect an EV's battery to supply system via charging plug of charger. The method has high efficiency when compares with wireless charging method. The method is very dangerous when is used without safety equipment. Nowadays, many charging topologies were presented for single phase charger and three phase charger (B. Singh et al., 2003) (B. Singh et al., 2004) which consists of AC/DC converter, power factor correction and DC/DC converter. The type of conductive charger can separate into two categories as follow: on-board charger and off-board charger. Generally, onboard charger of EV can charge an EV with slow charging which a charging process is simple by using charging plug connecting to household outlet. In case of off-board charger, the method can be given a fast-charging service to EV's battery by using wall charger. Which the component of each charger type as shown in FIGURE 2.10-2.11 (Yilmaz & Krein, 2012)



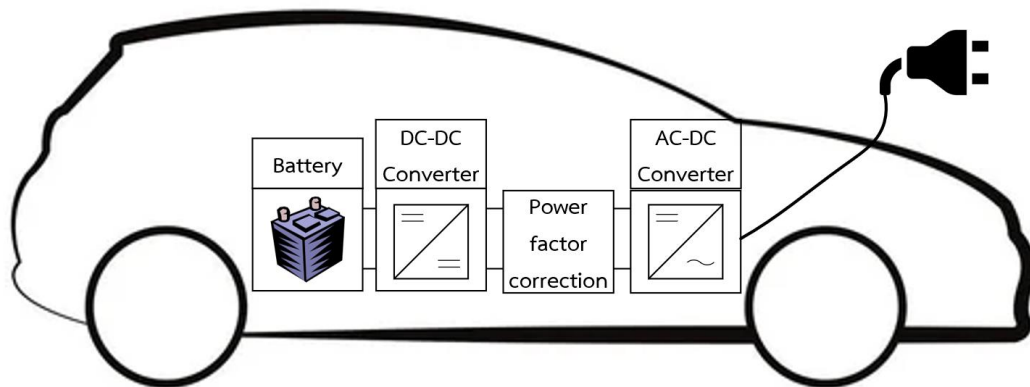


FIGURE 2.10 onboard EV charger component

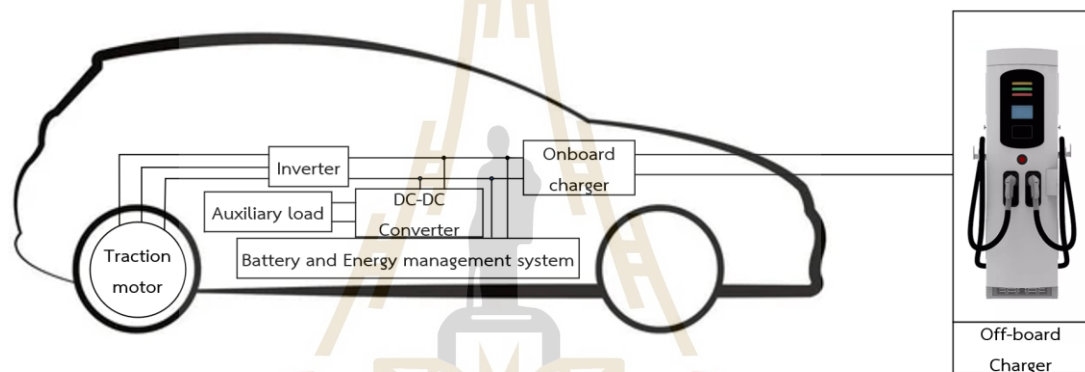


Figure 2.11 off board EV charger component

Infrastructure development and availability for EV charger infrastructure can decrease a capacity of EV battery which EV charger infrastructure have three power charging level. The charging level can be separated into 3 categories as follow: level1, level2, level 3 or DC fast charging which the most vehicle can be charged on level 1 and level 2 charger, but some model cannot charge at level 3 charger. Nowadays, the level 1 and level 2 charger are a primary option which suitable to household installation due to EV owner charges at home overnight which supports to EV's owner daily life. While level 3 charger is used to for commercial charging station (Botsford & Szczepanek, 2009).

Level 1 charging is the slow charging which does not require an additional charger device. So, the charging will use only wall outlet to charge an EV

battery with on-board charger which have a lowest cost but needs a long time to be fully charged due to the charging uses low power rating and low impacts on distribution grid. A slow charging is suitable to install at home, office or working place to service EVs in working period or resting period due to charging power is up to 2 kW with 120-220 V<sub>AC</sub> which have charging time 4 – 6 hr. so, the charging is suitable with EV owners that parks EV at parking lot in a long time.

Level 2 charging or primary charging uses 208 V or 240 V with current up to 80 A. which charging power is up to 19.2 kW. A charging time of level 2 charging is shorter than level 1 charger. To achieve level 2 charging, the EV need home or public additional EV supply equipment installation. So, the charging is suitable to distribute to other place such as office, restaurant or convenient store that the place has an activity time equal or higher than charging time (1 hr. to 3 hr.).

Level 3 charging is designed to operate as a refueling station which can be fully charged less than 1 hrs. which can be installed at main road or highways. A level 3 charging level need a 480 V or high voltage power supply to operate and available only as an off-board charger due to a charging power rate is up to 100 kW. So, a level 3 charging does not suitable to install at household due to many problems such high installation cost, safety issue and rated of power supply. The charger is installed in shopping centers, parking lots, restaurants, theaters or etc. which present an advantage of high charging power in term of charging time but it can be increased a peak demand in the distribution grid (Botsford & Szczepanek, 2009). So, the capability of EV is important to choosing power level type which the TABLE 2.9 show charger rated at different levels.

At each type can be classified based on power flow direction as follow:  
 1) unidirectional charging and 2) bidirectional charging which the detail of the category is discussed in next subsection. In future, a robot is developed to connect charging plug to EV's charging port. The charging method have a lot of standards that was developed by many organizations to support charging devices such as SAE J1722

standard or IEC 61851 standard. Which the standard discussion is presented in TABLE 2.9

The SAE standard is developed and used to determine a charging port type and charging connector that have many types with various countries. The charging port and charging connector based on SAE standard are shown in FIGURE 2.12 And 2.13, respectively.

Table 2.9 specification of charging level

| Power level type            | Power rate (current rated) | Voltage             | Charging time | Vehicle technology supported | Suitable Installation location |
|-----------------------------|----------------------------|---------------------|---------------|------------------------------|--------------------------------|
| Level 1<br>Slow charging    | 1.4 kW (12A)               | 120 V <sub>AC</sub> | 4-11 hours    | PHEVs(5-                     | Home<br>Office                 |
|                             | 1.9 kW(20)                 | 230 V <sub>AC</sub> | 11-36 hours   | 15kWh)<br>EVs(16-50kWh)      |                                |
| Level 2<br>Primary charging | 4 kW(17A)                  | 240 V <sub>AC</sub> | 1-4 hours     | PHEV(5-                      | Home,<br>department store      |
|                             | 8 kW(32A)                  | 400 V <sub>AC</sub> | 2-6 hours     | 15kWh)<br>EVs(16-30kWh)      |                                |
|                             | 19.2 kW(80A)               |                     | 2-3 hours     | EVs(3-50kWh)                 |                                |
| Level 3<br>Fast charging    | 50 kW                      | 208-600             | 0.4-1 hours   | EVs(20-                      | Commercial building            |
|                             | 100 kW                     | V <sub>AC</sub>     | 0.2-0.5 hours | 50kWh)                       |                                |
|                             |                            |                     |               |                              |                                |

|  | USA  | JAPAN  | EU   | CHINA  |
|--|--|--|--|--|
| <b>Single Phase/ 3-Phase AC Charging</b> | <br>SAE J1772<br>Level 1, Level 2<br>Single phase   | <br>SAE J1772<br>Level 1, Level 2<br>Single phase     |  <br>IEC 62196<br>Level 1<br>Single Phase | <br>IEC 62196<br>Level 1,2<br>Single/Three<br>Phase |
| <b>DC Fast Charging /AC-DC Combo</b>     |  <br>Level 1 + DC<br>SAE J1772 Combo | <br>JEVS G105-<br>1993<br>CHAdeMO DC<br>Fast Charging | <br>IEC 62196-3 Hybrid<br>Combo   | <br>GB/T 20234.3-<br>2011<br>DC Fast charging       |

Figure 2.12 charging port










|  | USA   | JAPAN   | EU   | CHINA   |
|--|---|---|--|---|
| <b>Single Phase/ 3-Phase AC Charging</b> | <br>SAE J1772<br>Level 1, Level 2<br>Single phase   | <br>SAE J1772<br>Level 1, Level 2<br>Single phase | <br>IEC 62196-2<br>Level 1, 2<br>Single/Three phase | <br>IEC 62196<br>Level 1,2<br>Single/Three<br>Phase |
| <b>DC Fast Charging /AC-DC Combo</b>     |  <br>SAE J1772<br>Level 2 + DC<br>Combo | <br>CHAdeMO DC<br>Fast Charging                  | <br>IEC 62196-3 Hybrid<br>Combo                   | <br>GB/T 20234.3-<br>2011<br>DC Fast charging      |

Figure 2.13 Charging connector

### Wireless charging method

A wireless charging method or inductive charging method is a charging method without directly connected but connected through magnetic field. Normally, the charging method is used to charged electric bus battery during stop at bus stop or charging point which the highest efficiency of charging method is 90 % (Yue Cao, Ahmad, Kaiwartya, Puturs, & Khalid, 2018; Y. Yang et al., 2018). There are three wireless charging method as follow: 1) inductive, 2) resonant inductive and 3) capacitive wireless charging (Musavi & Eberle, 2014; Zhenshi Wang, Wei, & Dai, 2016).

### Inductive wireless charging

Inductive wireless charging (IWC) is a basic idea of technology that contains AC/DC converter to convert AC power supplied from utility grid to DC power. Then, A DC power is converted again to high frequency AC power and fed to primary coil that all of component are installed in street underground. While an EV have to install secondary coil to receive power from primary coil via electromagnetic induction through the air gap. A received AC power have to converted to DC by AC/DC converter and charged to battery (Li & Mi, 2015). A inductive wireless charging simplified diagram is shown in FIUGRE 2.14 which IWC can classified into dynamic inductive charging and static inductive charging. For inductive charging, EV have to park over a primary coil during charging while dynamic inductive charging can charge EV during moving (Un-Noor, Padmanaban, Mihet-Popa, Mollah, & Hossain, 2017).

At present, WC is only supported to unidirectional power flow from grid to vehicle but in the future the technology is developed to discharge power to the grid. The advantages of this technologies are user convenience, electrical safety and not require charging cable but the challenges are less efficiency due to high power loss, large charging time and huge investment cost.

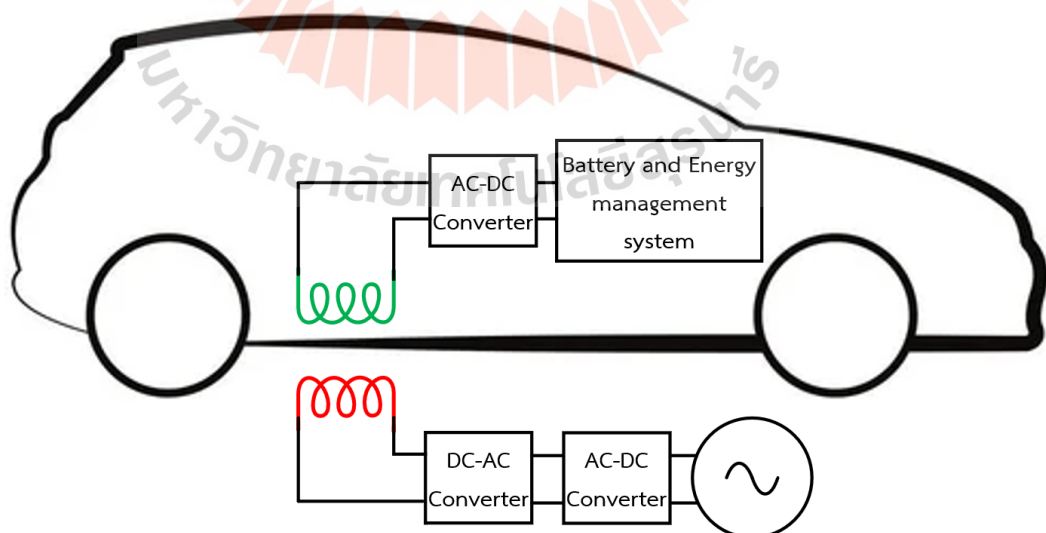


Figure 2.14 Simplified diagram of inductive charging

### Battery swapping method

Battery swapping station (BSS) replaces a drained or discharged battery by charged battery in few minutes which the advantage is no waiting time (Sarker, Pandžić, & Ortega-Vazquez, 2015). the method is suitable for electric motorcycle or electric folk lifts that have high battery capacity which have a long charging time by using conductive charging method. In case of transportation vehicle such as E-bus or E-car, the method is unsuitable to use because a reason of battery warranty, weight of battery and size of battery due to swapping station must stock many sizes of battery to support many models of EV. So, the station requires the huge investment (Zheng et al., 2014) (Sarker, Pandžić, & Ortega-Vazquez, 2013).

The advantage and disadvantage of each charging type is concluded and shown in Table 2.10

Table 2.10 advantage and disadvantage of each charging method

| Charging type       | Advantage   | Disadvantage   |
|---------------------|---|--|
| Conductive charging | Various charging power level<br>Support V2G service<br>High efficiency              |  |
| Slow charging       | Extending the battery lifecycle<br>Low heat generated during charging procedure     | Long time charging                                     |
| Fast charging       | Short charging duration time<br>Support transport infrastructure such as bus route. | High battery degradation rate.<br>Inefficient charging |

Table 2.10 advantage and disadvantage of each charging method (Continued)

| Charging type     | Advantage  | Disadvantage   |
|-------------------|--|--|
| Wireless charging | Non-wear and tear on connector<br>Effortless charging procedure<br>Enhanced safety | Lower efficiency<br>High investment cost<br>Limited Compatibility              |
| Battery swapping  | Low charging time<br>Increase EV range and driving flexibility                     | High infrastructure cost and operational cost<br>Require precision engineering |

### 2.3.2 EV's Charging Classification Strategy

A fleet of EV have to recharge battery for daily usage at various location such as home, working place or charging station which each location has difference electrical capabilities such as voltage level (low voltage or high voltage), voltage type (single phase or three phase) or electrical policies (restriction of charger power rated at each location). So, each place can install difference type of charger that have a difference charger level such as slow charging (level 1), primary charging (level 2) and fast charging (level 3).

The distribution system faces a lot of problem of EV penetration level due to various charging level which the charging impact of EV fleet has many factors such as charging level, number of EVs charging in same time and charging control method these factors can affect the system performance power loss. To discusses a charging method and EV charging impact, the EV charging method classification presents a charging strategy, charging approach, energy flow directional and, control architecture which as shown in FIGURE 2.15

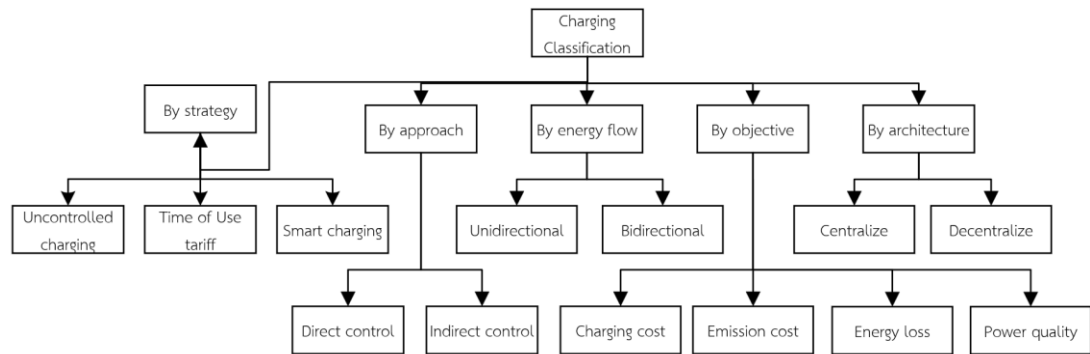


Figure 2.15 EV charging method classification

The charging strategy or charging behavior control method is a method for control EV's charging behavior to reduce impact on distribution grid which comprises of three methods as follow: 1) uncontrolled charging method, 2) Time of Use tariff and 3) controlled charging method or smart charging.

Uncontrolled charging method is a simple method and used frequently which an EV's owner can be charged their EV immediately or after defined time. During charging period, A grid operator can't be controlled charger and can't accessed to charging information, parameter etc. charging process. So, the charging load varies randomly within a specific time which can be produced many problems for distribution grid in term of under voltage, frequency fluctuation and power outage due to rapid peak power. Reference (Verzijlbergh, Grond, Lukszo, Slootweg, & Ilic, 2012) presented an impact of uncontrolled charging and controlled charging on medium voltage of distribution cable, transformer and substation. An issue of uncontrolled charging can be lead to a problem of management, control and operation of power system which can be decreased system stability due to high peak demand (Saldaña, San Martin, Zamora, Asensio, & Oñederra, 2019). EV charging station without control strategies can consume the power as high as 350 kW per charger. So, the EV charging station in some building such as office or department store can increase monthly peak power demand up to 250 % (Gilleran et al., 2021).

Time of Use tariffs or TOU tariffs is an electricity price changing based on time along the day which depends on power demand at each period. At each period of



the day, in case of off-peak period such as power demand less than power generated, the price is cheap to influence EV owner connecting EV to grid. In the other hand, the price can be risen when EV owner charges their EV during peak-time. So, TOU tariffs can be shift load demand or charging demand from peak load demand to off peak load demand. The method can be reduced stress of distribution grid.

Smart charging or controlled charging is an integration of uncontrolled charging and TOU tariff to achieve more benefit in technical term and economic reason. The method allows a grid operator communicating to EV for create an optimal charging schedule. A controlled charging method is used to reduce grid impact. The charge and discharge management can be centralized, decentralized and hierarchical method(Deilami, Masoum, Moses, & Masoum, 2011). In case of centralized control method, aggregator or operator can directly control and manage a behavior of EV's charging and discharging. The aggregator can control charger via control signal to optimize the charging and discharging rate of EV to search an optimal solution and give various service to grid. This method become with several limitation and challenge such as a backup system to support a system during a fail to solve the problem of aggregator. The other problem is solving time that depends on a number of EV so large-scale of EV fleet and time solving becomes a main problem of centralized control method (Nimalsiri et al., 2020) (Alshahrani, Khalid, & Almuahini, 2019). In present, a objective of optimization is used to planned for a EV's charging and discharging in distribution network to give a maximum benefit for grid utility and EV owner such as minimizing daily energy loss and maximizing EV's owner profit (Einaddin & Yazdankhah, 2020). A centralized control strategy determines a number of vehicle to control total charging demand via grid operator or aggregator which these strategy provides many benefits to the EV owner and the grid such as improve voltage profile, reduced power loss and reduce peak power by using valley-filling (Clement-Nyns, Haesen, & Driesen, 2010),(Sortomme, Hindi, MacPherson, & Venkata, 2011).

There are two control architecture method to control an EV charging as follow: A centralize charging method, a EV charging system have aggregator unit (AU) to decide to charge a EV battery by using EV information like state of charge, vehicle

location, parking time, amount of vehicle and etc. (García-Villalobos, Zamora, San Martín, Asensio, & Aperribay, 2014). which a main barrier of centralize are privacy and security policy due to aggregator can achieve to EV information. The architecture as shown in FIGURE 2.16 the aggregator function is keeping a benefit of grid utility and EV owner. The method is fully support to an ancillary service which the control method is high complexity and can support a EV consumer with limitation (Deng, Liang, Tan, & Wang, 2016). The method has high computation time to manage EV fleet in service area and requires many conditions to manage or schedule charging load which reduces flexibility.

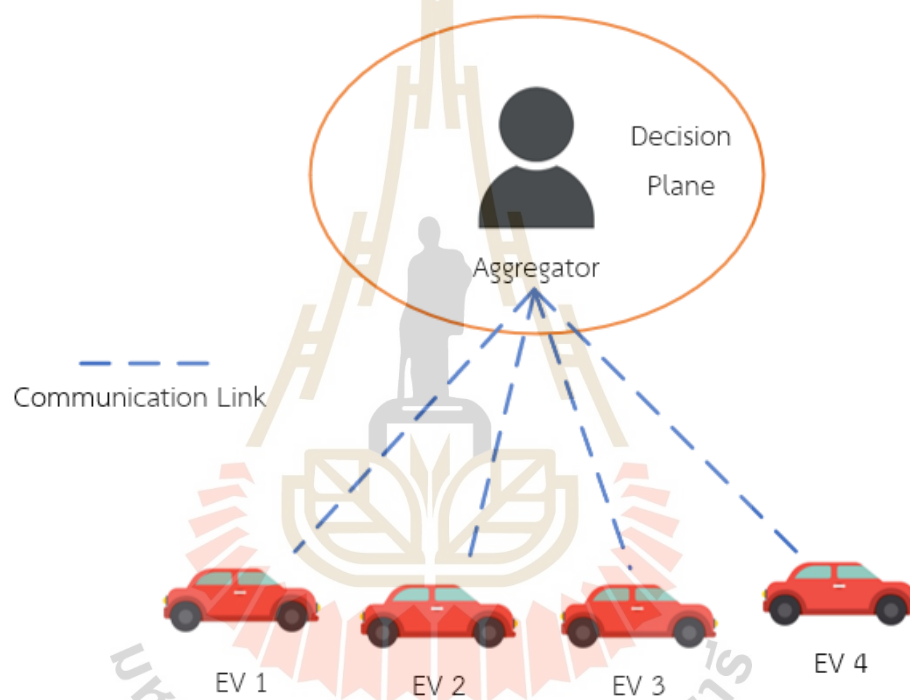


FIGURE 2.16 centralize charging method configuration

In case of decentralized control method, the method allows an EV owner and grid operator define some parameter to reach a specific target such as minimize charging cost so grid manager can indirect control charging or discharging behavior of EV user to achieve a pricing strategy and using price incentives strategy to transfer load from peak-hours to off-peak hours. The decentralized method lacks direct control which the optimal solution can't be guaranteed. So, ancillary service in decentralized control is more difficult than centralized control. The decentralized control is suitable for large-scale of EV fleets which EV's owner can be shared charging, discharging and state of

charge information. So, this method requires a communication system to communicate between EV's owner and aggregator (Aghajan-Eshkevari, Azad, Nazari-Heris, Ameli, & Asadi, 2022). The aggregator can be used the information to decision charging and discharging cost via price-based demand response strategy to take benefit for grid. A practical demand response was proposed in (Bahrami & Parniani, 2014) which consider an impact of EV charging strategy on the electricity price and optimize the charging cost of EV battery. In (Amiri, Jadid, & Saboori, 2018) implements valley filling in a distribution network with considering decentralized control which a decentralize charging control configuration is shown in FIGURE 2.17

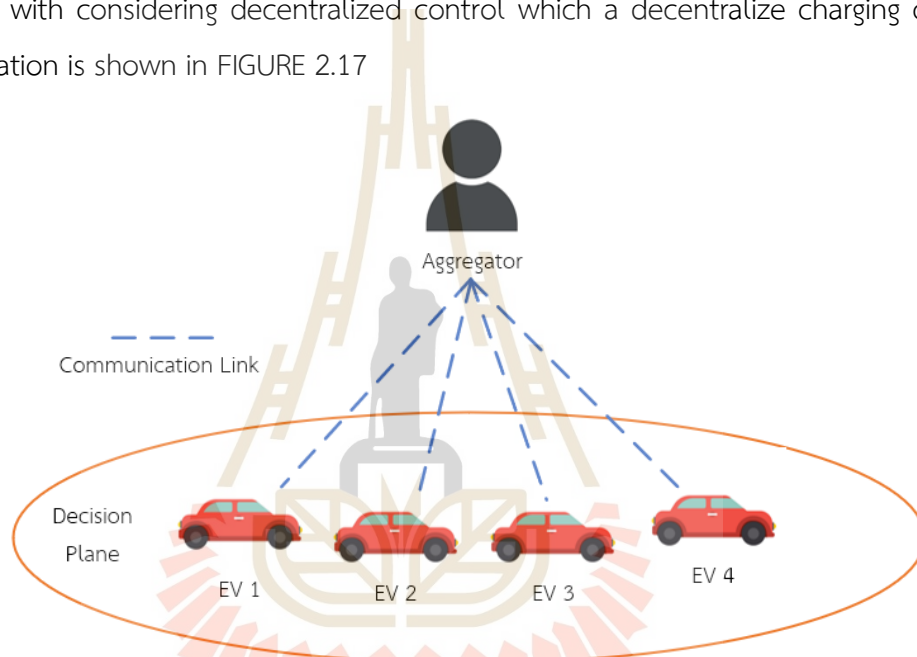


Figure 2.17 decentralize charging control configuration

Therefore, A comparison of centralize and decentralize charging control is presented in TABLE 2.11

Table 2.11 Comparison of centralize and decentralize charging control

| Characteristics   | Control architecture               |                     |
|-------------------|------------------------------------|---------------------|
|                   | Centralize                         | Decentralize        |
| Charging decision | The aggregator or network operator | EV owner            |
| Control action    | Direct control                     | Price-based control |
| Ancillary service | Fully supported                    | Partially supported |
| Complexity        | More                               | less                |
| Flexibility       | less                               | More                |
| Scalability       | less                               | More                |

The charging approaches can be classified into two approaches as follow: 1) direct controlled approach and 2) indirect control approach which a direct controlled approach allows an operator to control a charging procedure to reduce impact on grid, fulfil a user demand and achieve the financial performance. In the other hand, indirect control allows an EV's consumer to fully control charging procedure such as charging time, charger capacity and etc. the operator can't be directly controlled charging procedure, but they control via charging price such as off-peak or on-peak hours price. So, A smart charging approach is developed to control charger power output that can be controlled from zero to maximum power and controlled charging duration. while EV connected to charger, The EV is not charge all time because the power output of charger can be control to zero during peak hours by operator (Kong & Karagiannidis, 2016).

The energy flow directional comprises of two direction flow as follows: 1) unidirectional energy flow and bidirectional energy flow which the operation at each mode as shown in Figure 2.18

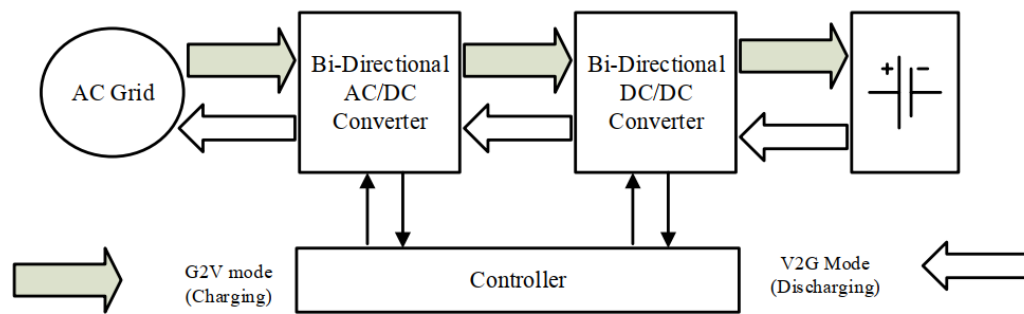


Figure 2.18 Unidirectional and bidirectional energy flow

A unidirectional energy flow is an energy flowing characteristic from grid to EV for recharge EV battery. In case of bidirectional directional energy flow, the method can be flown energy in two directions as follow: 1) charging mode (energy flow from grid to EV) 2) discharging mode (energy flow from EV to grid) which a bidirectional converter installed on EV or bidirectional charger can support V2X and V2G technology, respectively. In charging mode, An EV battery act as load to recharge energy from grid and discharging mode EV battery act as source to reserve or to release energy to grid for support grid operation. Which the method can be change a EV as a mobile energy source and flexible load (Hosseini, Badri, & Parvania, 2012).

The objective of charging method can be classified on many types of objectives such as charging time, waiting time, charging cost, system loss, emission and power quality issue to design or develop a charging station, strategy and equipment to improve efficiency of EV charger station. The EV charging infrastructures are shown in Figure .... Which comprises of power infrastructure, communication infrastructure and control system.

#### By objective function

The charging method can be classified on many types of objective function such as reduced charging time, waiting time, energy cost, emission, charging cost, system loss or power quality issue. For simulation, researcher can be used only one objective or multi-objective which TABLE 2.12 Reviews research paper with various objective function.

Table 2.12 literature review of various objective function simulation

| Author                                      | Objection function   | discussion  |
|---|--|---|
| (Mohsenian-Rad & Leon-Garcia, 2010)         | Charging cost minimization based on real time pricing                          | The research presents a comparison of real time pricing model for improve economic and environment with common current flat rate by using simple and efficient weight average price prediction based on data set from Illinois power company from January 2007 to December 2009   |
| (Deilami, Moses, Masoum, & Abu-Siada, 2013) | Power loss minimization with peak shaving strategy based on Time of use tariff | The paper proposes a smart load management approach for coordinating plug-in electric vehicle (PEV) chargers in distribution and residential networks. The approach aims to achieve peak shaving, minimize power losses, and improve voltage regulation. A simulation results based on the proposed SLM approach are presented and discussed a different charging scenario and the effects of charging stations are compared. |

Table 2.12 literature review of various objective function simulation (Continued)

| Author  | Objection function   | discussion  |
|---|--|---|
| (Y. Cao et al., 2012)   | Charging cost minimization with peak shaving and fill valley based on Time of use tariff | The paper proposes an optimized EV charging model that considers time-of-use (TOU) price and the state of charge (SOC) curve to minimize charging cost and flatten the load curve. The result of simulation presents a optimized charging pattern and flat load curve to reduce cost. |
| (Martinenas, Pedersen, Marinelli, Andersen, & Trreholt, 2014) | Charging cost minimization with real time pricing  | The paper proposes a real-time control strategy for charging electric vehicles using a dynamic price tariff to minimize charging costs. The result presents an optimal scheduling that generated by algorithm based on price signal.  |
| (Anderson, 2014)  | Charging cost minimization   | The paper proposes a dynamic, real-time, demand-influenced energy pricing mechanism for billing EVs charging process during congested timeslots.  |

Table 2.12 literature review of various objective function simulation (Continued)

| Author   | Objection function   | discussion  |
|--|--|---|
| (Misra, Bera, & Ojha, 2015)                        | Optimal charging cost and reduce load demand during peak hours                       | The paper proposes a distributed dynamic pricing policy for managing plug-in hybrid electric vehicles (PHEVs) in a smart grid architecture. The simulation result presents a Utility of PHEVs increases by approximately 34% with the proposed architecture.  |
| (Binetti, Davoudi, Naso, Turchiano, & Lewis, 2015) | Minimize power loss, voltage deviation, operational cost, load variance and emission | The paper proposes a decentralized algorithm for scheduling EV charging which the algorithm is non-iterative, scalable, and suitable for real-time implementation. A simulation result presents an effectiveness of proposed algorithm for scheduling a large population of EV in a decentralized charging control. |
| (Latinopoulos, Sivakumar, & Polak, 2017)           | EV load scheduling based on dynamic pricing  | The paper discusses how electric vehicle drivers respond to uncertain future prices when charging their vehicles away from home. It uses a survey to observe their preferences for hypothetical charging services and finds that most drivers are risk averse and prefer a certain price over an uncertain one.     |



Table 2.12 literature review of various objective function simulation (Continued)

| Author                                      | Objection function   | discussion   |
|---|--|--|
| (X. Zhang, Liang, Zhang, Bu, & Zhang, 2017) | Reduce peak or valley and improve economic with time of use tariff                   | The paper proposes a peak-valley time-of-use charging price model for private charging piles in Beijing to optimize the charging pricing and promote the large-scale adoption of private electric vehicles (PEVs). The case study suggests that the proposed peak, average, and valley price in Beijing should be 1.8, 1, and 0.4 yuan/kWh, respectively, to promote the large-scale adoption of PEVs. |
| (Moon & Kim, 2017)                          | Balance charging with time of use tariff   | The paper discusses a method for managing electric vehicle charging demand by considering both the costs and loads simultaneously, aiming to find a balanced state that satisfies both the users and system operators.   |
| (X. Zhang, Liang, & Liu, 2017)              | Optimal benefit of grid utility, charging station and EV user with real time pricing | The paper proposes a new optimal EV route model considering time-of-use electricity price and develops a learnable partheno-genetic algorithm to solve the problem. The feasibility and effectiveness of the proposed model and algorithm are verified through numerical tests.  |

## 2.4 Impact of EV charging demand

In the early EV era, charging station plays important role to support daily usage of EVs which charging time and lifetime of battery are related to charger characteristic. So, the charger must be reliable and efficient with high power density and low investment cost. The charger must draw the current with low distortion to minimize power quality impact on utility grid. The EV charging impact limitation on utility grid is determined by many standards such as IEEE1547, IEC1000-3-2 and the US National Electric Code (NEC) 690 standard that allow a DC current injection and harmonic into utility grid.

### 2.4.1 The impact of EV charging station on distribution grid

The charging impact of EV fleet has many factors such as charging level, number of EVs charging in same time and charging control method these factors can affect the system performance power loss. The charging control method comprises of two methods, which are uncontrolled charging and controlled charging (or smart charging).

A fleet of EV have many advantages on environment benefit like less air pollution, increase transportation system efficiency and reduce the dependency of fossil fuel transportation but an electricity demand fluctuation of EV charging can lead to grid instability. So, the section presents an effect of EV integration on grid stability such as power quality issue and energy loss increasing. Then, the section proposed a potential method to improve grid stability, grid reliability and reduce cost of EV integration.

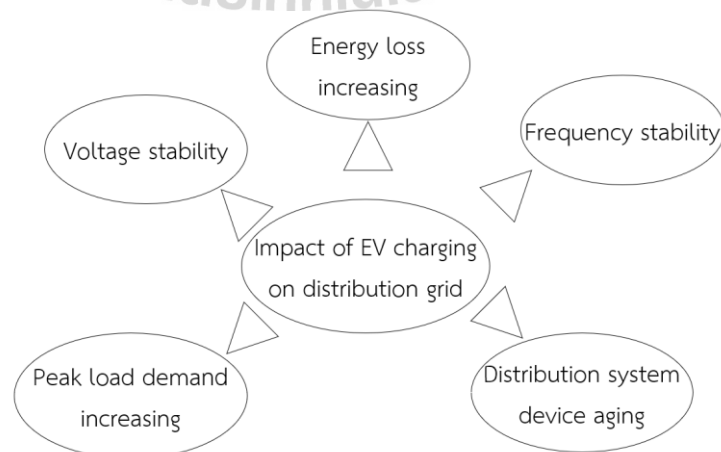


Figure 2.19 Impact of EV fleet on distribution system

A definition of power system stability is a self-restoration of power system to maintain a steady-state operational condition after under operate with disturbance which can be led to blackout due to power system instability. An EV charging load characteristic is non-linear load unlike generally load which can be stressed on the power system. An EV charging demand behavior evaluation is a complicated and unpredictable characteristic of EV charging time, duration and location which depends on EV's owner behavior. The behavior may a cause of power system stability problem if a huge of EV charging simultaneously. Voltage stability is a distribution system ability to maintain a steady state voltage of all the system bus while the system was disturbance from an operation point (Kothari, 2011). A load increasing plays an important role for voltage stability occurring which the author presents a voltage stability impact of EV charging station on 13 bus system by simulate a various location of EV charging to find a weakest bus in test system (Juanuwattanakul & Masoum, 2011). The paper calculates a voltage stability index at each node of 33 bus radial distribution system to find out a weakest node which have more sensitive to voltage collapse (L. KUMAR, SHARMA, & GOEL). The authors present an optimal scheme of charging station placement based in voltage sensitivity index (Rahman, Barua, Zohora, Hasan, & Aziz, 2013). The impact of EV charging is analyzed in 43 IEEE bus system to evaluate a static voltage stability margin (Dharmakeerthi, Mithulananthan, & Saha, 2014). Voltage instability represents a challenging issue and can result in system disruptions (Cutsem, 2000). the EVs consume more power in a short time to fully charge the battery. Furthermore, single phase EVs chargers may increase phase unbalance at distribution network. Phase unbalance results in unwanted negative effects at distribution network operation and connected loads and should remain in the acceptable limits. The impact of uncontrolled charging on voltage deviation at different daily durations to obtained results showed a large increase in voltage deviation which was close to exceeding the acceptable limits especially if EVs were charging at peak period (Clement-Nyns et al., 2010). The impact of uncontrolled charging of EV for three distribution networks including urban, suburban and rural which 25% of penetration level can be occurred high voltage drop in rural network with long feeder.

Frequency stability is a steady state frequency maintaining of power system after a serious disruption in the system that causes a large imbalance between the load and the generation (Kundur et al., 2004). when a power system can't maintain or reach a new equilibrium point after an imbalance between generation and load, a system frequency is unstable and decrease. In the other hand, the system tries to maintain frequency to acceptable level which a large disturbance can be led to generator tripping or load outage (Lokay & Burtnyk, 1968).

Several studies were conduct to peak load increasing due to charging behavior of EV's user which can led to increase power loss and reduce a voltage profile at each bus in the system. EVs have the potential to significantly increase load demand, particularly during peak charging times. Peak load growth is influenced by EV population, charging habits, and infrastructure. Peak electricity consumption is predicted to rise when EVs are widely used. The effects of EV charging on the US electrical grid were examined in several studies. Adoption of EVs might result in a 30% rise in peak power demand at night (M. Kumar et al., 2023). The study of 100 % of EV penetration with uncoordinated charging can be introduced to higher peak load demand per day which the system must require a higher capacity of electricity generation to support average load along a day (Habib, Khan, Abbas, & Tang, 2018). The research study an impact of EV on Western Australis Perth electricity grid with 100% of EV penetration and uncoordinated charging in the system. The result illustrated the peak load demand rising over a daily average power (Z. Wang & Paranjape, 2017). In a similar report, an effect of 30% of EV penetration with uncoordinated charging can increase peak demand up to 53% (Khalid, Alam, Sarwar, & Jamil Asghar, 2019). A 10% of EV penetration with uncontrolled charging in suburban area can significantly increase peak load demand. The impact can be reduced by using coordinate charging or smart charging strategy which the strategy with 30 % penetration of EV can increase 53% of peak demand (Jin, Tang, & Ghosh, 2013). Uncontrolled charging method usually increases the residential peak power demand and time of use pricing plan which the charging period are usually occurred at nighttime. An issue of uncontrolled charging can be lead to a problem of management, control and operation of power system which can be decreased system stability due to high peak demand

(Saldaña et al., 2019). EV charging station without control strategies can consume the power as high as 350 kW per charger. So, the EV charging station in some building such as office or department store can increase monthly peak power demand up to 250 % (Gilleran et al., 2021)

In case of device aging, to support the EV charging load, a large power is required which a distribution system can be operated under overload condition in a long time. The level 1 charging or slow charging with uncontrolled charging has impact on lifetime of transformer. At level 2 and level 3 charging with uncontrolled charging has very harmful impact on transformer life and system device which a large current flow can overload a distribution transformer based on penetration level of EVs. At overload condition of distribution transformer can be occurred transformer power loss increasing, voltage sag, harmonic distortion and maximum demand increasing. So, the system requires a large size of cable and high-capacity transformer to serve a EV charging load. While charging load increase, a transformer temperature also increases that can be reduced a transformer operating life and feeder can operate under overload condition. So, voltage profile of distribution is poor. To reduce an EV load charging impact. The demand response strategy is used. The strategy can control charging scheme which can be reduced degradation of transformer life. The delay charging is used to integrate with valley filling to move a charging load from peak hour to off-peak hours which can be improve voltage profile of distribution system. Reference (Verzijlbergh et al., 2012) presented an impact of uncontrolled charging and controlled charging on medium voltage of distribution cable, transformer and substation.

Extra power demand represented in EVs charging will lead to higher currents flowing and extra power losses in different system components, such as generators, transformers, and cables, which is the main concern for utilities. The EV charging impact on a Danish distribution network show that for uncontrolled charging with 50% penetration level the grid losses increased by 40% and increased only 10% for controlled charging (Pillai & Bak-Jensen, 2010). the impact of EVs charging on distribution transformer power losses was found that for penetration levels ranging from 2% to 40%, the transformer losses increased to more than 300% mainly due to

windings copper losses increase (Masoum, Moses, & Smedley, 2011). The distribution network supplies residential and commercial loads and located on a Korean island that have 40 % of EV penetration can be had daily energy losses increased by 66% (Chang, Bae, Yoon, Park, & Choy, 2019).

## 2.5 Literature Review

| Author and publication year           | Object  | Detail  |
|---------------------------------------|---|---|
| (Clement-Nyns et al., 2010)           | To improve power quality (Peak power, power loss)                                 | This paper compares power loss and power quality (peak power, voltage drop and line current) of demonstrate system in three cases including without EV, uncontrolled charging and controlled charging at 30% EV penetration.  |
| (Byeon, Yoon, Oh, & Jang, 2013).      | to reduce total energy costs by considering EV owner benefit                      | This paper proposes the energy management strategy based on the real-time acquisition data and determines the optimal behavior of the EV service model which results show that the EMS can be reduced the energy cost of EV owners and applied to DC distribution community |
| (Morais, Sousa, Vale, & Faria, 2014). | to minimize operation costs and reschedule distribution energy resources and EVs. | This paper presents the impact of EVs in system operation cost and load demand of distribution networks with large penetration of DG and proposes an efficient management method for charging and discharging EVs. The  |

| Author and publication year                 | Object   | Detail   |
|---|--|--|
|   |  | results of the simulation show the impact of the load factor of EV. As an example, the operation cost can increase by 0.03 % when the load factor increases by 5 %.  |
| (Rabiee, Sadeghi, Aghaeic, & Heidari, 2016) | to reduce operation costs by using peak shaving and load curve modification method | This paper presents the scheduling of electric vehicles which can be separated into two stages. The first stage is generation cost-minimizing by using PSO algorithm and the second stage is charging schedule design. The result of this paper shows the benefit of EV to reduce operation cost while considering the uncertainties of wind and PV. |
| (Farahani, 2017)                            | To minimize VUF  | This paper compares VUF of uncontrolled and controlled charging and discharging of EVs to study impact of EV to VUF which VUF of base case distribution system is 1.93 %. For uncontrolled charging of EV can be increased significantly to 7.7 % of VUF and controlled charging and discharging can be declined the VUF to 0.71 %                   |
| (Lee, Oh, Sim, Kim, & Kim, 2017)            | To reduce peak demand with various   | This paper proposes an algorithm for shaving the peak load which is a one  |

| Author and publication year | Object  | Detail   |
|-----------------------------|---|--|
|                             | penetration level of EV                               | of V2G function in distribution system. The simulation result, The V2G system with 10 % penetration level can improve well with proposed algorithm   |
| (Bian et al., 2019)         | Maximize return of investment                         | This paper propose a Mixed Integer Linear Programming model based on Geographic Information System to use as important inputs, and six important constraints are in cities   |
| (Yu, Nduka, & Pal, 2020)    | Minimize power loss with peak shaving with EV battery | In this article, A two-stage optimization framework-based EV charging/discharging approach that minimizes DCMG network losses and EV battery degradation has been described. The simulation result can be discussed as follow: 24-hours case, the system losses can reduce 4.4 % and reduce DG capacity. 17.8%. In the case of residential, the system loss can reduce up to 13.9 %, and 27.0% of DG capacity was saved. |
| (Liu, Xie, & Huang, 2020)   | To evaluate profit, voltage quality, load fluctuation | This paper presents a multi objective optimization of DG and electric charging station placement to integrated with V2G Technology based on PSO algorithm. The result of this  |



| Author and publication year            | Object  | Detail   |
|--|---|--|
|  |   | paper shows an investment cost, voltage quality, load fluctuation and charging satisfaction of EV of 3 scenarios   |
| Author and publication year            | Object  | Detail   |
| (Arnaudo, Topel, & Laumert, 2020)      | To reduce peak demand caused by heat pump with peak shaving from EV battery discharging                         | Hammarby Sjostad district faces a peak demand from heat pump which can be overloaded the local grid. The simulation shows an EV discharging can reduce the overload amplitude of heat pump during peak hour which depend on EV penetration and SOC   |
| (Attou, Zidi, Hadjeri, & Khatir, 2021) | To reduce critical customer demand and fill off peak period by peak shaving and load leveling energy management | This study presents a peak shaving, load balancing and load leveling based with tree-based decision algorithm in a microgrid. the simulation result shows the performance of the V2G technology in peak management applications during high demand periods and valley filling during off-peak hours to a smoothing of the load curve |

| Author and publication year | Object  | Detail   |
|-----------------------------|---|--|
| (S et al., 2022)            | To schedule EV charging based on solar PV power | The proposed algorithm can be reduced overall charging cost form 10-20 % with only schedule EV while integrating a PV system and charging method can save cost 50-100% based on location, system size and charging point |

## 2.6 Reference

- Abeynayake, G., Li, G., Joseph, T., Liang, J., & Ming, W. (2021). Reliability and Cost-Oriented Analysis, Comparison and Selection of Multi-Level MVdc Converters. *IEEE Transactions on Power Delivery*, 36(6), 3945-3955. doi:10.1109/TPWRD.2021.3051531
- Aghajan-Eshkevari, S., Azad, S., Nazari-Heris, M., Ameli, M. T., & Asadi, S. (2022). Charging and Discharging of Electric Vehicles in Power Systems: An Updated and Detailed Review of Methods, Control Structures, Objectives, and Optimization Methodologies. *Sustainability*, 14(4). doi:10.3390/su14042137
- Alshahrani, S., Khalid, M., & Almuahini, M. (2019). Electric Vehicles Beyond Energy Storage and Modern Power Networks: Challenges and Applications. *IEEE Access*, 7, 99031-99064. doi:10.1109/ACCESS.2019.2928639
- Amiri, S. S., Jadid, S., & Saboori, H. (2018). Multi-objective optimum charging management of electric vehicles through battery swapping stations. *Energy*, 165, 549-562. doi:https://doi.org/10.1016/j.energy.2018.09.167
- Anderson, E. (2014). Real-Time Pricing for Charging Electric Vehicles. *The Electricity Journal*, 27(9), 105-111. doi:https://doi.org/10.1016/j.tej.2014.10.002

- Arnaudo, M., Topel, M., & Laumert, B. (2020). Vehicle-To-Grid for Peak Shaving to Unlock the Integration of Distributed Heat Pumps in a Swedish Neighborhood. *Energies*, 13(7). doi:10.3390/en13071705
- Attou, N., Zidi, S. A., Hadjeri, S., & Khatir, M. (2021, 27-28 May 2021). *Improved peak shaving and valley filling using V2G technology in grid connected Microgrid*. Paper presented at the 2021 Third International Conference on Transportation and Smart Technologies (TST).
- Bahrami, S., & Parniani, M. (2014). Game Theoretic Based Charging Strategy for Plug-in Hybrid Electric Vehicles. *IEEE Transactions on Smart Grid*, 5(5), 2368-2375. doi:10.1109/TSG.2014.2317523
- Bathurst, G., Hwang, G., & Tejwani, L. (2015, 10-12 Feb. 2015). *MVDC - The New Technology for Distribution Networks*. Paper presented at the 11th IET International Conference on AC and DC Power Transmission.
- Bian, C., Li, H., Wallin, F., Avelin, A., Lin, L., & Yu, Z. (2019). Finding the optimal location for public charging stations – a GIS-based MILP approach. *Energy Procedia*, 158, 6582-6588. doi:10.1016/j.egypro.2019.01.071
- Binetti, G., Davoudi, A., Naso, D., Turchiano, B., & Lewis, F. L. (2015). Scalable Real-Time Electric Vehicles Charging With Discrete Charging Rates. *IEEE Transactions on Smart Grid*, 6(5), 2211-2220. doi:10.1109/TSG.2015.2396772
- Botsford, C., & Szczepanek, A. (2009). Fast Charging vs. Slow Charging: Pros and cons for the New Age of Electric Vehicles.
- Byeon, G., Yoon, T., Oh, S., & Jang, G. (2013). Energy Management Strategy of the DC Distribution System in Buildings Using the EV Service Model. *IEEE Transactions on Power Electronics*, 28(4), 1544-1554. doi:10.1109/TPEL.2012.2210911
- Cao, Y., Ahmad, N., Kaiwartya, O., Puturs, G., & Khalid, M. (2018). Intelligent Transportation Systems Enabled ICT Framework for Electric Vehicle Charging in Smart City. In M. Maheswaran & E. Badidi (Eds.), *Handbook of Smart Cities: Software Services and Cyber Infrastructure* (pp. 311-330). Cham: Springer International Publishing.

- Cao, Y., Tang, S., Li, C., Zhang, P., Tan, Y., Zhang, Z., & Li, J. (2012). An Optimized EV Charging Model Considering TOU Price and SOC Curve. *IEEE Transactions on Smart Grid*, 3(1), 388-393. doi:10.1109/TSG.2011.2159630
- Chang, M., Bae, S., Yoon, G. g., Park, S. h., & Choy, Y. (2019, 18-21 Feb. 2019). *Impact of Electric Vehicle Charging Demand on a Jeju Island Radial Distribution Network*. Paper presented at the 2019 IEEE Power & Energy Society Innovative Smart Grid Technologies Conference (ISGT).
- Clement-Nyngs, K., Haesen, E., & Driesen, J. (2010). The Impact of Charging Plug-In Hybrid Electric Vehicles on a Residential Distribution Grid. *IEEE Transactions on Power Systems*, 25(1), 371-380. doi:10.1109/TPWRS.2009.2036481
- Cutsem, T. V. (2000). Voltage instability: phenomena, countermeasures, and analysis methods. *Proceedings of the IEEE*, 88(2), 208-227. doi:10.1109/5.823999
- Deilami, S., Masoum, A., Moses, P., & Masoum, M. (2011). Real-Time Coordination of Plug-In Electric Vehicle Charging in Smart Grids to Minimize Power Losses and Improve Voltage Profile. *Smart Grid, IEEE Transactions on*, 2, 456-467. doi:10.1109/TSG.2011.2159816
- Deilami, S., Moses, P., Masoum, M. A. S., & Abu-Siada, A. (2013). Smart load management of plug-in electric vehicles in distribution and residential networks with charging stations for peak shaving and loss minimisation considering voltage regulation. *IET Gener. Transm. Distrib*, 7, 866-873.
- Deng, C., Liang, N., Tan, J., & Wang, G. (2016). Multi-Objective Scheduling of Electric Vehicles in Smart Distribution Network. *Sustainability*, 8(12). doi:10.3390/su8121234
- Dharmakeerthi, C., Mithulananthan, N., & Saha, T. (2014). Impact of electric vehicle fast charging on power system voltage stability. *International Journal of Electrical Power & Energy Systems*, 57, 241-249.
- Einaddin, A. H., & Yazdankhah, A. S. (2020). A novel approach for multi-objective optimal scheduling of large-scale EV fleets in a smart distribution grid considering realistic and stochastic modeling framework. *International Journal of Electrical Power & Energy Systems*, 117, 105617. doi:https://doi.org/10.1016/j.ijepes.2019.105617

- Emadi, A., Rajashekara, K., Williamson, S. S., & Lukic, S. M. (2005). Topological overview of hybrid electric and fuel cell vehicular power system architectures and configurations. *IEEE Transactions on Vehicular Technology*, *54*(3), 763-770. doi:10.1109/TVT.2005.847445
- Farahani, H. F. (2017). Improving voltage unbalance of low-voltage distribution networks using plug-in electric vehicles. *Journal of Cleaner Production*, *148*, 336-346. doi:https://doi.org/10.1016/j.jclepro.2017.01.178
- García-Villalobos, J., Zamora, I., San Martín, J. I., Asensio, F. J., & Aperribay, V. (2014). Plug-in electric vehicles in electric distribution networks: A review of smart charging approaches. *Renewable and Sustainable Energy Reviews*, *38*, 717-731. doi:https://doi.org/10.1016/j.rser.2014.07.040
- Giannakis, A., & Pefitsis, D. (2018, 17-21 Sept. 2018). *MVDC Distribution Grids and Potential Applications: Future Trends and Protection Challenges*. Paper presented at the 2018 20th European Conference on Power Electronics and Applications (EPE'18 ECCE Europe).
- Gillera, M., Bonnema, E., Woods, J., Mishra, P., Doebber, I., Hunter, C., . . . Mann, M. (2021). Impact of electric vehicle charging on the power demand of retail buildings. *Advances in Applied Energy*, *4*, 100062. doi:https://doi.org/10.1016/j.adapen.2021.100062
- Habib, S., Khan, M. M., Abbas, F., & Tang, H. (2018). Assessment of electric vehicles concerning impacts, charging infrastructure with unidirectional and bidirectional chargers, and power flow comparisons. *International Journal of Energy Research*, *42*(11), 3416-3441. doi:https://doi.org/10.1002/er.4033
- Hosseini, S. S., Badri, A., & Parvania, M. (2012, 9-12 Sept. 2012). *The plug-in electric vehicles for power system applications: The vehicle to grid (V2G) concept*. Paper presented at the 2012 IEEE International Energy Conference and Exhibition (ENERGYCON).
- Hrishikesan, V. M., Das, D., Kumar, C., Gooi, H. B., Mekhilef, S., & Guo, X. (2021). Increasing Voltage Support Using Smart Power Converter Based Energy Storage System and Load Control. *IEEE Transactions on Industrial Electronics*, *68*(12), 12364-12374. doi:10.1109/TIE.2020.3042165

- Jang, B., Hejazi, A., Rad, R. E., Qaragoz, Y. M., Ali, I., Pu, Y., . . . Lee, K. Y. (2021). A 15-W Triple-Mode Wireless Power Transmitting Unit With High System Efficiency Using Integrated Power Amplifier and DC–DC Converter. *IEEE Transactions on Industrial Electronics*, *68*(10), 9574-9585. doi:10.1109/TIE.2020.3026290
- Jhunjhunwala, A., Lolla, A., & Kaur, P. (2016). Solar-dc Microgrid for Indian Homes: A Transforming Power Scenario. *IEEE Electrification Magazine*, *4*(2), 10-19. doi:10.1109/MELE.2016.2543950
- Jin, C., Tang, J., & Ghosh, P. (2013). Optimizing Electric Vehicle Charging: A Customer's Perspective. *IEEE Transactions on Vehicular Technology*, *62*(7), 2919-2927. doi:10.1109/TVT.2013.2251023
- Jovcic, D., Taherbaneh, M., Taisne, J. P., & Nguéfeu, S. (2015). Offshore DC Grids as an Interconnection of Radial Systems: Protection and Control Aspects. *IEEE Transactions on Smart Grid*, *6*(2), 903-910. doi:10.1109/TSG.2014.2365542
- Juanuwattanakul, P., & Masoum, M. A. S. (2011, 13-16 Nov. 2011). *Identification of the weakest buses in unbalanced multiphase smart grids with Plug-in Electric Vehicle charging stations*. Paper presented at the 2011 IEEE PES Innovative Smart Grid Technologies.
- Kakigano, H., Miura, Y., Ise, T., & Uchida, R. (2007, 2-5 April 2007). *DC Voltage Control of the DC Micro-grid for Super High Quality Distribution*. Paper presented at the 2007 Power Conversion Conference - Nagoya.
- Karppanen, J., Kaipia, T., Nuutinen, P., Lana, A., Peltoniemi, P., Pinomaa, A., . . . Kim, J. (2015, 10-12 Feb. 2015). *Effect of Voltage Level Selection on Earthing and Protection of LVDC Distribution Systems*. Paper presented at the 11th IET International Conference on AC and DC Power Transmission.
- Khalid, M. R., Alam, M. S., Sarwar, A., & Jamil Asghar, M. S. (2019). A Comprehensive review on electric vehicles charging infrastructures and their impacts on power-quality of the utility grid. *eTransportation*, *1*, 100006. doi:https://doi.org/10.1016/j.etrans.2019.100006
- Kong, P. Y., & Karagiannidis, G. K. (2016). Charging Schemes for Plug-In Hybrid Electric Vehicles in Smart Grid: A Survey. *IEEE Access*, *4*, 6846-6875. doi:10.1109/ACCESS.2016.2614689

- Kothari, D. P. (2011). *Modern Power System Analysis* [1 online resource]. Retrieved from <http://www.mylibrary.com?id=343740>
- Kumar, D., Zare, F., & Ghosh, A. (2017). DC Microgrid Technology: System Architectures, AC Grid Interfaces, Grounding Schemes, Power Quality, Communication Networks, Applications, and Standardizations Aspects. *IEEE Access*, 5, 12230-12256. doi:10.1109/ACCESS.2017.2705914
- KUMAR, L., SHARMA, D., & GOEL, S. AN EFFICIENT LOAD FLOW SOLUTION AND VSI ANALYSIS FOR RADIAL DISTRIBUTION SYSTEM.
- Kumar, M., Panda, K. P., Naayagi, R. T., Thakur, R., & Panda, G. (2023). Comprehensive Review of Electric Vehicle Technology and Its Impacts: Detailed Investigation of Charging Infrastructure, Power Management, and Control Techniques. *Applied Sciences*, 13(15). doi:10.3390/app13158919
- Kundur, P., Paserba, J., Ajarapu, V., Andersson, G., Bose, A., Canizares, C., . . . Vittal, V. (2004). Definition and classification of power system stability IEEE/CIGRE joint task force on stability terms and definitions. *IEEE Transactions on Power Systems*, 19(3), 1387-1401. doi:10.1109/TPWRS.2004.825981
- Latinopoulos, C., Sivakumar, A., & Polak, J. W. (2017). Response of electric vehicle drivers to dynamic pricing of parking and charging services: Risky choice in early reservations. *Transportation Research Part C: Emerging Technologies*, 80, 175-189. doi:<https://doi.org/10.1016/j.trc.2017.04.008>
- Lee, S.-J., Oh, Y.-S., Sim, B.-S., Kim, M.-S., & Kim, C.-H. (2017). Analysis of peak shaving effect of demand power using Vehicle to Grid system in distribution system. *Journal of International Council on Electrical Engineering*, 7(1), 198-204. doi:10.1080/22348972.2017.1324275
- Li, S., & Mi, C. C. (2015). Wireless Power Transfer for Electric Vehicle Applications. *IEEE Journal of Emerging and Selected Topics in Power Electronics*, 3(1), 4-17. doi:10.1109/JESTPE.2014.2319453
- Liu, L., Xie, F., & Huang, Z. (2020). Multi-Objective Coordinated Optimal Allocation of DG and EVCSs Based on the V2G Mode. *Processes*, 9, 18. doi:10.3390/pr9010018

- Lokay, H. E., & Burtnyk, V. (1968). Application of Underfrequency Relays for Automatic Load Shedding. *IEEE Transactions on Power Apparatus and Systems, PAS-87*(3), 776-783. doi:10.1109/TPAS.1968.292193
- Ma, Z., Li, Y., Sun, Y., & Sun, K. (2023). Low Voltage Direct Current Supply and Utilization System: Definition, Key Technologies and Development. *CSEE Journal of Power and Energy Systems, 9*(1), 331-350. doi:10.17775/CSEEJPES.2022.02130
- Martinenas, S., Pedersen, A. B., Marinelli, M., Andersen, P. B., & Trreholt, C. (2014, 17-19 Dec. 2014). *Electric vehicle smart charging using dynamic price signal*. Paper presented at the 2014 IEEE International Electric Vehicle Conference (IEVC).
- Masoum, M. A. S., Moses, P. S., & Smedley, K. M. (2011, 17-19 Jan. 2011). *Distribution transformer losses and performance in smart grids with residential Plug-In Electric Vehicles*. Paper presented at the ISGT 2011.
- Misra, S., Bera, S., & Ojha, T. (2015). D2P: Distributed Dynamic Pricing Policy in Smart Grid for PHEVs Management. *IEEE Transactions on Parallel and Distributed Systems, 26*(3), 702-712. doi:10.1109/TPDS.2014.2315195
- Mohsenian-Rad, A. H., & Leon-Garcia, A. (2010). Optimal Residential Load Control With Price Prediction in Real-Time Electricity Pricing Environments. *IEEE Transactions on Smart Grid, 1*(2), 120-133. doi:10.1109/TSG.2010.2055903
- Moon, S.-K., & Kim, J.-O. (2017). Balanced charging strategies for electric vehicles on power systems. *Applied Energy, 189*, 44-54. doi:https://doi.org/10.1016/j.apenergy.2016.12.025
- Morais, H., Sousa, T., Vale, Z., & Faria, P. (2014). Evaluation of the electric vehicle impact in the power demand curve in a smart grid environment. *Energy Conversion and Management, 82*, 268-282. doi:https://doi.org/10.1016/j.enconman.2014.03.032
- Morris, B., Federica, F., & Dario, Z. (2018). DC Railway Electrification Systems. In *Electrical Railway Transportation Systems* (pp. 99-176): IEEE.
- Musa, A., Rehan, S., Sabug, L., Ponci, F., & Monti, A. (2017, 26-29 Sept. 2017). *Modeling and design of hybrid distribution network: Operational and technical features*. Paper presented at the 2017 IEEE PES Innovative Smart Grid Technologies Conference Europe (ISGT-Europe).



- Musavi, F., & Eberle, W. (2014). Overview of wireless power transfer technologies for electric vehicle battery charging. *IET Power Electronics*, 7(1), 60-66. doi:<https://doi.org/10.1049/iet-pel.2013.0047>
- Muthukumar, M., Rengarajan, N., Velliyangiri, B., Omprakas, M. A., Rohit, C. B., & Kartheek Raja, U. (2021). The development of fuel cell electric vehicles – A review. *Materials Today: Proceedings*, 45, 1181-1187. doi:<https://doi.org/10.1016/j.matpr.2020.03.679>
- Nicoletti, L., Mayer, S., Brönnner, M., Schockenhoff, F., & Lienkamp, M. (2020). Design Parameters for the Early Development Phase of Battery Electric Vehicles. *World Electric Vehicle Journal*, 11(3). doi:10.3390/wevj11030047
- Nimalsiri, N. I., Mediwaththe, C. P., Ratnam, E. L., Shaw, M., Smith, D. B., & Halgamuge, S. K. (2020). A Survey of Algorithms for Distributed Charging Control of Electric Vehicles in Smart Grid. *IEEE Transactions on Intelligent Transportation Systems*, 21(11), 4497-4515. doi:10.1109/TITS.2019.2943620
- Pillai, J. R., & Bak-Jensen, B. (2010, 1-3 Sept. 2010). *Impacts of electric vehicle loads on power distribution systems*. Paper presented at the 2010 IEEE Vehicle Power and Propulsion Conference.
- Pinto, R. T., Rodrigues, S., Bauer, P., & Pierik, J. (2013, 3-6 June 2013). *Operation and control of a multi-terminal DC network*. Paper presented at the 2013 IEEE ECCE Asia Downunder.
- Prakash, K., Lallu, A., Islam, F. R., & Mamun, K. A. (2016, 5-6 Dec. 2016). *Review of Power System Distribution Network Architecture*. Paper presented at the 2016 3rd Asia-Pacific World Congress on Computer Science and Engineering (APWC on CSE).
- Rabiee, A., Sadeghi, M., Aghaei, J., & Heidari, A. (2016). Optimal operation of microgrids through simultaneous scheduling of electrical vehicles and responsive loads considering wind and PV units uncertainties. *Renewable and Sustainable Energy Reviews*, 57, 721-739. doi:<https://doi.org/10.1016/j.rser.2015.12.041>
- Rahman, M. M., Barua, S., Zohora, S. T., Hasan, K., & Aziz, T. (2013, 8-11 Dec. 2013). *Voltage sensitivity based site selection for PHEV charging station in commercial distribution system*. Paper presented at the 2013 IEEE PES Asia-Pacific Power and Energy Engineering Conference (APPEEC).

- Ryndzionek, R., & Sienkiewicz, Ł. (2020). Evolution of the HVDC Link Connecting Offshore Wind Farms to Onshore Power Systems. *Energies*, *13*(8). doi:10.3390/en13081914
- S, S. M., Titus, F., Thanikanti, S. B., M, S. S., Deb, S., & Kumar, N. M. (2022). Charge Scheduling Optimization of Plug-In Electric Vehicle in a PV Powered Grid-Connected Charging Station Based on Day-Ahead Solar Energy Forecasting in Australia. *Sustainability*, *14*(6). doi:10.3390/su14063498
- Saldaña, G., San Martin, J. I., Zamora, I., Asensio, F. J., & Oñederra, O. (2019). Electric Vehicle into the Grid: Charging Methodologies Aimed at Providing Ancillary Services Considering Battery Degradation. *Energies*, *12*(12). doi:10.3390/en12122443
- Sanguesa, J. A., Torres-Sanz, V., Garrido, P., Martinez, F. J., & Marquez-Barja, J. M. (2021). A Review on Electric Vehicles: Technologies and Challenges. *Smart Cities*, *4*(1), 372-404. doi:10.3390/smartcities4010022
- Sarker, M. R., Pandžić, H., & Ortega-Vazquez, M. A. (2013, 2-6 Dec. 2013). *Electric vehicle battery swapping station: Business case and optimization model*. Paper presented at the 2013 International Conference on Connected Vehicles and Expo (ICCVE).
- Sarker, M. R., Pandžić, H., & Ortega-Vazquez, M. A. (2015). Optimal Operation and Services Scheduling for an Electric Vehicle Battery Swapping Station. *IEEE Transactions on Power Systems*, *30*(2), 901-910. doi:10.1109/TPWRS.2014.2331560
- Simiyu, P., Xin, A., Wang, K., Adwek, G., & Salman, S. (2020). Multiterminal Medium Voltage DC Distribution Network Hierarchical Control. *Electronics*, *9*(3). doi:10.3390/electronics9030506
- Singh, B., Singh, B. N., Chandra, A., Al-Haddad, K., Pandey, A., & Kothari, D. P. (2003). A review of single-phase improved power quality AC-DC converters. *IEEE Transactions on Industrial Electronics*, *50*(5), 962-981. doi:10.1109/TIE.2003.817609
- Singh, B., Singh, B. N., Chandra, A., Al-Haddad, K., Pandey, A., & Kothari, D. P. (2004). A review of three-phase improved power quality AC-DC converters. *IEEE*

- Transactions on Industrial Electronics*, 51(3), 641-660.  
doi:10.1109/TIE.2004.825341
- Singh, K. V., Bansal, H. O., & Singh, D. (2019). A comprehensive review on hybrid electric vehicles: architectures and components. *Journal of Modern Transportation*, 27(2), 77-107. doi:10.1007/s40534-019-0184-3
- Soman, R., Steurer, M. M., Toshon, T. A., Faruque, M. O., & Cuzner, R. M. (2017). Size and Weight Computation of MVDC Power Equipment in Architectures Developed Using the Smart Ship Systems Design Environment. *IEEE Journal of Emerging and Selected Topics in Power Electronics*, 5(1), 40-50. doi:10.1109/JESTPE.2016.2625030
- Sortomme, E., Hindi, M. M., MacPherson, S. D. J., & Venkata, S. S. (2011). Coordinated Charging of Plug-In Hybrid Electric Vehicles to Minimize Distribution System Losses. *IEEE Transactions on Smart Grid*, 2(1), 198-205. doi:10.1109/TSG.2010.2090913
- Stieneker, M., & Doncker, R. W. D. (2016, 27-30 June 2016). *Medium-voltage DC distribution grids in urban areas*. Paper presented at the 2016 IEEE 7th International Symposium on Power Electronics for Distributed Generation Systems (PEDG).
- Tran, D.-D., Vafaeipour, M., El Baghdadi, M., Barrero, R., Van Mierlo, J., & Hegazy, O. (2020). Thorough state-of-the-art analysis of electric and hybrid vehicle powertrains: Topologies and integrated energy management strategies. *Renewable and Sustainable Energy Reviews*, 119, 109596. doi:https://doi.org/10.1016/j.rser.2019.109596
- Un-Noor, F., Padmanaban, S., Mihet-Popa, L., Mollah, M. N., & Hossain, E. (2017). A Comprehensive Study of Key Electric Vehicle (EV) Components, Technologies, Challenges, Impacts, and Future Direction of Development. *Energies*, 10(8). doi:10.3390/en10081217
- Verzijlbergh, R. A., Grond, M. O. W., Lukszo, Z., Slootweg, J. G., & Ilic, M. D. (2012). Network Impacts and Cost Savings of Controlled EV Charging. *IEEE Transactions on Smart Grid*, 3(3), 1203-1212. doi:10.1109/TSG.2012.2190307

- Wang, F., Wang, L., Zhang, X., Wang, J., Li, S., & Liu, Y. (2021, 22-24 Jan. 2021). *Voltage Level Study for DC Distribution Grid Based on Comprehensive Evaluation*. Paper presented at the 2021 IEEE International Conference on Power Electronics, Computer Applications (ICPECA).
- Wang, X., He, H., Sun, F., Sun, X., & Tang, H. (2013). Comparative Study on Different Energy Management Strategies for Plug-In Hybrid Electric Vehicles. *Energies*, 6(11), 5656-5675. doi:10.3390/en6115656
- Wang, Z., & Paranjape, R. (2017). Optimal Residential Demand Response for Multiple Heterogeneous Homes With Real-Time Price Prediction in a Multiagent Framework. *IEEE Transactions on Smart Grid*, 8(3), 1173-1184. doi:10.1109/TSG.2015.2479557
- Wang, Z., Wei, X., & Dai, H. (2016). Design and Control of a 3 kW Wireless Power Transfer System for Electric Vehicles. *Energies*, 9(1). doi:10.3390/en9010010
- Yang, M., Xie, D., Zhu, H., & Lou, Y. (2015, 10-12 Feb. 2015). *Architectures and Control for Multi-terminal DC (MTDC) Distribution Network-A Review*. Paper presented at the 11th IET International Conference on AC and DC Power Transmission.
- Yang, Y., El Baghdadi, M., Lan, Y., Benomar, Y., Van Mierlo, J., & Hegazy, O. (2018). Design Methodology, Modeling, and Comparative Study of Wireless Power Transfer Systems for Electric Vehicles. *Energies*, 11(7). doi:10.3390/en11071716
- Yilmaz, M., & Krein, P. T. (2012, 4-8 March 2012). *Review of charging power levels and infrastructure for plug-in electric and hybrid vehicles*. Paper presented at the 2012 IEEE International Electric Vehicle Conference.
- Yoldaş, Y., Önen, A., Muyeen, S. M., Vasilakos, A. V., & Alan, İ. (2017). Enhancing smart grid with microgrids: Challenges and opportunities. *Renewable and Sustainable Energy Reviews*, 72, 205-214. doi:https://doi.org/10.1016/j.rser.2017.01.064
- Yu, Y., Nduka, O. S., & Pal, B. C. (2020). Smart Control of an Electric Vehicle for Ancillary Service in DC Microgrid. *IEEE Access*, 8, 197222-197235. doi:10.1109/ACCESS.2020.3034496
- Zhang, L., Tang, W., Liang, J., Li, G., Cai, Y., & Yan, T. (2016, 28-29 May 2016). *A medium voltage hybrid AC/DC distribution network and its economic evaluation*. Paper

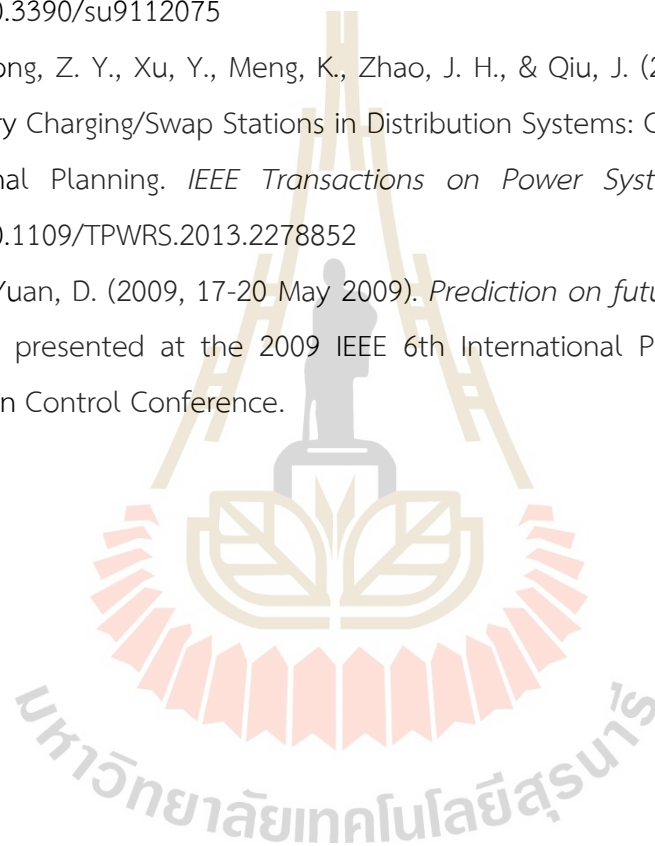
presented at the 12th IET International Conference on AC and DC Power Transmission (ACDC 2016).

Zhang, X., Liang, Y., & Liu, W. (2017). Pricing model for the charging of electric vehicles based on system dynamics in Beijing. *Energy*, 119, 218-234. doi:<https://doi.org/10.1016/j.energy.2016.12.057>

Zhang, X., Liang, Y., Zhang, Y., Bu, Y., & Zhang, H. (2017). Charge Pricing Optimization Model for Private Charging Piles in Beijing. *Sustainability*, 9(11). doi:10.3390/su9112075

Zheng, Y., Dong, Z. Y., Xu, Y., Meng, K., Zhao, J. H., & Qiu, J. (2014). Electric Vehicle Battery Charging/Swap Stations in Distribution Systems: Comparison Study and Optimal Planning. *IEEE Transactions on Power Systems*, 29(1), 221-229. doi:10.1109/TPWRS.2013.2278852

Zhou, Q., & Yuan, D. (2009, 17-20 May 2009). *Prediction on future DC power system*. Paper presented at the 2009 IEEE 6th International Power Electronics and Motion Control Conference.



## CHAPTER III

### METHODOLOGY

#### 3.1 Introduction

This section presents a calculation method of bipolar DC power flow, load balancing method and EV load demand evaluation to evaluate effect on unbalance load and EV charging demand on bipolar DC distribution grid via voltage profile, system power loss and VUF which the overall calculation program of bipolar DC distribution grid integrated with EV charging load demand is expressed in FIGURE 3.1.

The program comprises of two main components as follow: 1) EV load demand evaluation and 2) particle swarm optimization using the load-balancing approach with bipolar DC power flow calculation.

EV load demand evaluation uses a mean and standard deviation of survey EV's owner to evaluation probabilistic of plug-in time, daily travel distance and charging time to evaluate EV charging load profile at each bus. after that, the EV charging load and load profile at each bus was calculate voltage profile, power loss and VUF by using DC power flow calculation which connection type of load was solve by particle swarm optimization to find a optimal connection type of load. So, the detail of calculation method as proposed in next subsection.

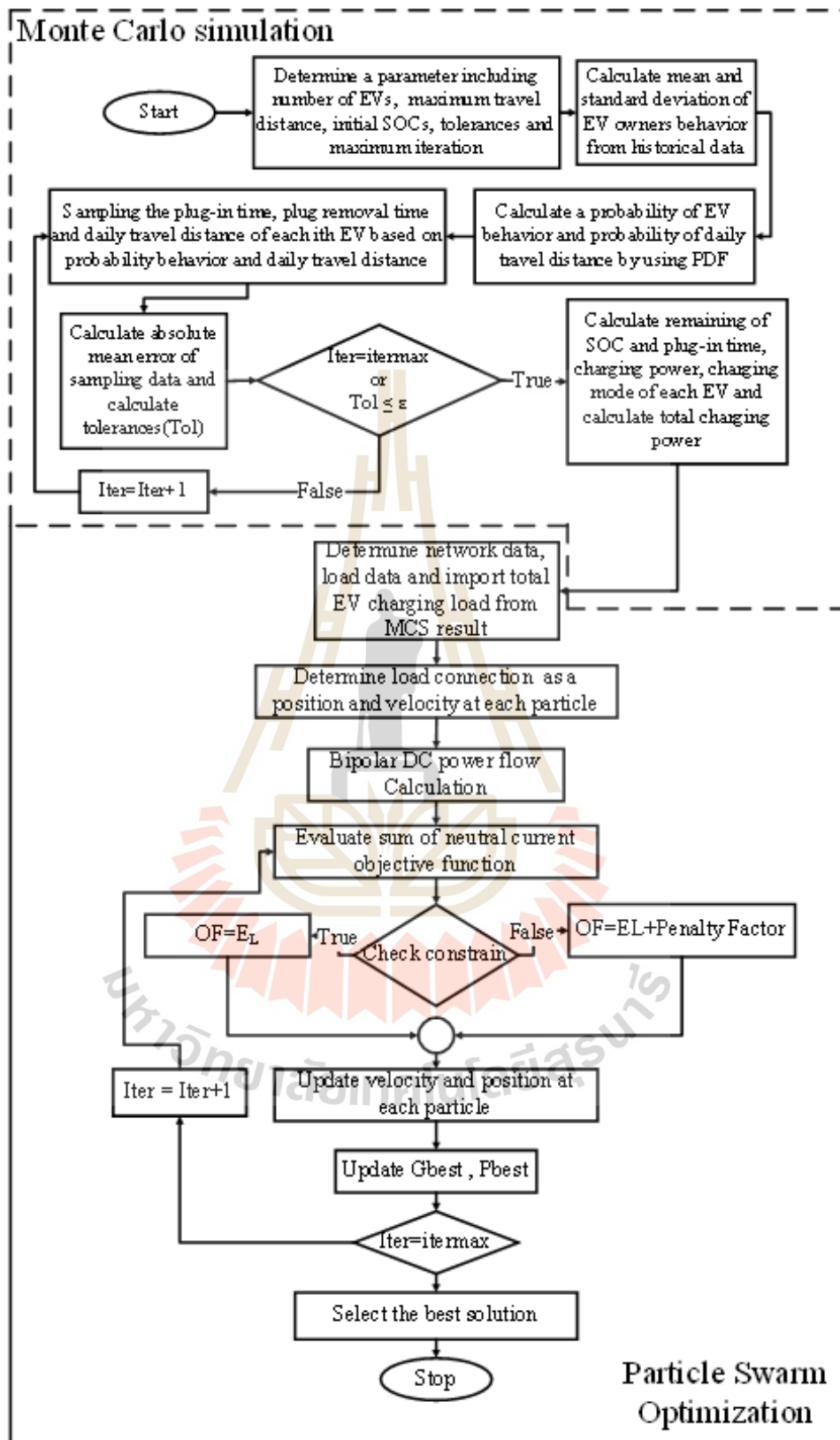


Figure 3.1 Overall calculation program

### 3.2 Bipolar DC Power flow Calculation with Gauss's iteration method

The Gauss iteration approach is employed in this subsection to solve the bipolar DC distribution system's bipolar DC power flow problem. An iterative approach for solving systems of linear equations is the Gauss Iteration method, often referred to as the Jacobi method. Equation 3.1 expresses the system of equations using this way.

$$Ax = b \quad 3.1$$

where 'A' is the coefficient matrix, 'x' is the vector of unknowns, and 'b' is the constant vector. The method involves rearranging the equation to isolate each unknown on the diagonal of the coefficient matrix and then iteratively updating the values of the unknowns until convergence

let's consider a 'n' linear equation system, Equation 3.1 can be represented as Equation 3.2 in matrix form and Equation 3.3 in general equation form.

$$[A]_{n \times n} [x]_{1 \times n} = [b]_{1 \times n} \quad 3.2$$

$$\left. \begin{aligned} A_{11}x_1 + A_{12}x_2 + \dots + A_{1n}x_n &= b_1 \\ A_{21}x_1 + A_{22}x_2 + \dots + A_{2n}x_n &= b_2 \\ \vdots & \\ A_{n1}x_1 + A_{n2}x_2 + \dots + A_{nn}x_n &= b_n \end{aligned} \right\} \quad 3.3$$

Which the iteration formula for the Gauss's iteration method is expressed in Equation 3.4

$$x_i^{(k+1)} = \frac{(b_i - \sum A_{ij} \times x_j^k)}{A_{ii}} \quad 3.4$$

Where  $i$  and  $j$  subscriptions are row and column of matrix A and B. in case of  $k$  is iteration index of iteration method.

So,  $x_i^{(k+1)}$  represents the updated value of the  $i$  of unknown vector at the  $(k+1)$  iteration.



$x_j^k$  represents the value of the  $j$  unknown vector at the  $k$  iteration.

$A_{ij}$  represents the elemental matrix of matrix A

$A_{ii}$  represents the diagonal element of matrix A for the  $i$  row.

To terminate a simulation iteration, The unknown vector of  $k$  iteration and  $k+1$  iteration have to convergence or have a tolerance of unknown vector less than determined tolerance which can be expressed in Equation 3.5

$$\varepsilon = x_i^{k+1} - x_i^k \quad 3.5$$

The procedure can be expressed into 3 steps as follow:

Firstly, determine an initial value of all unknown value  $x_i^{(0)}$  to calculate first iteration of  $n$  equation system. second, each  $x_i^{(k)}$  ( $i=1$  to  $n$ ) is used to calculate and updated value using Equation 3.4 third, repeat step 2 until tolerance of each  $x_i^{(k)}$  less than specified tolerance or reach maximum number of iterations. lastly, the final value of unknowns vector  $[x]$  are the solution of the system. which the procedure of Gauss's iteration is expressed in FIGURE 3.2

To solve the DC power flow problem by using Gauss's iteration. A bipolar DC distribution system have to change in form of linear equation that refers as Equation 3.2 The component of bipolar DC distribution system such as substation, transmission network and load as shown in FIGURE 3.2 have to change in form of voltage at each bus, network conductance and load demand current, respectively. in bipolar DC distribution system, A load in the system can be connected between positive pole and neutral pole (unipolar connection) and connected between positive pole and negative pole (bipolar connection) which present in FIGURE 3.4 – 3.5

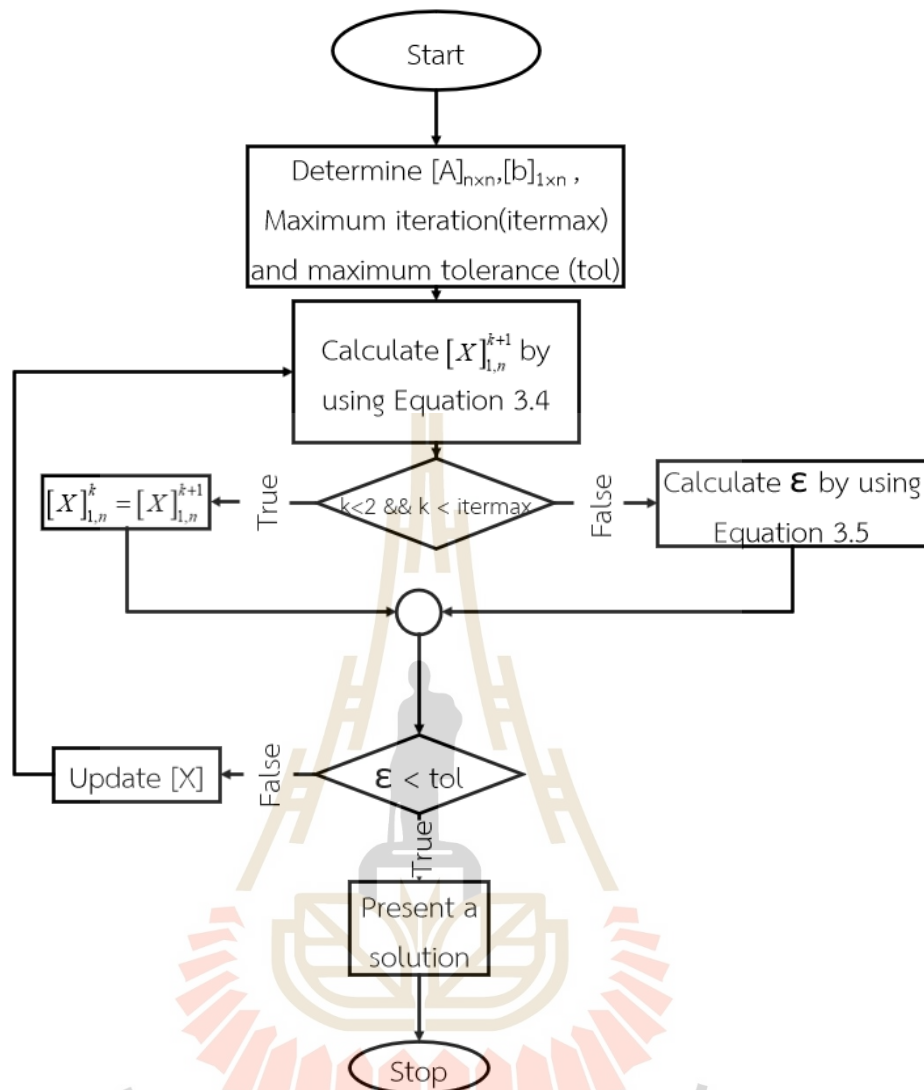


Figure 3.2 Gauss's iteration procedure

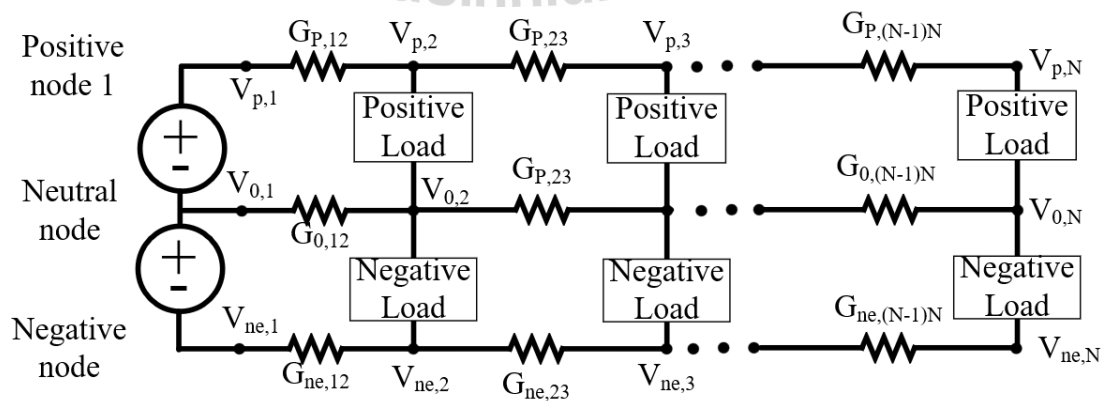


Figure 3.3 DC power system component

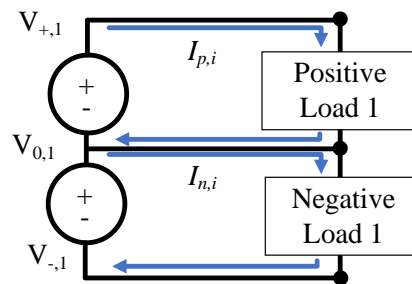


Figure 3.4 Unipolar load connection

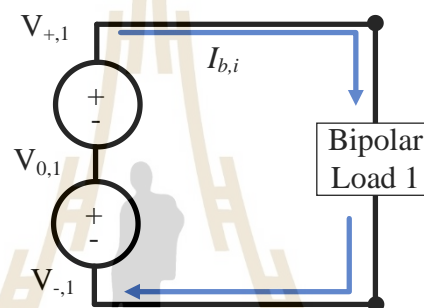


Figure 3.5 Bipolar load connection

FIGURE 3.3 illustrates the bipolar DC power system's elements, including the transmission line, the DC substation, and the loads (positive load, negative load, and bipolar load). For the study of the DC load flow, the G-Matrix Method (GMM) is used in this paper. The network component consists of two different types of buses, known as source and load buses, to create a power flow model. The slack bus, or index '1', takes the role of a source bus, while the load bus starts at index '2' and finishes at index 'n'.  $G_{ij}$  contributes the conductance of each transmission line between buses, where the beginning and ending buses of conductance in  $[G]$  are designated by index 'i' to index 'j'. There are three wires in a bipolar DC network. As a result,  $[G]$  must contain  $G_{+,0/-}$ . This displays the positive, neutral, and negative cable conductance from bus i to bus j. The load current of each pole is denoted by  $I_{p/n/b}$ , and there are three voltages present at bus i: positive, neutral, and negative. Unipolar loads, such as  $I_p$  and  $I_n$ , draw current from either the positive or negative poles and return to the substation via the neutral pole.  $I_b$  is a bipolar load that uses the positive pole to draw power and uses

the negative pole to return to the substation. As a result, nodal analysis is used to construct the single line diagram, which depicts the link between unipolar and bipolar load current. FIGURES 3.4 and 3.5 depict the direction of loading currents.

Equations 3.6 to 3.7 may be used to calculate a load voltage drop by accounting for the voltage differential at the connecting pole.

$$V_{p,i} = V_{+,i} - V_{0,i} \quad 3.6$$

$$V_{ne,i} = V_{0,i} - V_{-,i} \quad 3.7$$

When referring to a positive pole or negative pole with a neutral pole, the values  $V_{p,i}$  and  $V_{n,i}$  indicate a positive and negative voltage drop at bus i. The voltage at each of bus i's poles is  $V_{+,i}$ ,  $V_{-,i}$ , and  $V_{0,i}$ , respectively. Consequently, when the positive and negative poles are indicated, the voltage drop of a unipolar load at bus i is represented by  $V_{+,i}$  and  $V_{-,i}$ , respectively.

To calculate load current demand at each pole, the voltage drop at each pole from Equation 3.6 and Equation 3.7 is used to calculate the current by Equation 3.8 and Equation 3.9, respectively.

$$I_{p,i} = \frac{P_{p,i}}{V_{p,i}} \quad 3.8$$

$$I_{ne,i} = \frac{P_{ne,i}}{V_{ne,i}} \quad 3.9$$

When  $I_{p,i}$  and  $I_{ne,i}$  are load current of positive and negative pole at each bus and  $P_{p,i}$  and  $P_{ne,i}$  are positive and negative load in an unipolar type.

According to FIGURE 3.4, in a bipolar load connection, the load is connected to both the positive and negative poles. As a result, the load's nominal voltage is 2VDC. Equation 3.10 allows the bipolar load voltage drop to be determined.

$$V_{b,i} = V_{+,i} - V_{-,i} \quad 3.10$$

When  $V_{b,i}$ ,  $V_{+,i}$  and  $V_{-,i}$  are voltage drop of bipolar load, positive and negative voltage at each pole, respectively. so, the bipolar load current can compute by using Equation 3.11

$$I_{b,i} = \frac{P_{b,i}}{V_{b,i}} \quad 3.11$$

Where  $I_{b,i}$ ,  $P_{b,i}$  and  $V_{b,i}$  are bipolar load current, bipolar power demand and bipolar voltage drop at bus  $i$ , respectively. the substation is assumed as a slack bus which have nominal voltage 1 p.u., 0 p.u. and -1 p.u. at positive bus, neutral bus and negative bus respectively. the transmission resistance are replaced by transmission conductance between bus. so, the power flow equation of DC distribution system can be expressed as Equation 3.12. from Equation 3.12 can be modeled in form of bipolar DC distribution system as shown in Equation 3.13

$$[\mathbf{I}] = [\mathbf{G}][\mathbf{V}] \quad 3.12$$

$$\begin{bmatrix} \mathbf{I}_p \\ \mathbf{I}_0 \\ \mathbf{I}_{ne} \end{bmatrix} = \begin{bmatrix} \mathbf{G}_p & 0 & 0 \\ 0 & \mathbf{G}_0 & 0 \\ 0 & 0 & \mathbf{G}_{ne} \end{bmatrix} \begin{bmatrix} \mathbf{V}_p \\ \mathbf{V}_0 \\ \mathbf{V}_{ne} \end{bmatrix} \quad 3.13$$

Where

$$\mathbf{V}_p = \begin{bmatrix} V_{p,1} & V_{p,2} & \cdots & V_{p,N} \end{bmatrix}^T \quad 3.14$$

$$\mathbf{V}_0 = \begin{bmatrix} V_{0,1} & V_{0,2} & \cdots & V_{0,N} \end{bmatrix}^T \quad 3.15$$

$$\mathbf{V}_{ne} = \begin{bmatrix} V_{ne,1} & V_{ne,2} & \cdots & V_{ne,N} \end{bmatrix}^T \quad 3.16$$

$$\mathbf{I}_p = \begin{bmatrix} I_{p,1} + I_{b,1} & I_{p,2} + I_{b,2} & \cdots & I_{p,N} + I_{b,N} \end{bmatrix}^T \quad 3.17$$

$$\mathbf{I}_0 = \begin{bmatrix} I_{0,1} & I_{0,2} & \cdots & I_{0,N} \end{bmatrix}^T \quad 3.18$$

$$\mathbf{I}_{ne} = \begin{bmatrix} I_{ne,1} + I_{b,1} & I_{ne,2} + I_{b,2} & \cdots & I_{ne,N} + I_{b,N} \end{bmatrix}^T \quad 3.19$$

$$\mathbf{G}_p = \begin{bmatrix} \sum_{i \leftrightarrow 1} G_{p,1i} & -G_{p,12} & \cdots & -G_{p,1N} \\ -G_{p,21} & \sum_{i \leftrightarrow 1} G_{p,2i} & -G_{p,23} & -G_{p,2N} \\ \vdots & \vdots & \ddots & \vdots \\ -G_{p,N1} & -G_{p,N2} & \cdots & \sum_{i \leftrightarrow 1} G_{p,NN} \end{bmatrix} \quad 3.20$$

$$\mathbf{G}_0 = \begin{bmatrix} \sum_{i \leftrightarrow 1} G_{0,1i} & -G_{0,12} & \cdots & -G_{0,1N} \\ -G_{0,21} & \sum_{i \leftrightarrow 1} G_{0,2i} & -G_{0,23} & -G_{0,2N} \\ \vdots & \vdots & \ddots & \vdots \\ -G_{0,N1} & -G_{0,N2} & \cdots & \sum_{i \leftrightarrow 1} G_{0,NN} \end{bmatrix} \quad 3.21$$

$$\mathbf{G}_{ne} = \begin{bmatrix} \sum_{i \leftrightarrow 1} G_{ne,1i} & -G_{ne,12} & \cdots & -G_{ne,1N} \\ -G_{ne,21} & \sum_{i \leftrightarrow 1} G_{ne,2i} & -G_{ne,23} & -G_{ne,2N} \\ \vdots & \vdots & \ddots & \vdots \\ -G_{ne,N1} & -G_{ne,N2} & \cdots & \sum_{i \leftrightarrow 1} G_{ne,NN} \end{bmatrix} \quad 3.22$$

When  $[G]$ ,  $[I]$  and  $[V]$  represent conductance matrix, current matrix and voltage matrix of bipolar DC distribution system, respectively. which Equation 12 can be modeled as a bipolar DC distribution system as shown in Equation 3.13 to calculate voltage profile and current flow at each bus by using Gauss's iteration method which the power flow calculation procedure is presented in FIGURE 3.6.

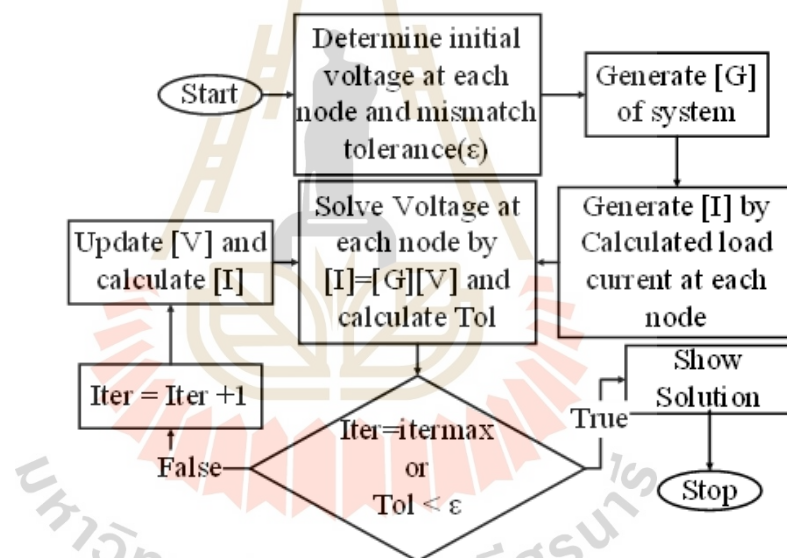


Figure 3.6 power flow calculation procedure

### 3.3 Particle Swarm Optimization based Load balancing method

An unbalance problem is differential of load demand at positive and negative bus which those load current returns to substation via neutral cable at each bus. normally, neutral current at balance situation must be equal zero due to positive current and negative current are equal and deduct at neutral bus as shown in FIGURE 3.7 (a)

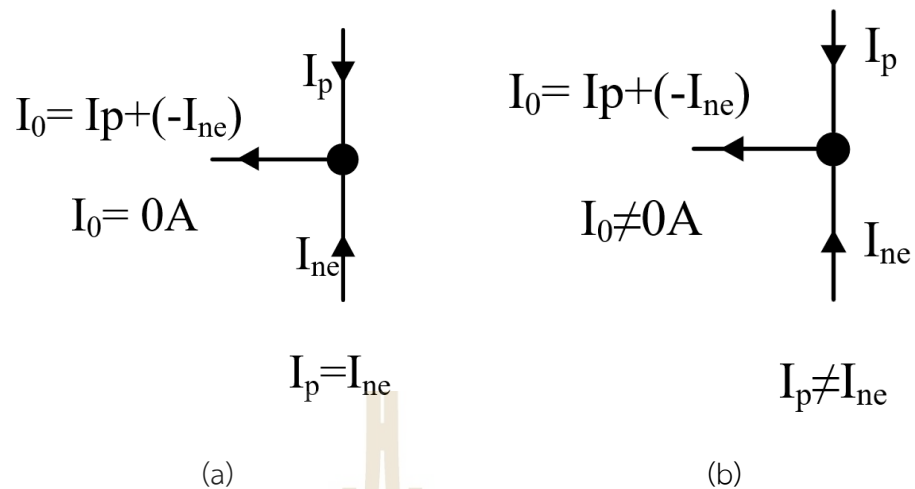


Figure 3.7 neutral current characteristic

In case of unbalance load, a positive and negative load current are not equal. when those current flow to neutral bus, the current magnitude cannot deduct to zero as shown in FIGURE 3.7 (b). So that can be led to current flow in neutral conductor and increase power loss at neutral bus, respectively. so, to reduce the unbalance problem the load balancing method is proposed which unbalance problem can be estimated by using voltage unbalance factor (VUF) as shown in Equation 3.23

$$\%VUF = \left( \frac{\frac{|V_{p,i}| - |V_{ne,i}|}{|V_{p,i}| + |V_{ne,i}|}}{2} \right) \times 100\% \quad 3.23$$

The concept of load balancing method is to adjust a connection type of load at each pole to reduce load demand difference between positive and negative pole by using static switch to reduce neutral current flow in the system. to evaluate an efficient of load balancing method on the system, the voltage unbalance factor and neutral power loss are used as a criteria index. An unbalanced loads in bipolar DC distribution system is not equal of positive and negative pole's load capacity which leads to increase voltage drop in the transmission line by line resistance. The unbalance problem can be increased neutral power loss on neutral wire due to neutral current flow when positive and negative load demand at each bus is not equal

(Sakulphaisan & Chayakulkheeree, 2022). Thus, as seen in FIGURE 4, the primary issue with bipolar DCDG is the load imbalance condition, which results from the load's ability to be attached to either the positive or negative pole. Generally speaking, unexpected homes' and EV charging loads are the root cause of load imbalance issues.(Sharma, Cañizares, & Bhattacharya, 2014). This issue causes the neutral wire's current flow to rise, which raises the system's total power loss. A voltage balancer, which regulates the DC/DC converter's voltage at the point of common coupling (PCC) to offset voltage loss at each bus, is one method of reducing voltage imbalance in LVDC. One alternate way to lessen load imbalance is to use an energy price to manage the load demand characteristic of a DC bipolar distribution grid and lessen the power differential between the poles. This is known as demand response or load balancing using electrical pricing.(Chiş, Rajasekharan, Lundén, & Koivunen, 2016) which the problem formulation of the method can be modeled as shown in Equation 3.24 to Equation 3.27 as follow

$$[P] = [P_{1,1}, P_{2,1}, P_{1,2}, P_{2,2}, P_{3,1}, P_{3,2}, \dots, P_{n,i}] \quad 3.24$$

$$x_i = \begin{cases} 1 & ; P_{p,i} = P_i \\ 2 & ; P_{ne,i} = P_i \end{cases} \quad 3.25$$

$$P_{p,i} = P_i \quad ; \quad x_i = 1 \quad 3.26$$

$$P_{ne,i} = P_i \quad ; \quad x_i = 2 \quad 3.27$$

In Equation 3.25,  $x_i$  presents a load connection type of  $[P]$  in Equation 3.24 at each bus which  $n$  subscription and  $i$  subscription of  $[P]$  present a number of load and bus location of load. In case of  $x_i = 1$  means, load at this bus have to connected to positive pole. In case of  $x_i = 2$ , load have to connected to negative pole as shown in Equation 3.26 to 3.27. after that, load demand that connected to each pole have to calculate load current by using Equation 3.6 to 3.11. lastly, calculate voltage profile by using Equation 3.13.

To search optimize load connection type for minimum power loss, the PSO was used. A particle of PSO is assumed as a load connection type at each bus ( $x_i$ ).in every iteration of PSO, a group of particles is used to determine a connection type at



each load in the system. after that, the power flow calculation was solved by Gauss's iteration method which the result of power flow comprises of voltage profile, power loss and VUF. In this study uses daily energy loss as an objective function as shown in Equation 3.28 and constrain that expressed in Equation 3.29 to Equation 3.31. then, the best result of objective function at each iteration of PSO is determined as Pbest and the best result of every iteration is determined as Gbest. Finally, the velocity and position of PSO was updated and calculate until last iteration. the PSO based load balancing method is expressed in FIGURE 3.8

$$\text{Minimize } E_L = \sum_{t=1}^{48} [P_{L,p}(t) + P_{L,0}(t) + P_{L,ne}(t)] \quad 3.28$$

When

$$P_{L,p} = \frac{\sum_{i=1}^{n-1} I_{p,(i,j+1)}^2}{G_{p(i,i+1)}} \quad 3.29$$

$$P_{L,0} = \frac{\sum_{i=1}^{n-1} I_{0,(i,i+1)}^2}{G_{0(i,i+1)}} \quad 3.30$$

$$P_{L,ne} = \frac{\sum_{i=1}^{n-1} I_{ne,(i,i+1)}^2}{G_{ne(i,i+1)}} \quad 3.31$$

Subject to constrain

$$V_{p \min,i} \leq V_{p,i} \leq V_{p \max,i} \quad 3.32$$

$$V_{0 \min,i} \leq V_{0,i} \leq V_{0 \max,i} \quad 3.33$$

$$V_{ne \min,i} \leq V_{ne,i} \leq V_{ne \max,i} \quad 3.34$$

$$\%VUF < \%VUF_{\max} \quad 3.35$$

Where subscript  $p$ ,  $0$  and  $n$  represent positive pole, negative pole, and neutral pole. To present an effect of total energy loss, the total energy loss has to compare

in form of percentage of total usage energy of simulation system which the usage energy can be calculated by using Equation 3.36

$$E_T = \sum_{t=1}^{48} \sum_{i=1}^n [P_{i,p}(t) + P_{i,ne}(t) + P_{i,bi}(t)] \quad 3.36$$

Where  $P_{i,p}$ ,  $P_{i,ne}$  and  $P_{i,bi}$  are positive negative and bipolar load demand.

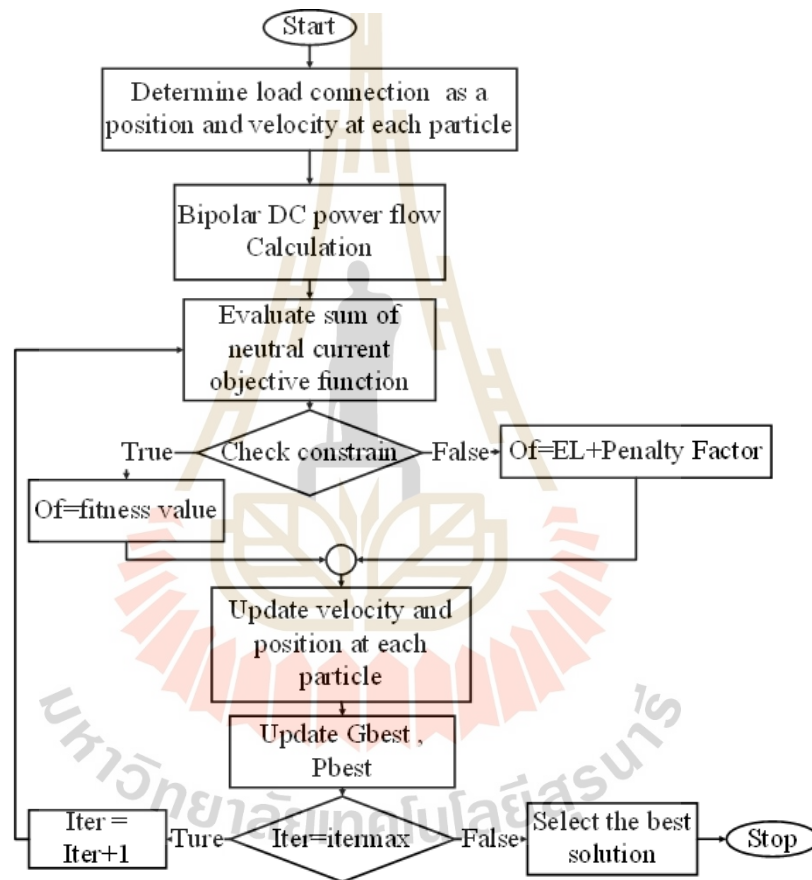


Figure 3.8 PSO based load balancing method

### Probabilistic EV Load Demand Evaluation based on Monte Carlo Simulation

The Monte-Carlo simulation-based multivariate probabilistic EV charging load is based on survey research on EV charging behavior. the Monte-Carlo simulation, as seen in Figure 3.9, to assess charging demand

The figure 3.8 shows a procedure to evaluate an EV charging demand which comprises of two parts as follow: Monte-Carlo simulation and charging demand calculation. The Monte-Carlo simulation used a survey data to evaluate daily mileage, charging mode, plug-in time, determine initial SOC and charging duration.

The EV charging behavior evaluation is a random variable including driving pattern and daily distance. A multivariate probabilistic model is used to evaluate charging demand based on survey and statistic data. Daily travel distance, plug-in duration, and the probability that an EV will recharge are uncertainty variables taken into account while predicting the need for 24-hour EV charging. An uncertainty of each EV are defined as a probability distribution function (PDF) which the PDF of daily distance can be defined into two type including log normal distribution type and normal distribution type, as respectively expressed by Equation 3.37 – 3.38

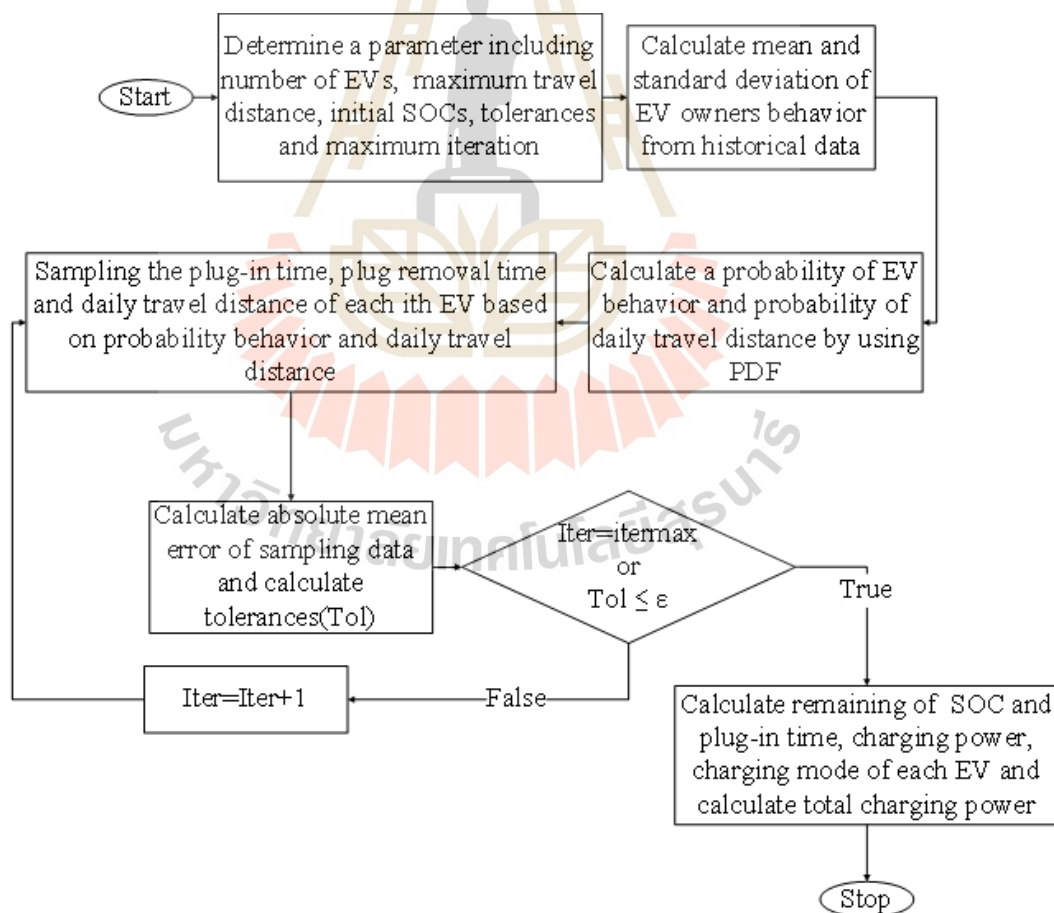


Figure 3.9 EV charging demand based on Monte Carlo

$$f_{1d}(x_{i,j}) = \frac{1}{x_{i,j} \sigma_{d,j} \sqrt{2\pi}} e^{\left( \frac{(\ln x_{i,j} - \mu_{d,j})^2}{2\sigma_{d,j}^2} \right)} \quad 3.37$$

$$f_{2d}(x_{i,j}) = \frac{1}{\sigma_{d,j} \sqrt{2\pi}} e^{-\frac{1}{2} \left( \frac{(x_{i,j} - \mu_{d,j})^2}{\sigma_{d,j}^2} \right)} \quad 3.38$$

Where  $x$  represent daily distance of  $i$ th EV ,  
 $j$  represent EV type  
 $\mu_d$  represent mean value  
 $\sigma_d$  represent standard deviation value

The state of charge (SOC) of EV battery remain from daily travel distance can be determined using Eq 3.39

$$SOC_{i,j} = 1 - \frac{d_{i,j}}{D_j \times \eta_1} \quad 3.39$$

Where  $d_{i,j}$  represent daily mileage distance of EV before charge  
 $D$  is Full mileage range  
 $\eta_1$  is efficiency of battery

Plug-in time is a duration of  $i$ th EV which connects to power grid and make a request to charge. The uncertainly of plug-in time of each EV are random variables in form of normal probability distribution function which expressed by Eq 3.40

$$f_t(tp_{i,j}) = \frac{1}{\sigma_{d,j} \sqrt{2\pi}} e^{-\frac{1}{2} \left( \frac{tp_{i,j} - \mu_{t,j}}{\sigma_{t,j}} \right)^2} \quad 3.40$$

Where  $tp_{i,j}$  is plug-in time of  $i$ th EV

$\mu_t$  represent mean value

$\sigma_t$  represent standard deviation value

The charging time of EV can be expressed by Eq 3.41 – 3.42

$$tp_{i,j} = (1 - SOC_{i,j}) \times \frac{Cap_{i,j}}{Pc_{i,j} \times \eta_2} \quad 3.41$$

$$td_{i,j} = tp_{i,j} + tc_{i,j} \quad 3.42$$

Where  $Cap_{i,j}$  is battery capacity

$Pc_{i,j}$  is charging power rate

$\eta_2$  is efficiency of charger

$tc_{i,j}$  is complete charging time

The all-EV charging demand is calculated by aggregator that observe all EV charging demand at each 24-h period as shown in Eq 3.43 – 3.44

$$P_{EV,i,j}(t) = \begin{cases} Pc_{i,j} & : t_p \leq t \leq t_d \\ 0 & : \text{other time} \end{cases} \quad 3.43$$

$$P_{EV,i}(t) = \sum_{i=j}^{N_j} \sum_{i=1}^{N_i} Pc_{i,j}(t) \quad 3.44$$

To add base load to summation of EV charging demand. The total system load profile at time step can be expressed Eq 3.45 based on connection type at each bus

$$P_T(t) = \begin{cases} P_{p,i}(t) + P_{EV,i}(t) & ; x_i = 1 \\ P_{ne,i}(t) + P_{EV,i}(t) & ; x_i = 2 \end{cases} \quad 3.45$$

Where  $P_{p,i}(t)$ ,  $P_{ne,i}(t)$  and  $x_i$  are load demand at positive pole, negative pole at time interval and load connection type, respectively.

### 3.4 Conclusion

This chapter presents a methodology of bipolar DC distribution system integrated with EV probabilistic simulation to solve an unbalance problem and daily energy load by using load balancing method with PSO. The methodology chapter proposed a bipolar DC power flow calculation which the calculation is solved by using Gauss's iteration method to calculate voltage profile, power loss and daily energy loss. A particle swarm optimization based on load balancing method is used to search optimal connection type of load at each bus with minimum daily energy loss as an objective function and probabilistic EV load demand evaluation based on Monte Carlo Simulation to evaluate EV load charging demand of EV based on mean and standard deviation of EV's owner behavior.

### 3.5 Reference

- Chiş, A., Rajasekharan, J., Lundén, J., & Koivunen, V. (2016, 29 Aug.-2 Sept. 2016). *Demand response for renewable energy integration and load balancing in smart grid communities*. Paper presented at the 2016 24th European Signal Processing Conference (EUSIPCO).
- Sakulphaisan, G., & Chayakulkheeree, K. (2022, 9-11 March 2022). *Improve a Voltage Unbalance Index of Bipolar DC Distribution Grid By using Particle Swarm Optimization Based on Load Balancing Method*. Paper presented at the 2022 International Electrical Engineering Congress (iEECON).
- Sharma, I., Cañizares, C., & Bhattacharya, K. (2014). Smart Charging of PEVs Penetrating Into Residential Distribution Systems. *IEEE Transactions on Smart Grid*, 5(3), 1196-1209. doi:10.1109/TSG.2014.2303173

## CHAPTER IV

### SIMULATION RESULT

#### 4.1 Introduction

This section presents an introductory analysis of a preliminary simulation pertaining to a bipolar DC distribution grid. The simulation encompasses various components, including the calculation of DC power flow, the implementation of a load balancing technique, and an evaluation of the load demand associated with electric vehicle charging. The purpose of conducting these simulations is to validate the system and establish it as a fundamental reference case. A visual representation of the proposed simulation cases can be observed in FIGURE 4.1.

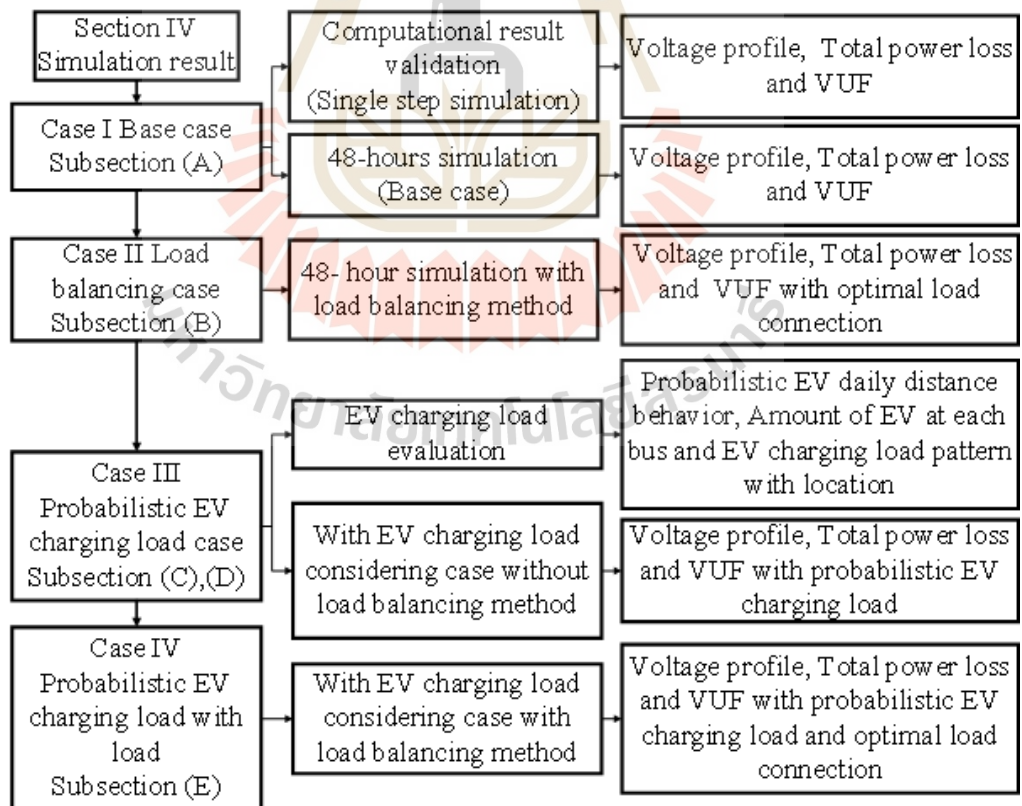


Figure 4.1 simulation case

Based on simulations, four different situations may be identified: Base case, Load balancing case, Probabilistic EV charging load case, and Probabilistic EV charging load with load balancing case. The simulation study comprises two primary categories: 1) a single step simulation and 2) a 48-hour simulation encompassing 192 time slots. In order to validate the computational outcomes, a single step simulation was employed to illustrate the impact of load on voltage profile and voltage unbalance factor (VUF), as well as to evaluate system power loss. Additionally, the effectiveness of the load balancing method was evaluated through a 48-hour simulation using Monte Carlo simulation (MCS), under both EV charging load and non-EV charging load conditions.

## 4.2 Validation Simulation

In this subsection, a simulation is conducted to verify the accuracy and reliability of the MATLAB source code employed in the referenced article, where the article utilizes the PSCAD program as a simulator. The simulation encompasses two distinct systems: a 4-bus bipolar DC distribution grid and a 21-bus bipolar DC distribution grid. The validation process involves the application of the GMM method, as described in Equations 3.3 to 3.17, with Gauss's iteration utilized to solve the bipolar DC power flow problem. The calculation flowchart for this process can be observed in FIGURE 3.5, as presented in Chapter 3.

The 4-bus bipolar DC distribution grid, as discussed in Chew (2019), employs the PSCAD program to effectively determine the voltage solution within the network. The simulation system consists of a balanced 4-bus bipolar DC distribution system with both unipolar and bipolar loads, where the existing infrastructure is an AC voltage system. The system is interconnected with a three-phase AC grid through an AC to DC converter, with the converter's DC voltage output set at  $\pm 18.7$  kV. Consequently, the DC voltage output of the converter is regarded as the slack bus. The simulation results, presented in TABLE 4.1 and Figure 4.3, are utilized to validate the accuracy of the source code and a numerical simulation result is presented in Appendix A.1 which a simulation system is illustrated in Figure 4.2 with a detail of system data.



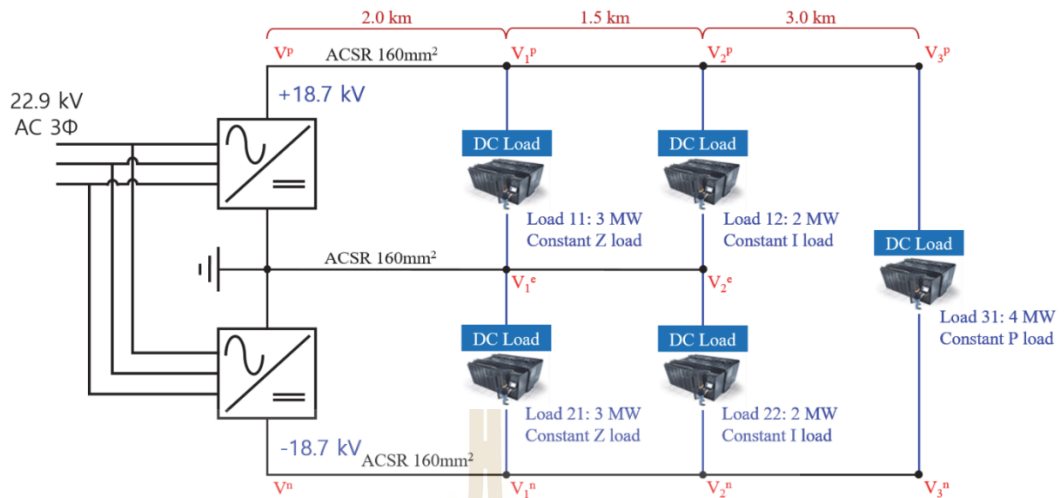


Figure 4.2 4-bus bipolar DC distribution grid

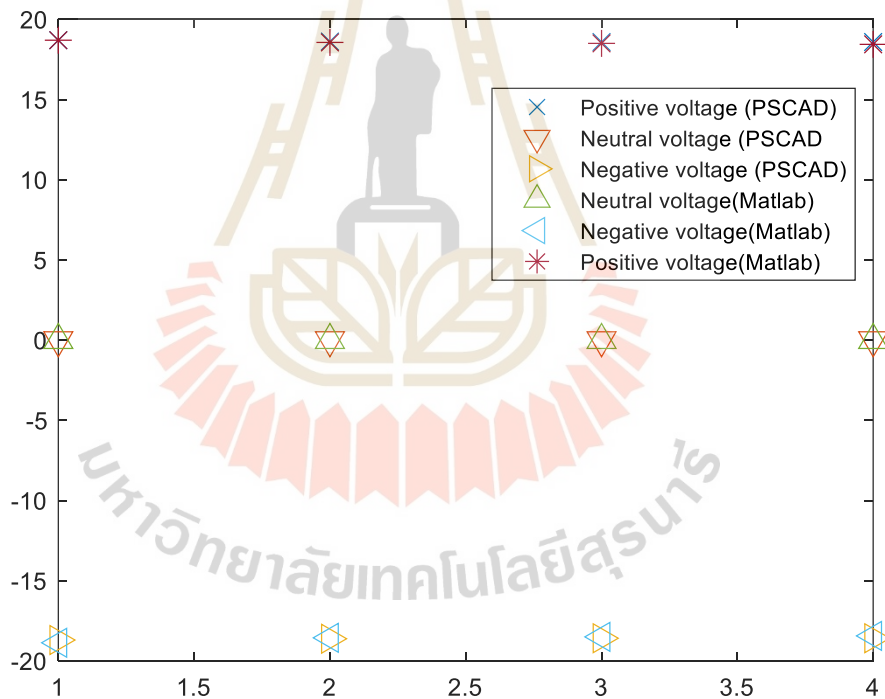


Figure 4.3 4-bus bipolar DC distribution grid validation result

Table 4.1 4-bus simulation result

|                                  |      |
|----------------------------------|------|
| The average simulation error (%) | 0.31 |
|----------------------------------|------|

A simulation result validation of source code with an average error of 0.31% is shown in TABLE 4.1. Line resistance and iteration technique, which are not precisely determined in the reference study article, may be the cause of mistake.

In case of 21 bipolar DC distribution system that presented in Figure 4.4, the system comprises of several type of load at each bus which the detail of load connection and system data was presented in Figure 4.5 and addition data was presented in Appendix A in TABLE A.2 to TABLE A.3. The simulation result was presented in TABLE 4.2 and addition simulation result is illustrated in TABLE A.4 in Appendix A.2 (Chew, Xu, & Wu, 2019)

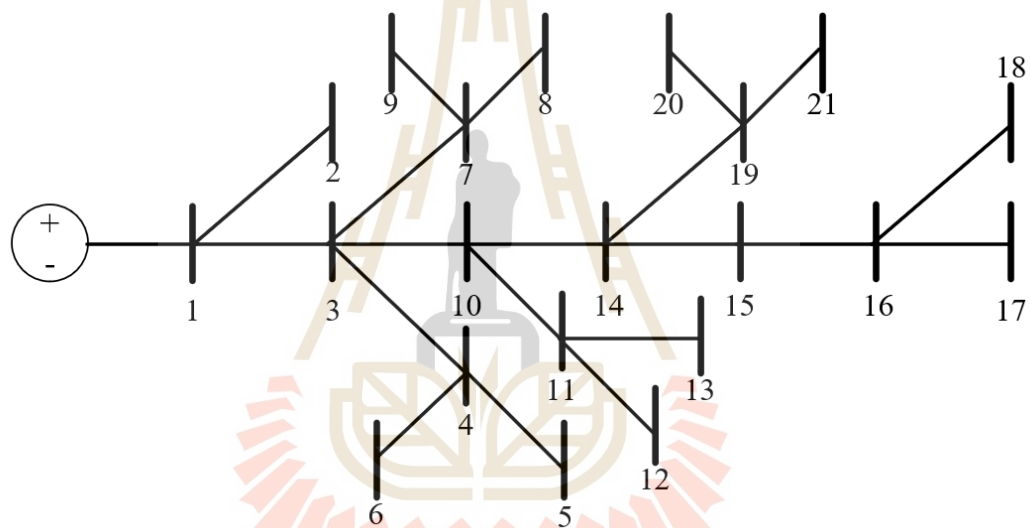


Figure 4.4 21-bus bipolar DC distribution grid

In TABLE 4.2 unbalance factor, are discussed. The positive VUF is caused by each bus's negative pole having a larger load than the positive pole. On the other side, the positive pole load is greater than the negative pole load, which causes the negative VUF. The largest VUF of -2.7% was observed in Bus 17, and the total power loss was 95.42 kW with a mismatch error of less than 0.01%. Figure 4.6, on the other hand, shows the voltage profile at each bus in comparison to a simulation of a 21-bus bipolar DC distribution grid created using the PSCAD software.

Table 4.2 Validation result of 21-bus bipolar DC distribution grid

|                       |                     |
|-----------------------|---------------------|
| Validation error (%)  | <0.01%              |
| Total power loss (kW) | 95.42               |
| Maximum VUF (%)       | -2.7<br>(At bus 17) |

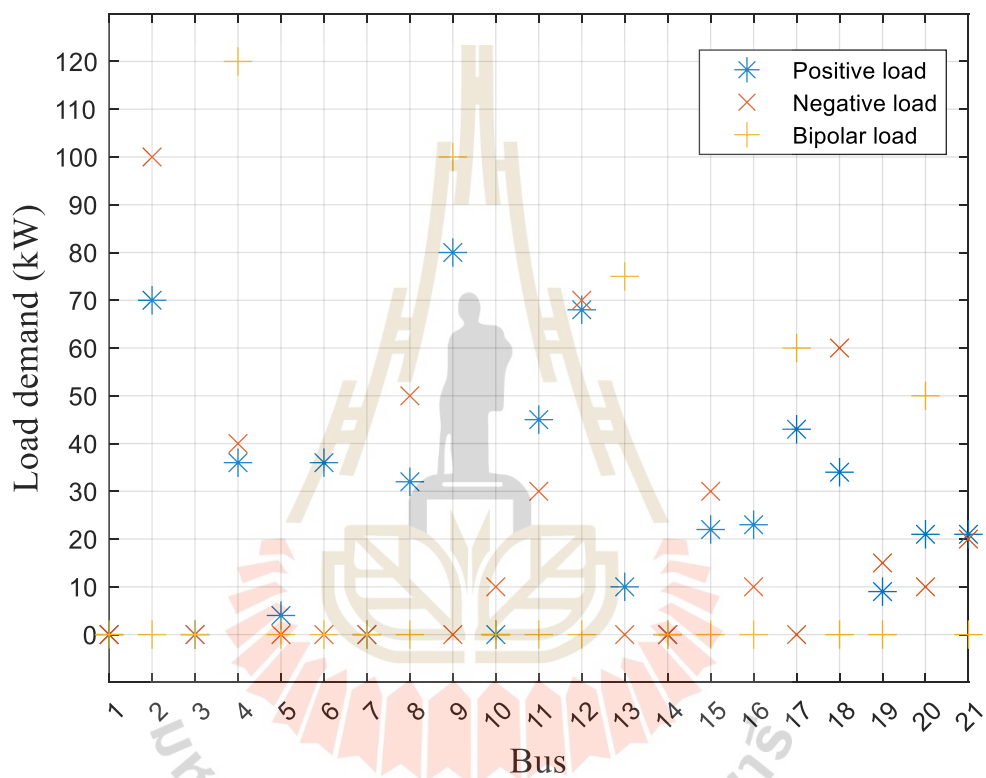


Figure 4.5 21-bus bipolar DC distribution grid validation result

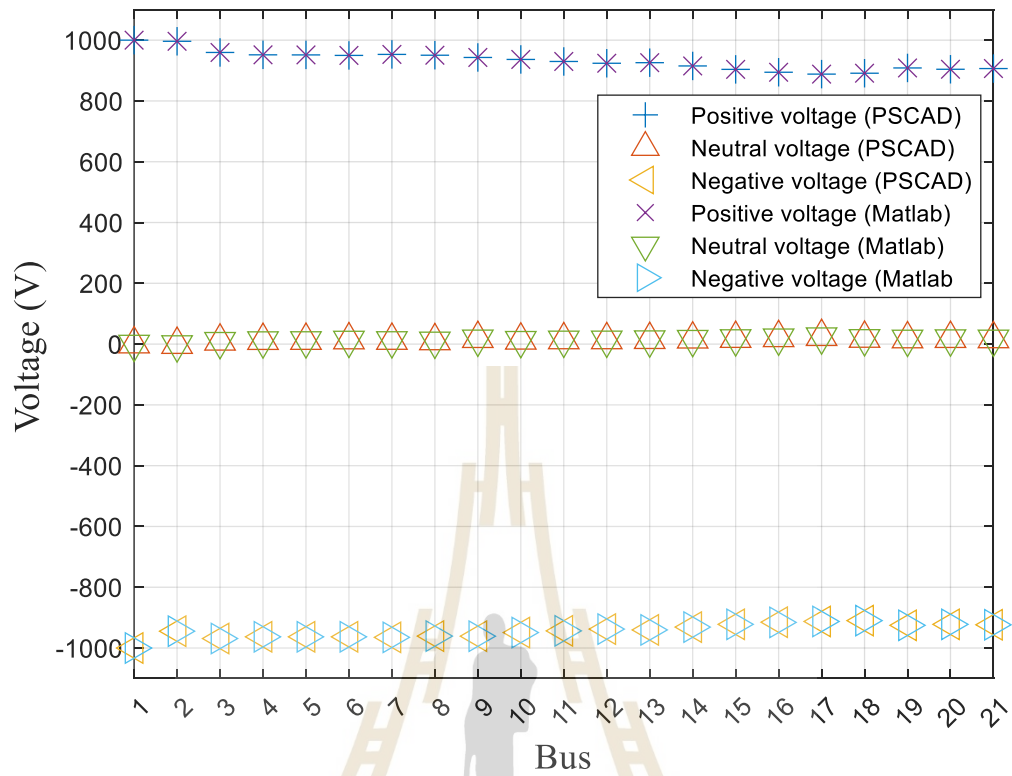


Figure 4.6 21-bus bipolar DC distribution grid simulation result

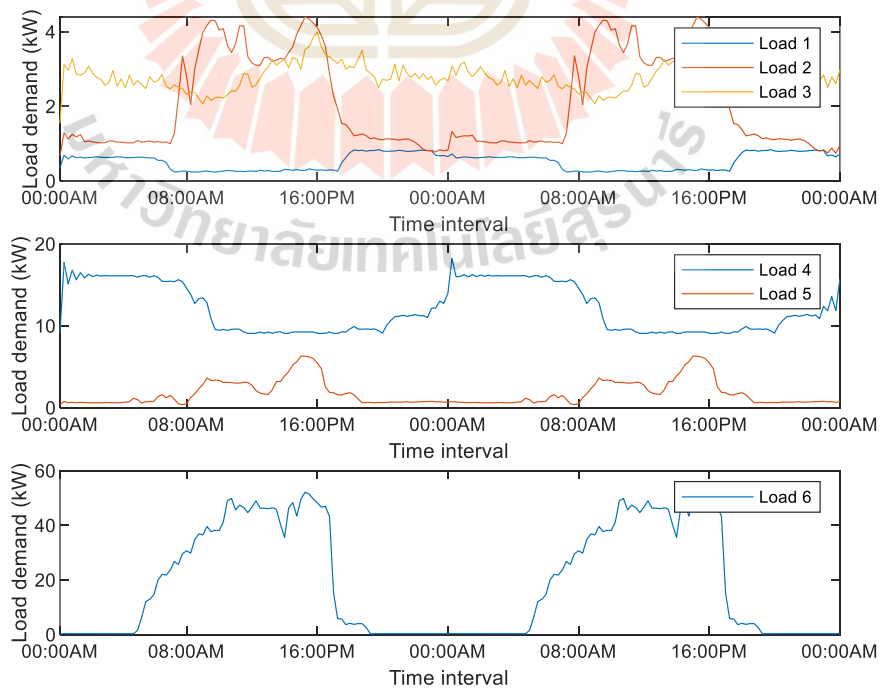


Figure 4.7 48 hrs. load profile

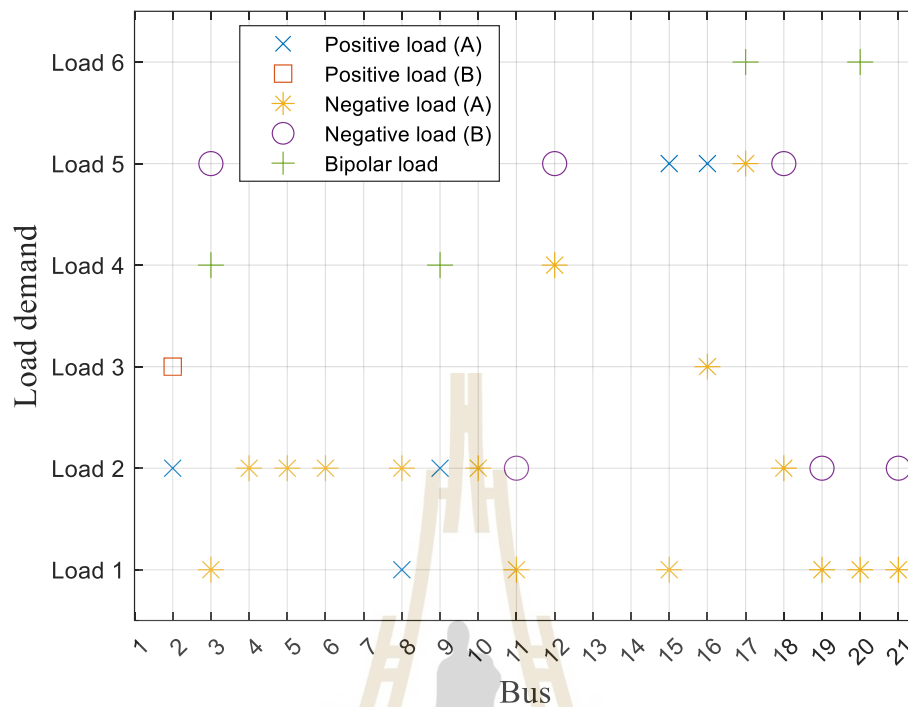


Figure 4.8 Load connection type of base case

### 4.3 Case I: Base Case Simulation

The base case power flow results are shown in this subsection. The GMM technique is used to compute power flow every 15 minutes (192 timestep) using a 21-bus bipolar DC distribution system as a simulation system. So, the 48-hours load profile and load connection detail as shown in Figure 4.7 and FIGURE 4.8.

A load connection type for load A and load B to the positive and negative pole is shown in FIGURE 4.8 and is referred to in TABLE A.5 in Appendix A. A positive voltage profile, negative voltage profile, and VUF are shown in FIGURES 4.9 to 4.11, depending on the load profile in Figure 4.7 and the load connection from FIGURE 4.8. At timeslot 61 or 15.30 p.m., the maximum VUF is found at bus 18 with 3.34% of VUF, while the lowest magnitude positive and negative voltage is found at bus 17 which have 0.983 p.u. and -0.950 p.u. The load demand at bus 17 consists of 6.34 kW at the negative pole and 9.26 kW with a bipolar connection, which accounts for the positive magnitude being larger than the negative magnitude. so, the voltage drops of positive pole is influenced by bipolar load and transmission resistance. In the other hand, the voltage

drops of negative pole occurred by negative load, bipolar load and transmission resistance. The major power loss occurs around 15.30 (slot 61) in the evening. The system's overall energy loss was 958.100 kWh at 15.30 p.m. because bus 18's load demand was only connected to the negative pole, resulting in an unbalanced voltage at the bus. So, the system's overall energy loss was 3.53 % of total energy consumption of the system.

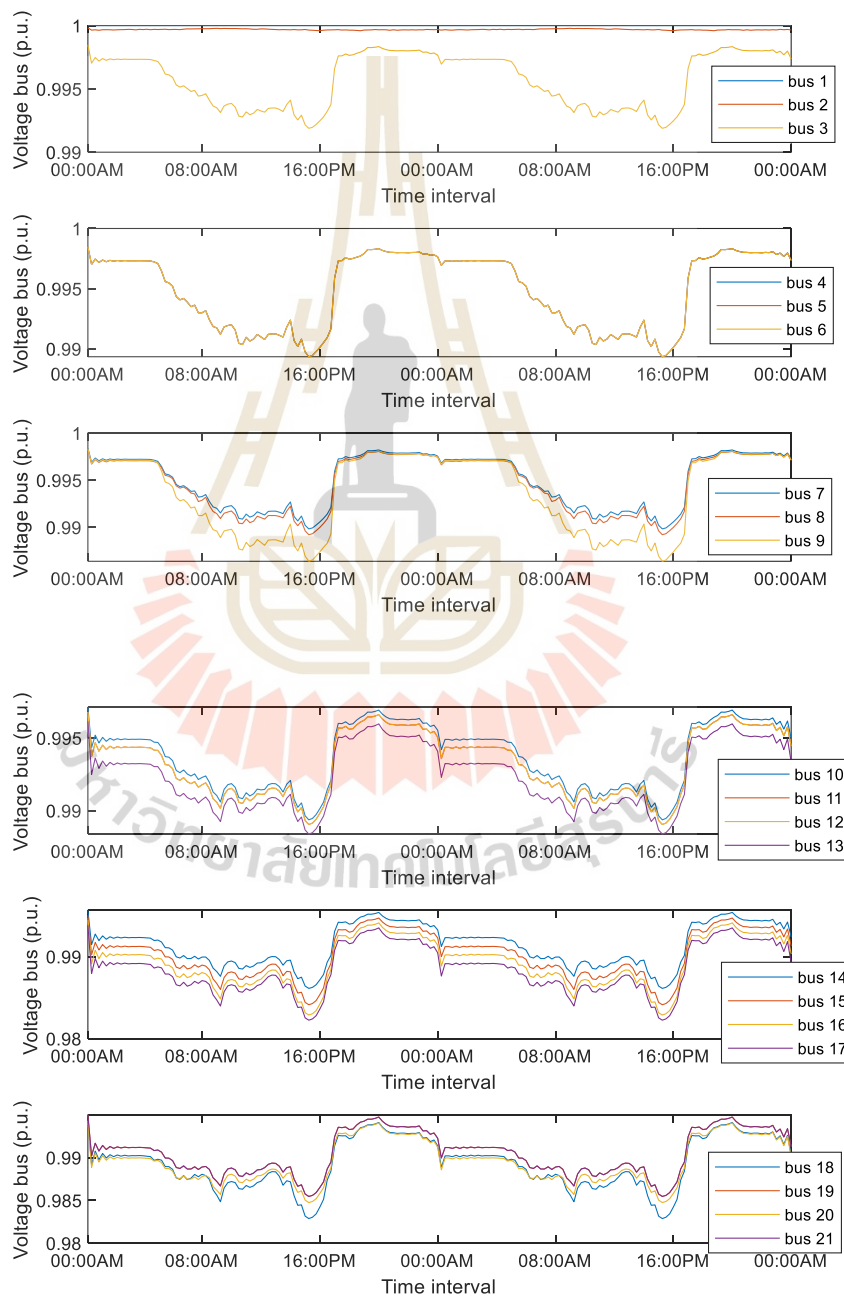


Figure 4.9 Positive voltage profile of case I

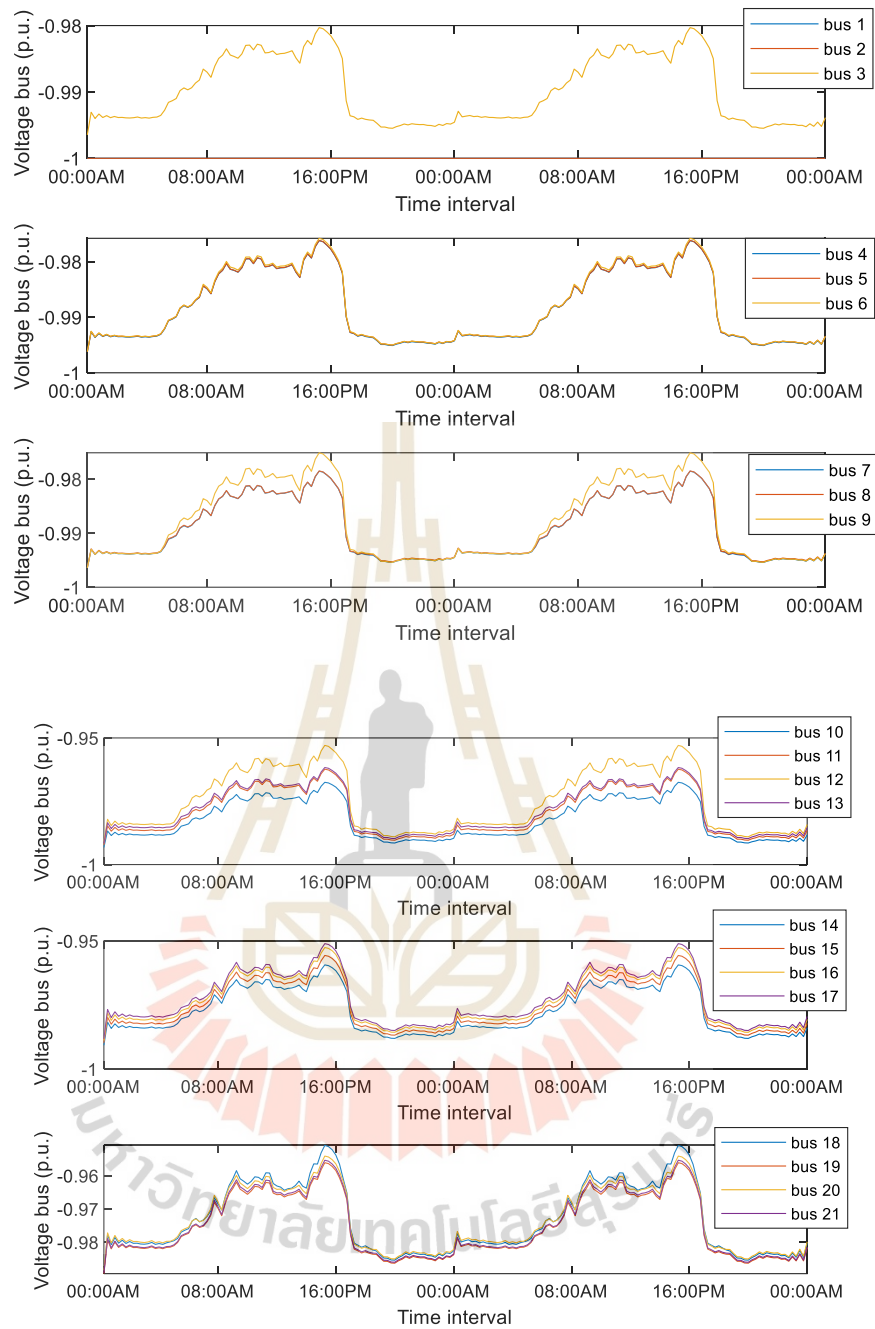


Figure 4.10 Negative voltage profile of case I

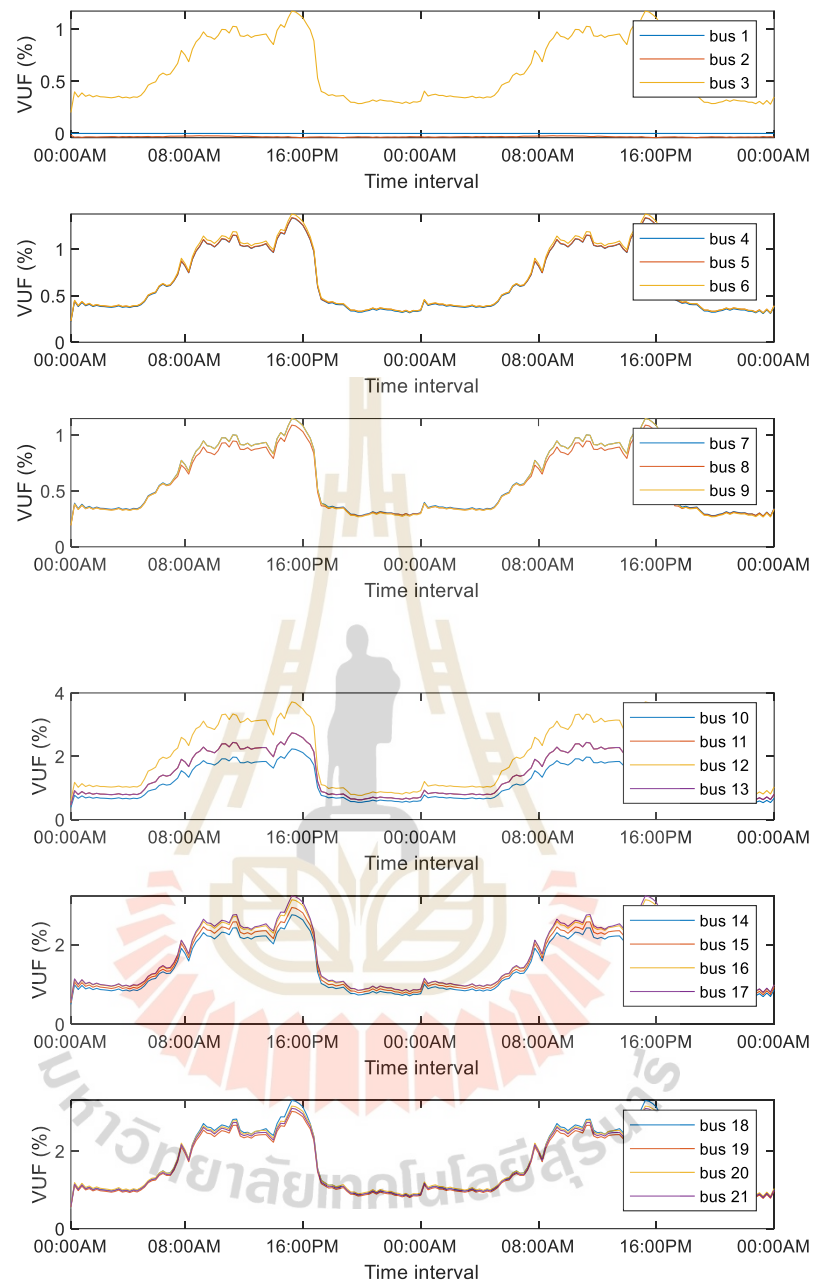


Figure 4.11 48 hours VUF of case I



#### 4.4 Case II Load Balancing Case Simulation

This subsection presents the load balancing method as a simulation result aimed at minimizing system power loss using Particle Swarm Optimization (PSO). The proposed approach involves selecting the appropriate connection types for each load during the planning phase, with the goal of reducing both system power loss and Voltage Unbalance Factor (VUF). FIGURES 4.12 to 4.16 illustrate the simulation results, which include PSO convergence characteristics, load types, power loss, and voltage profile. It should be noted that the study's maximum VUF limit limitation is 3%.

FIGURE 4.12 illustrates the convergence of the optimization approach, with iteration 8 yielding the best fitness function value of 471,200. FIGURE 4.13 showcases the outcome of selecting the optimal load connection types. Meanwhile, FIGURES 4.14 to 4.16 present the voltage profile and VUF. A comparison between the load connection types of the balancing case and the base case is shown in FIGURE 4.13. By switching load connection types to minimize the disparity between positive and negative load demands, the load balancing method aims to reduce overall system power loss. Consequently, the power loss at each bus in the system is diminished.

The voltage profile at the positive and negative poles is shown in FIGURES 4.14 to 4.15. The simulation findings indicate that the voltage drop between each bus's positive and negative poles may be reduced with the right load connection plan. FIGURE 4.16 presents a VUF of the system which VUF decreased by 0.124% as a result of the minimum voltage magnitudes at bus 17 increasing to 0.967 p.u. for the positive pole and -0.966 p.u. for the negative pole. The positive and negative pole voltages climbed to 0.967 p.u. and -0.968 p.u. at bus 18, which showed the lowest negative pole voltage. Bus 18 showed a variable VUF of 0.372 % and a neutral voltage of  $-0.356 \times 10^{-6}$  p.u. depending on the difference in voltage between the positive and negative buses. In this particular case, the VUF improvement contributed to a reduction in the system's neutral current flow, ultimately leading to a 50.821% decrease in system energy loss (from 958.100 kWh to 471.175 kWh). The energy loss is 1.73 % of total energy demand

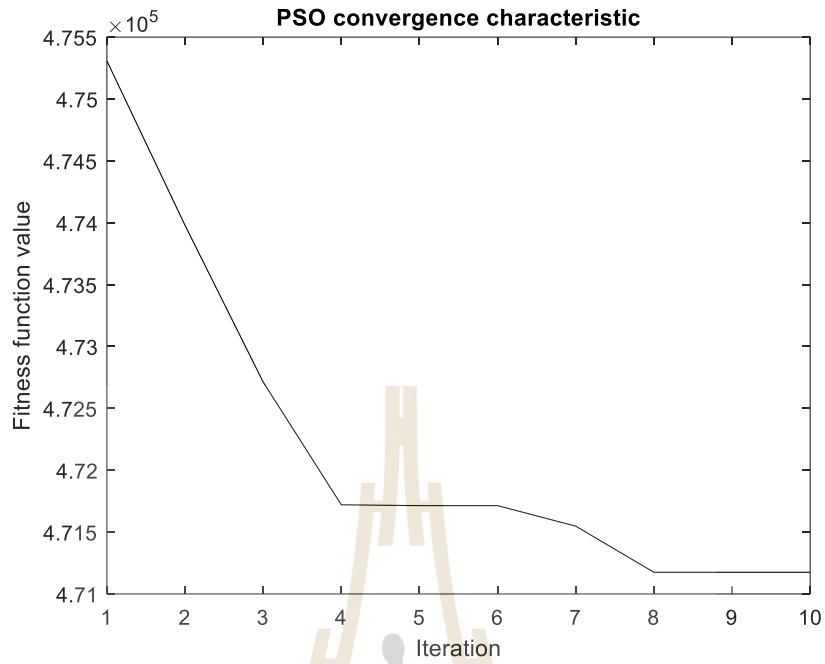


Figure 4.12 PSO convergence characteristic

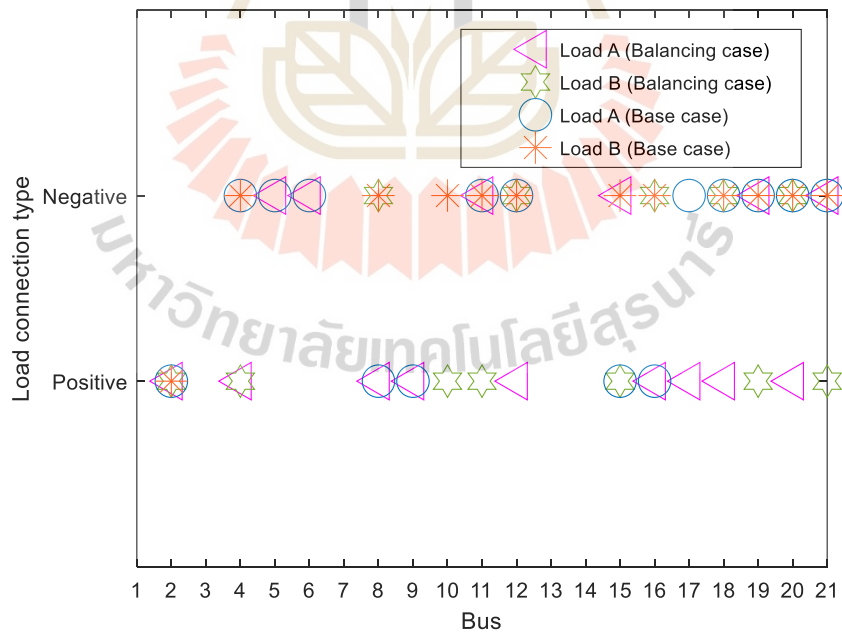


Figure 4.13 Load connection type comparisons of case I and case II

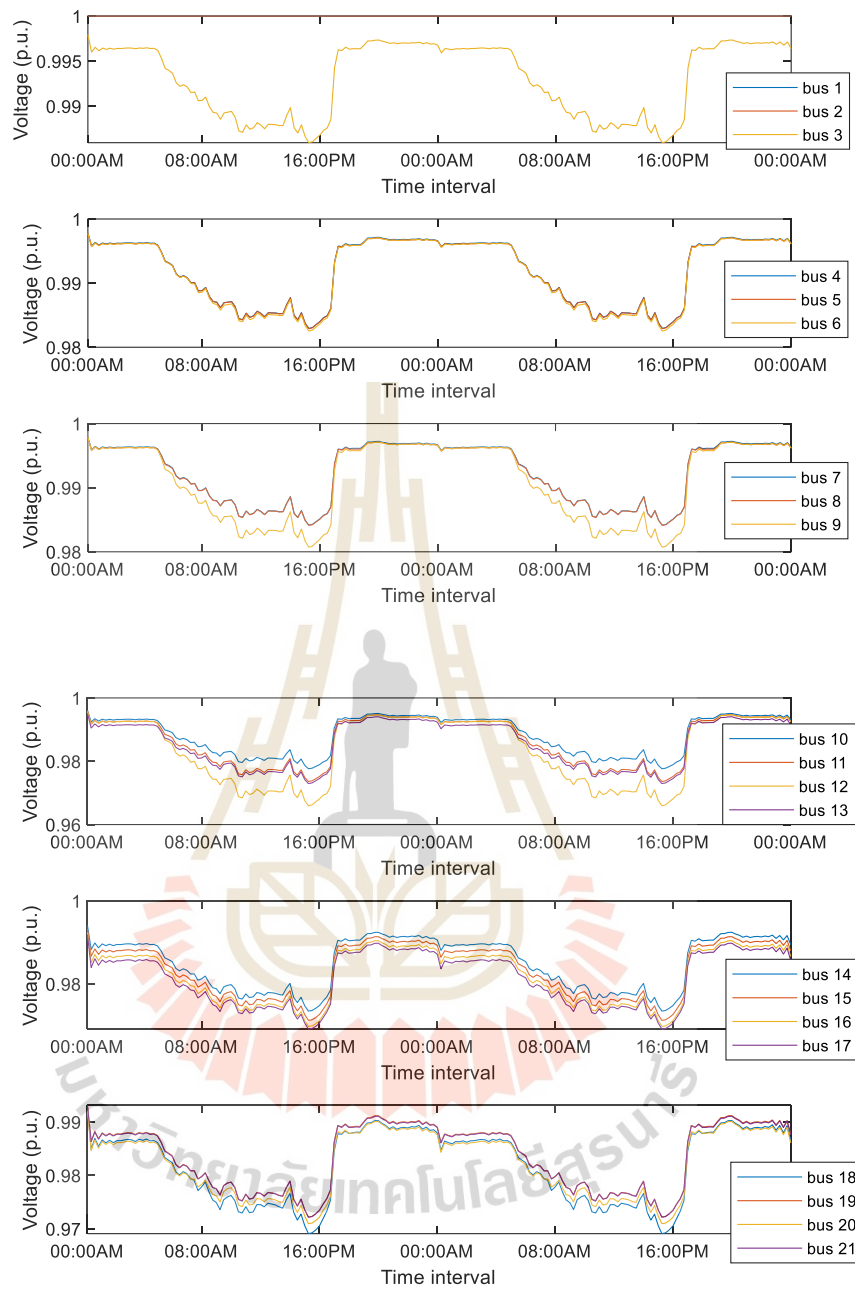


Figure 4.14 positive voltage profile of case II

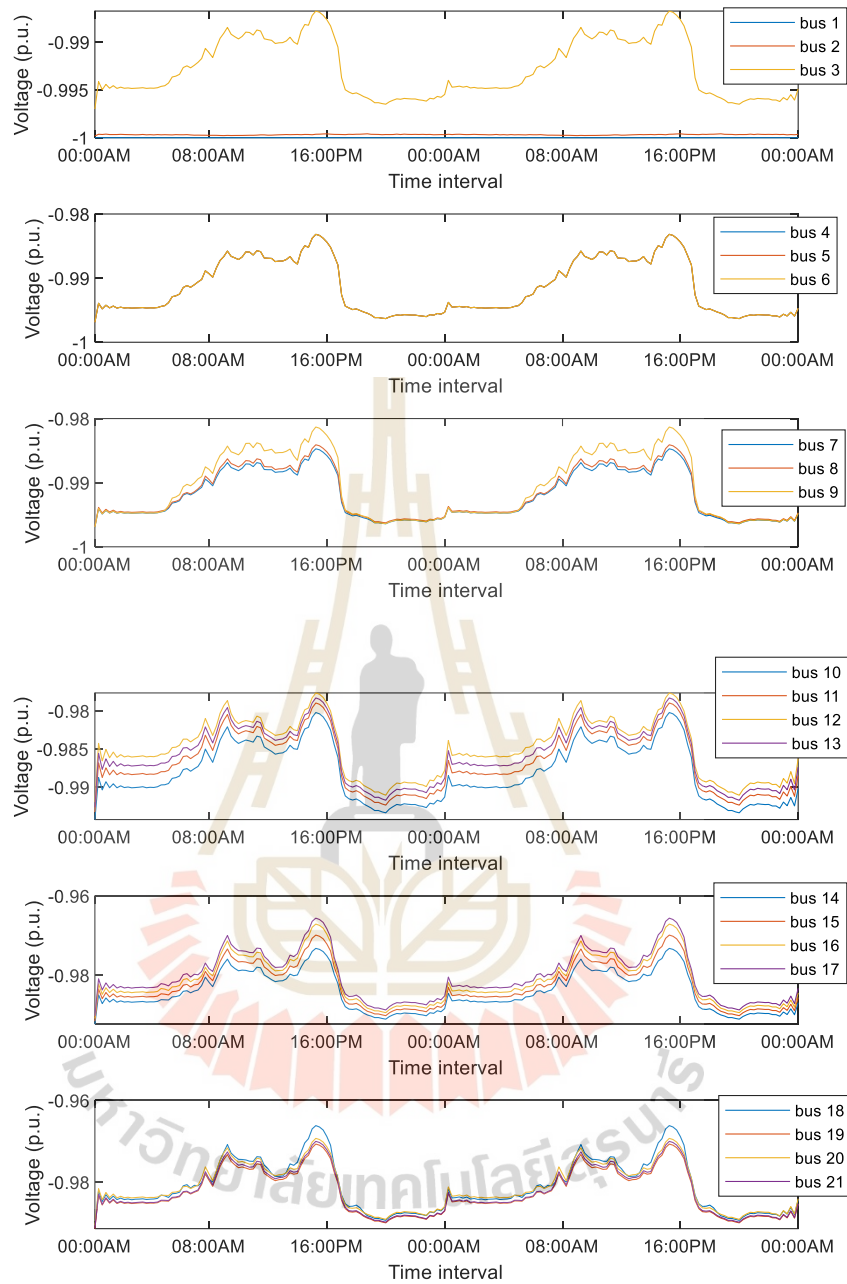


Figure 4.15 Negative voltage profile of case II

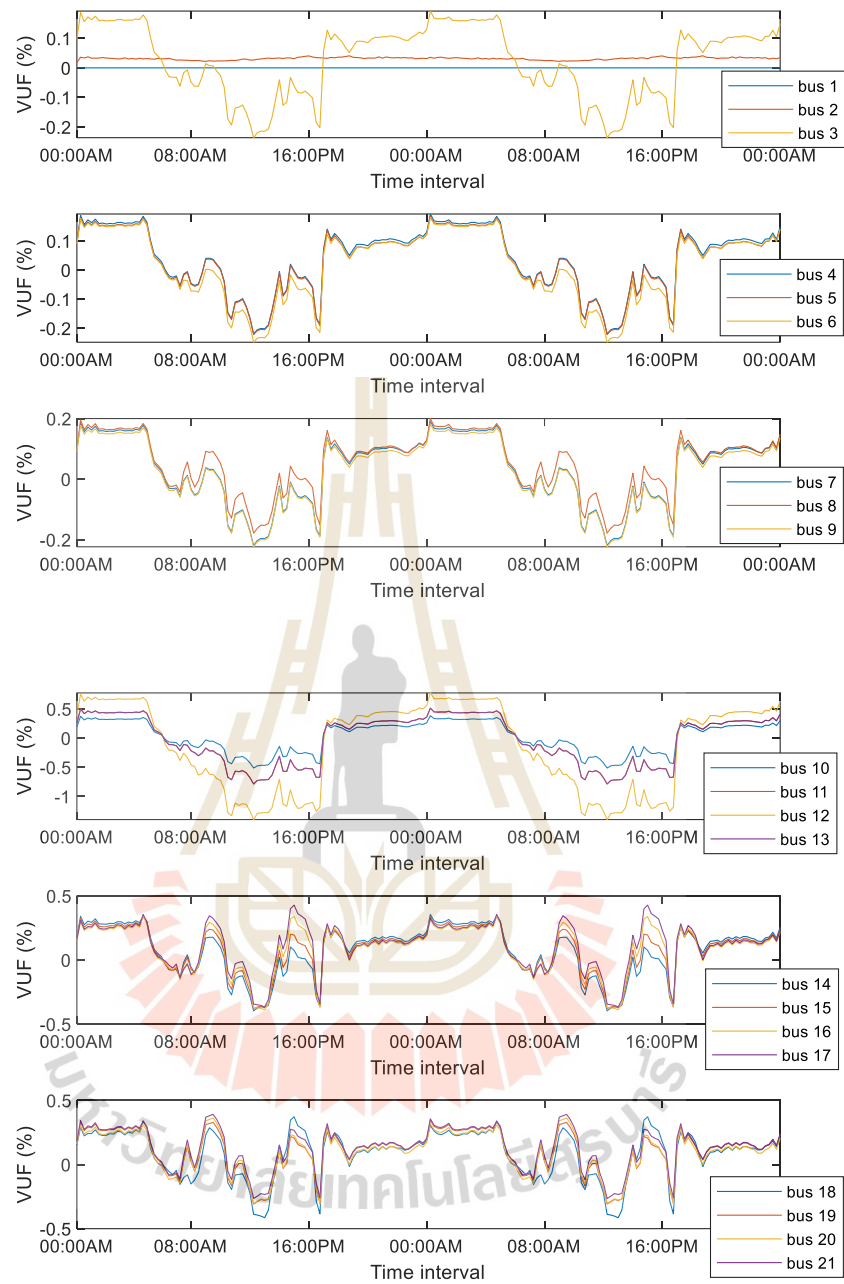


Figure 4.16 Voltage unbalance factor (VUF) of case II

#### 4.5 Probabilistic EV Load Demand Simulation

This section presents an MCS method for evaluating the demand for EV charging, starting with a probability calculation for daily trip distance and a random sample of EV owner behavior. After that, charging time and load demand are

determined using sample data, an MCS simulation requirement that is present at table 4.3

Table 4.3 Monte Carlo Simulation data

| Data type                                | value  |
|--|--|
| Amount of EV                             | 50   |
| Charger installation boundary            | Every bus  |
| Initial State of Charge (SOC) of all EV  | 100 %  |
| Charger plug-in time period              | Depend on sampling of PDF based on plug-in mean and standard deviation |
| Charger removal time period              | 08:00 AM   |
| Plug-in time standard deviation          | 18   |
| Plug-in time mean                        | 3.3  |
| Daily travel distance standard deviation | 94.42  |
| Daily travel distance mean               | 40   |
| Maximum EV milage                        | 400  |
| Charging power                           | 1.9  |
| Charging efficiency                      | 90%  |
| Battery capacity                         | 44.5 kWh   |

In order to assess the demand for EV charging, a Monte Carlo simulation was performed using the plug-in time simulation from Equation 3.40 and the charging time probability density function of the home-charging pattern as shown in FIGURE 4.17 and FIGURE 4.18.

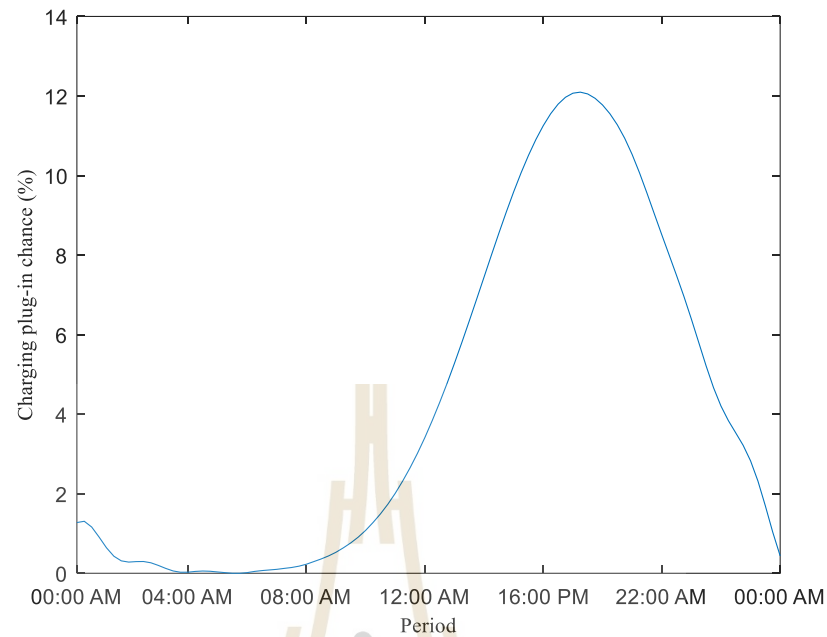


Figure 4.17 Plug-in time of home charger

A home charger's behavior while charging an EV is described in FIGURE 4.17. The simulation results are then utilized to generate random plug-in times for EV owner behavior. FIGURE 4.18 and TABLE 4.4 show some of the results of the sample data.

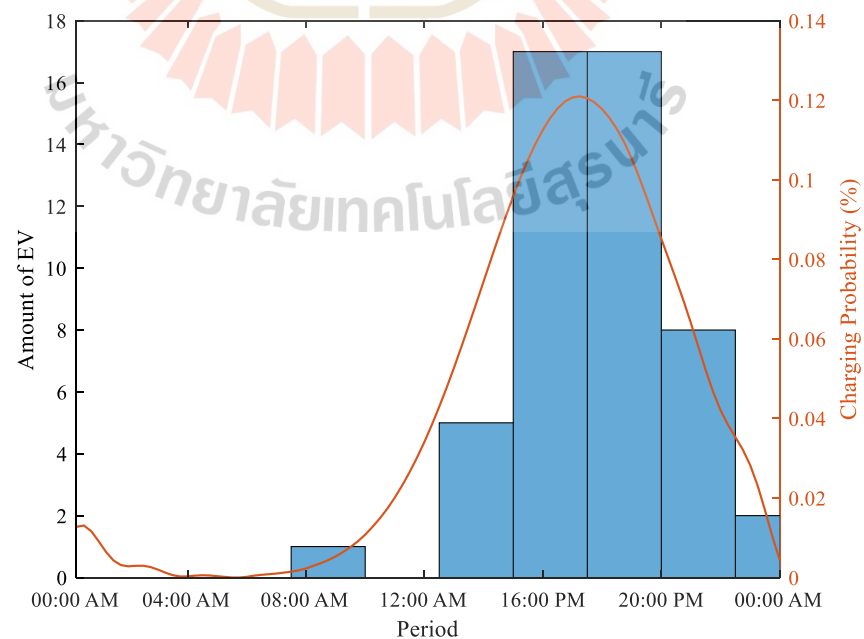


Figure 4.18 EV charging behavior of home charger

Table 4.4 Amount of EV at each bus based on charging time interval

| Interval of time  | Quantity of EV | Interval of time  | Quantity of EV |
|-------------------|----------------|-------------------|----------------|
| 07:30 AM-10:00AM  | 1              | 17:30 PM-20:00 PM | 17             |
| 12:30 PM-15:00 PM | 5              | 20:00 PM-22:30 PM | 8              |
| 15:00 PM-17:30 PM | 17             | 22:30 PM-00:00 AM | 2              |

TABLE 4.4 displays the total quantity of EV at interval times, and FIGURE 4.18 displays a sample of data from EV charging based on charging probability at interval intervals. The likelihood of daily distance travel or the owner of an EV's daily distance travel behavior may then be calculated using Equation 3.37 or Equation 3.38. FIGURE 4.19 shows the resultant figure.

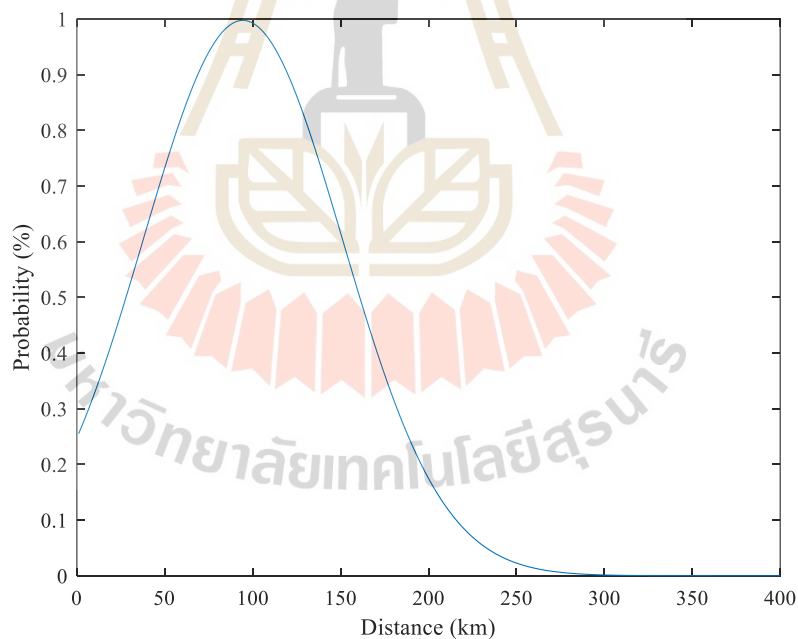


Figure 4.19 Probabilistic of daily distance travel



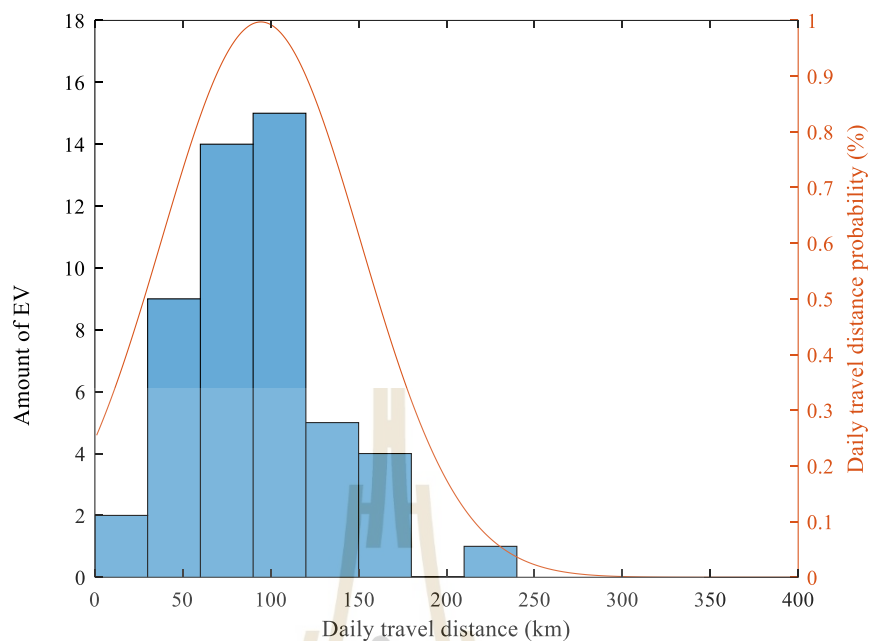


Figure 4.20 sampling of EV based on daily travel distance probability

Figure 4.19 displays the probabilities of daily distance traveled by EV owners, which ranges from 0 km to 283 km. The probability is utilized to generate a random sample of the daily travel distance for each EV. The sampling's results, as shown in FIGURE 4.20 and TABLE 4.5

Table 4.5 Quantity of EV based on daily travel mileage

| Daily travel mileage (km) | Amount of EV | Daily travel mileage (km) | Amount of EV |
|---------------------------|--------------|---------------------------|--------------|
| 0-30                      | 2            | 121-150                   | 5            |
| 31-60                     | 9            | 151-180                   | 4            |
| 61-90                     | 14           | 181-210                   | 0            |
| 91-120                    | 15           | 211-240                   | 1            |

The results in TABLE 4.5 provide a sample of the daily distance traveled by each electric vehicle (EV), from which the simulation results are used to calculate the amount of remaining SOC before charging at home and estimate the demand for EVs at each bus. Using the data in TABLE 4.3, it is possible to generate a random number of EVs at each bus, with the outcome displayed in TABLE 4.6. As previously noted, FIGURE 4.21 illustrates the SOC and EV charging load need as a consequence.

The remaining EV SOC sample data based on PDF related to daily trip distance is shown in FIGURE 4.21. As indicated, the simulation results are utilized to predict the time each EV will take to charge.

An EV load demand simulation presents a charging demand at each bus based on quantity of EV at each bus which is shown in FIGURE 4.22. a time interval of load demand is separated in to 192 timeslot or 48 hours (15 minute per timeslot) to simulate an EV owner behavior. The behavior likes to charge their EV in evening after finishing daily routine and end in a next day morning before daily routine.

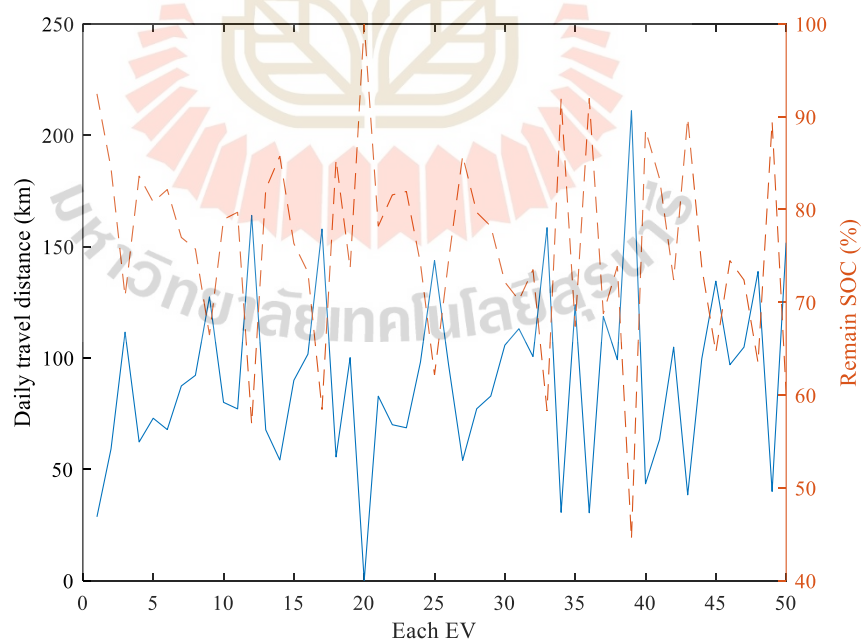


Figure 4.21 Remain SOC of each EV and daily distance travel

Table 4.6 Amount of EV at each bus

| Bus | Amount of EV | Bus | Amount of EV | Bus | Amount of EV |
|-----|--------------|-----|--------------|-----|--------------|
| 1   | 2            | 8   | 4            | 15  | 4            |
| 2   | 4            | 9   | 1            | 16  | 1            |
| 3   | 2            | 10  | 1            | 17  | 1            |
| 4   | 3            | 11  | 2            | 18  | 5            |
| 5   | 1            | 12  | 2            | 19  | 2            |
| 6   | 3            | 13  | 3            | 20  | 3            |
| 7   | 2            | 14  | 2            | 21  | 2            |

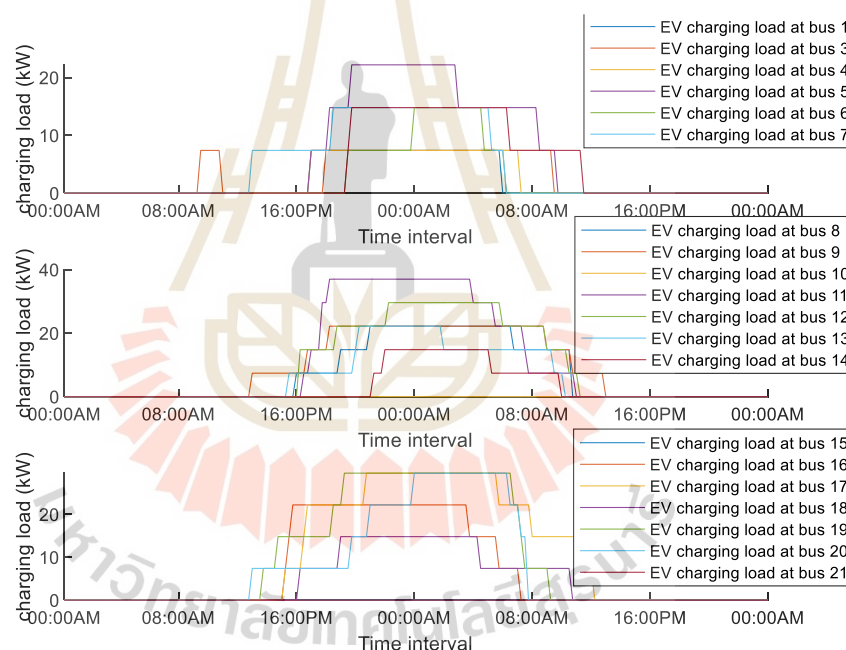


Figure 4.22 EV charging demand of home charging pattern

#### 4.6 Case III: Load Balancing Case with Unbalancing Probabilistic EV Load Demand

A bipolar DC distribution grid that accounts for the demand for uncoordinated electric vehicle (EV) charging is introduced in this chapter with the goal of estimating the overall system's voltage profile, energy loss, and Voltage Unbalance Factor (VUF). The EV charging demand is derived from the simulation results obtained in the previous

section. To simulate the impact of charging demand on the bipolar DC distribution grid, a random load connection type for EV charging demand is employed. The simulation results showcase the voltage profile, total energy loss, and VUF of the entire system.

A load connection type for the load balancing scenario with an EV charging demand is shown in FIGURE 4.23 and voltage profile of the system is presented in FIGURE 4.24 to FIGURE 4.26. The load connection type for EV charging demand is determined by utilizing Particle Swarm Optimization (PSO) with voltage constraints, as specified in Equations 3.32 to 3.35, to simulate the effects of load demand on the grid.

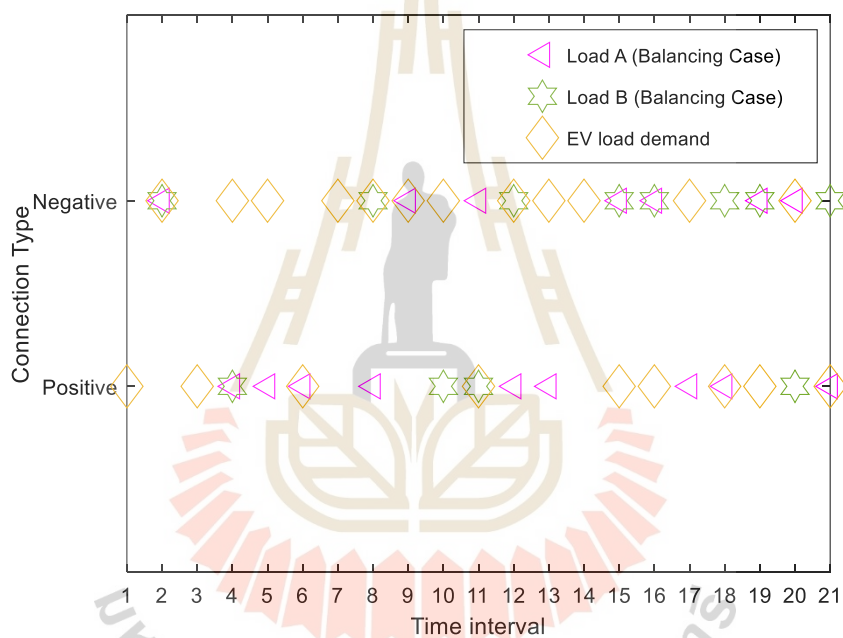


Figure 4.23 Load connection type of case III

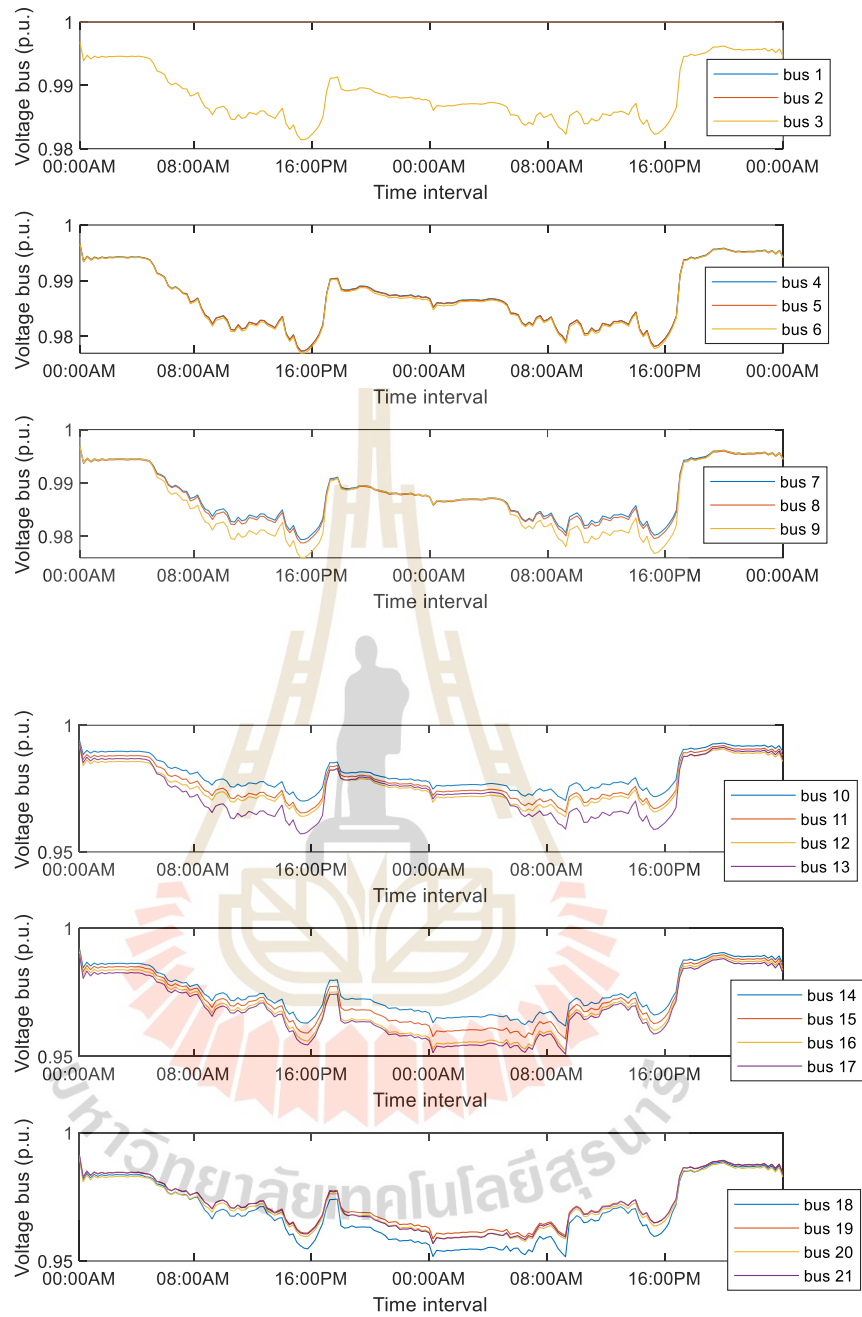


Figure 4.24 Positive voltage profile of bipolar DC distribution grid

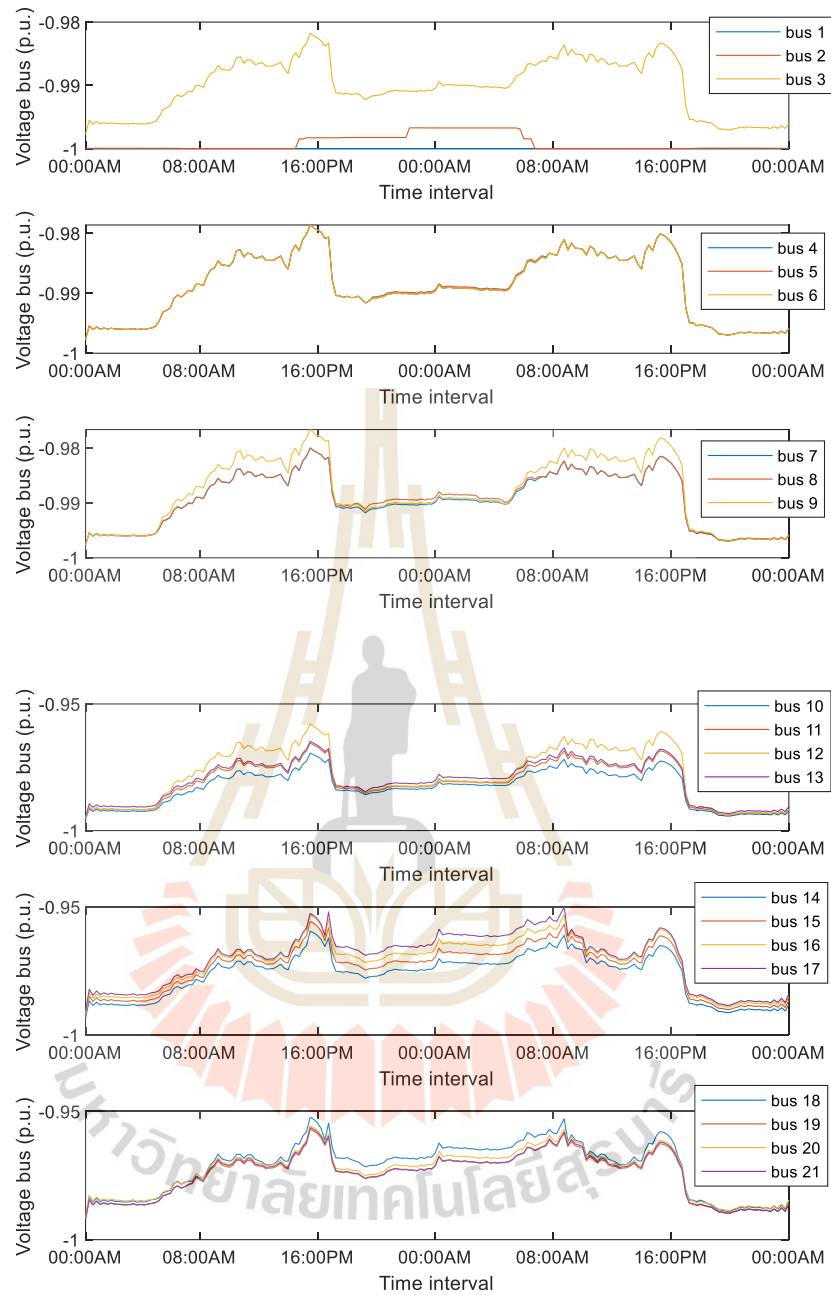


Figure 4.25 Negative voltage profile on bipolar DC distribution grid

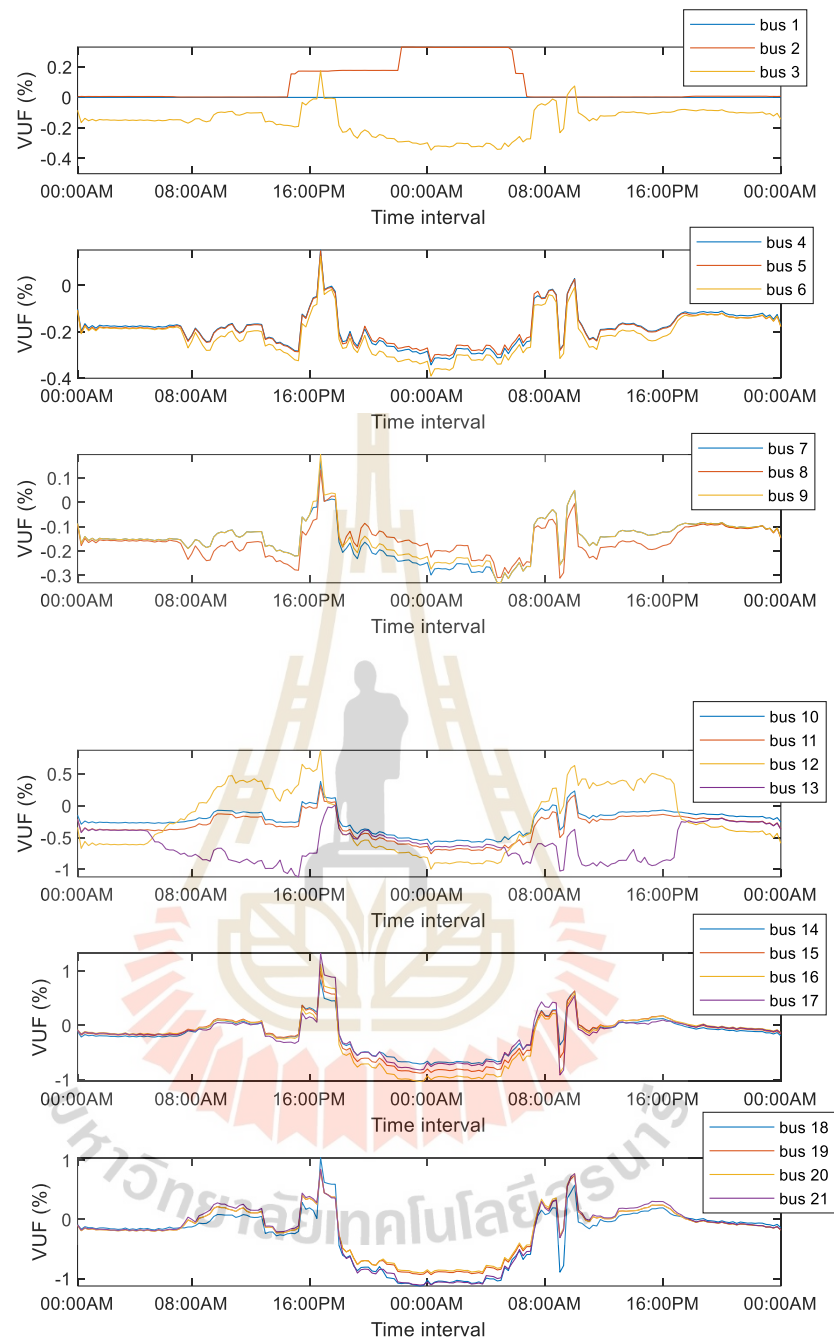


Figure 4.26 Voltage Unbalance Factor on bipolar DC distribution grid

To investigate the impact of electric vehicles (EVs) on the bipolar DC distribution grid, The voltage profile at each bus's positive and negative poles is shown by the simulation results. At various time intervals, Bus 17 displays the lowest positive and negative voltage. In particular, the lowest positive voltage recorded is 0.952 p.u. at 09:15 a.m. (time slot 133). attributed to the presence of EV load charging and the

existing load. At this moment, only one EV is connected to bus 17, with a charger power rating of 4.5 kW, and the charging window extending from 8:00 p.m. to 10:45 a.m. the following day. However, it should be noted that the positive pole is solely connected to the load demand, indicating that the voltage drop observed at this instance is not caused by the EV load demand itself. On the other hand, the lowest negative voltage at bus 17 occurs at 08:45 a.m. (time slot 131), where a 16 kW EV charger and bipolar load are present. The negative voltage at this bus decreased from -0.975 p.u. to -0.952 p.u. due to the influence of the EV charger. As a result of higher current flow at each bus and the resulting imbalance state, the EV load demand can have an impact on the overall power loss of the system. Thus, TABLE 4.7 provides a comparison between the results of the load balancing scenario with integrated EV load demand and the non-balancing case.

Table 4.7 simulation result comparison

| Scenario                                   | Highest VUF   | Total energy loss (kWh) |
|--|---------------|-------------------------|
| Load balancing case without EV load demand | 1.347(Bus 12) | 471.125                 |
| Load balancing case with EV load demand    | 1.326(Bus 17) | 1,132.833               |

So, the TABLE 4.8 can be concluded a significant of EV load demand impact which can be increased total energy loss of the system up to 140.462 % and a proportion of energy loss rises to 4.17 % of total energy demand or increases 2.44 % of without EV load demand.

#### 4.7 Case IV: Load Balancing Case with Balancing Probabilistic EV Load Demand

In this subsection, the load balancing scenario introduced in the previous section is employed as a simulation system to address the impact of probabilistic electric vehicle (EV) load demand on the distribution grid. The best connection type



for the EV load requirement is found using the Particle Swarm Optimization (PSO) method, which minimizes the impact on the grid and lowers system power loss. A optimal solution of load balancing method for the case is presented in FIGURE 4.27 and voltage profiles are presented in FIGURE 4.28 to FIGURE 4.30

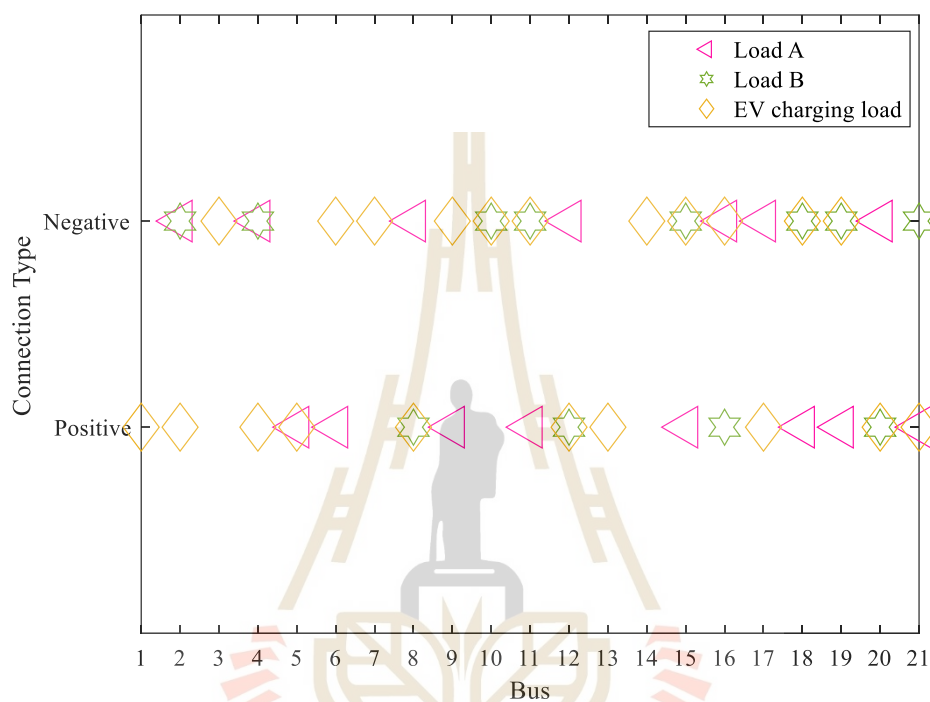


Figure 4.27 Load connection type of bipolar DC distribution grid

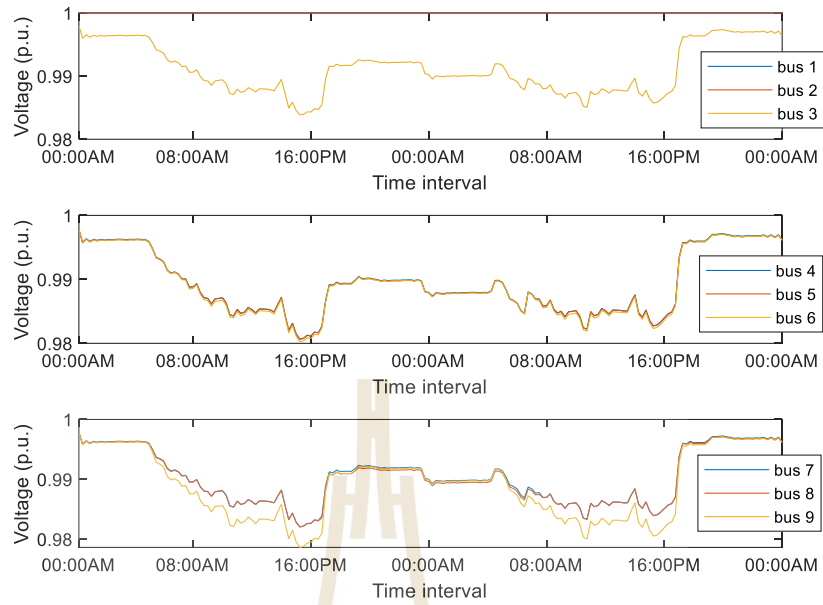


Figure 4.28 Positive voltage profile of case IV

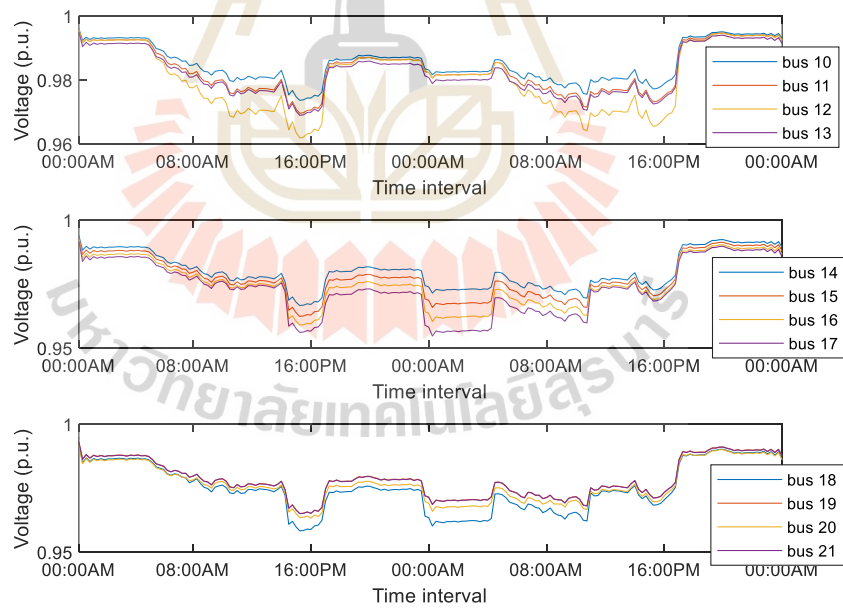


Figure 4.28 Positive voltage profile of case IV (cont.)

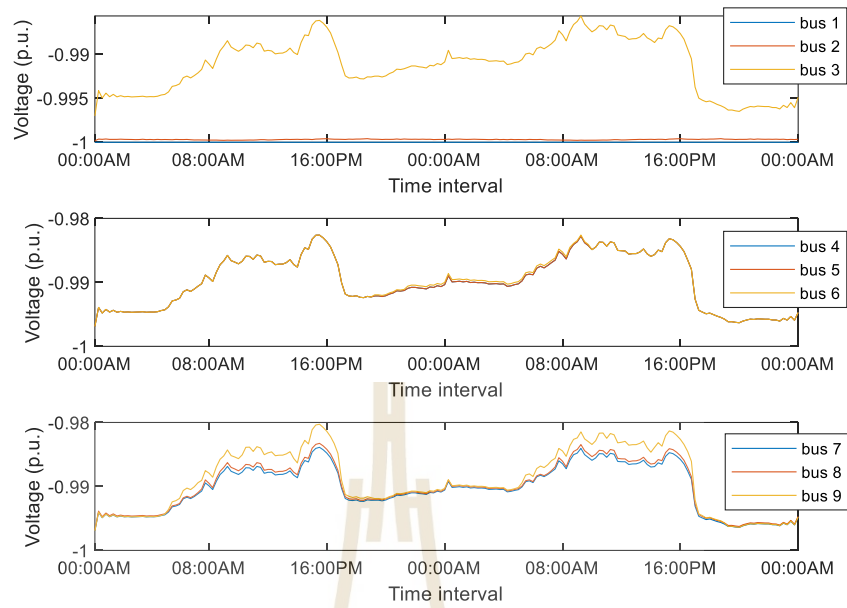


Figure 4.29 Negative voltage profile of case IV

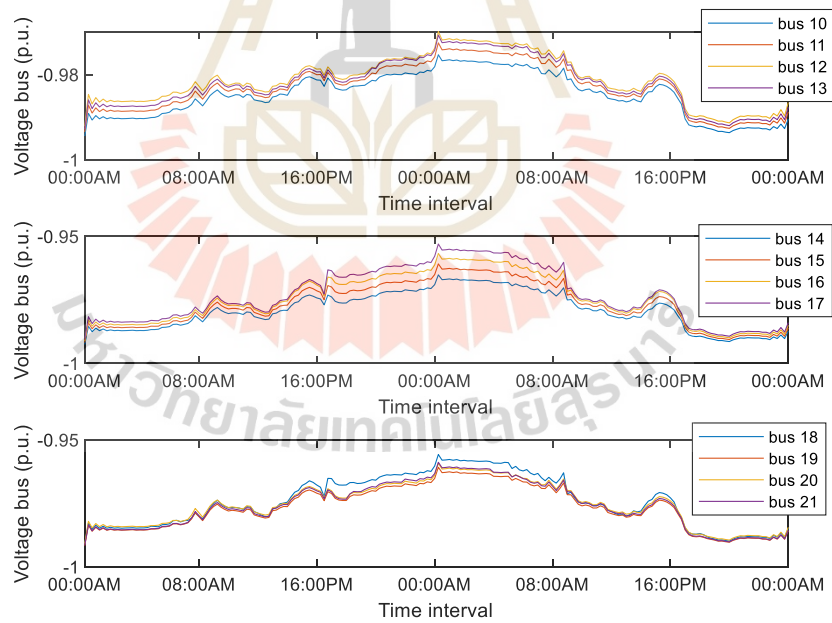


Figure 4.29 Negative voltage profile of case IV (cont.)

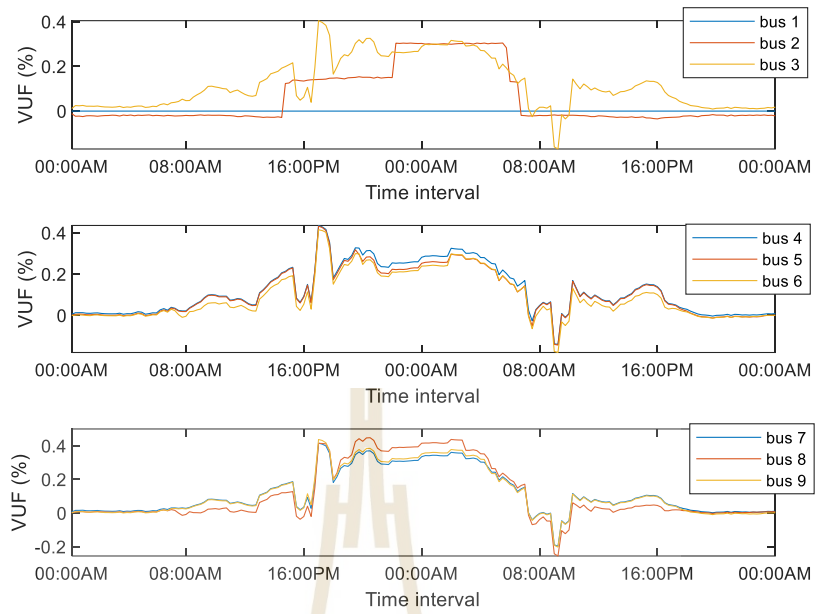


Figure 4.30 Voltage unbalance factor of case IV

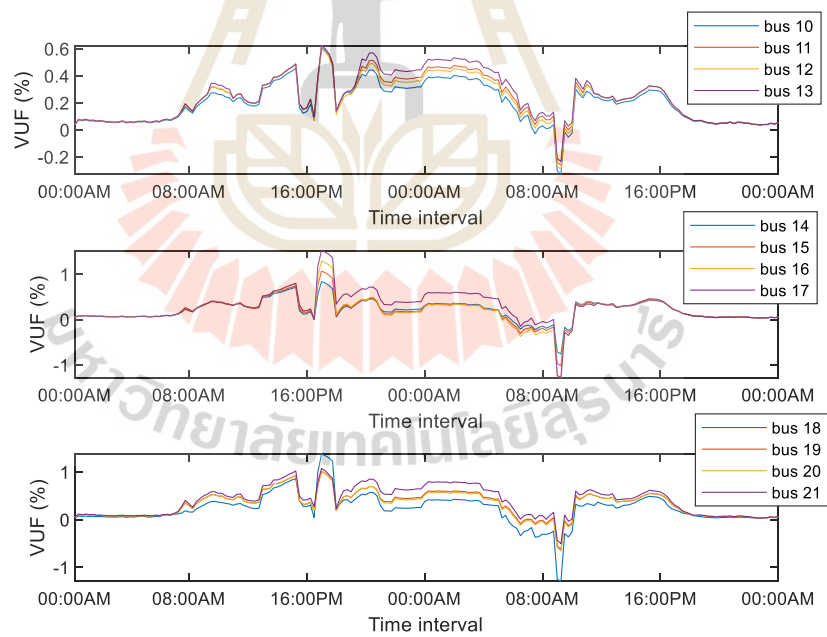


Figure 4.30 Voltage unbalance factor of case IV (cont.)

Bus 17 has the lowest voltage for both poles, based on the simulation results. With a positive voltage magnitude of 0.948 p.u., bus 17 in time slot 97 has the lowest voltage magnitude, and bus 17 in time slot 133 has the lowest negative voltage magnitude of 0.957 p.u. Therefore, the proposed approach may reduce the VUF and total power loss of the entire system by lowering the difference in load demand across poles. A comparison of the simulation results for examples III and IV is shown in TABLE 4.9. The optimal connection type for the example study might reduce the system's daily loss to 655.060 kWh, or around 17.61%. which compares with total energy demand of the system, the total energy loss is 2.41 %.

Table 4.8 The Highest VUF and Total Daily Loss Comparison of Cases III and IV

| Scenario | Highest VUF (%) | Total energy loss (kWh) |
|----------|-----------------|-------------------------|
| Case III | 1.326(Bus 17)   | 1,132.833               |
| Case IV  | 1.523(Bus 17)   | 655.060                 |

#### 4.8 Conclusion

This section showcases the results of a comprehensive simulation of a bipolar DC distribution grid, encompassing two distinct types of simulations: validation simulation and study case simulation. The validation simulation entails a comparison of the voltage profile obtained from a reference article utilizing PSCAD with the MATLAB source code that employs the Gauss's Method of Moments (GMM) for power flow calculations. On the other hand, the study case simulation consists of four case studies with 48-hour simulations, focusing on the integration of electric vehicle (EV) charging demand. The EV charging demand is modeled using Monte Carlo Simulation techniques. To minimize the total daily loss of the distribution grid, a load balancing method is employed, where the determination of the optimal load connection type is achieved through the use of Particle Swarm Optimization (PSO). The reduction in Voltage Unbalance Factor (VUF) is an additional outcome resulting from the pursuit of minimizing the total daily loss. The simulation results demonstrate that, when

considering the probabilistic nature of EV charging demand, the proposed load balancing strategy can significantly reduce the total daily loss and enhance the VUF of the bipolar DC distribution grid.



## CHAPTER V

### CONCLUSION

The presentation of this thesis comprises of 5 chapter which comprises of introduction, literature review, methodology, simulation result and conclusion.

Introduction chapter presents background, problem statement, objective and structure of thesis to overview a detail and problem of bipolar DC distribution grid with EV charging demand integration.

Literature review presents overview of DC distribution grid such as structure (unipolar and bipolar structure), voltage level in view of end's user or grid operator, impact of EV and concept of V2G technology.

Methodology presents a calculation method of bipolar DC power flow, load balancing method and EV load demand evaluation to evaluate effect on unbalance load and EV charging demand on bipolar DC distribution grid via voltage profile, system power loss and VUF

Simulation result can be separated into 4 parts as follow:

First part is a base case simulation which validate a source code with other article and simulate a 48-hours base case of bipolar DC distribution system to evaluate voltage profile, daily energy loss and VUF of unbalance condition. After that in second part, a load balancing method is used to reduce daily energy loss and VUF of base case system.

A conclusion of first part presents a validation which uses balanced 4-bus DC bipolar distribution grid and unbalanced 21-bus DC bipolar distribution grid. The referred simulation result of the system is solved by using PSCAD program which this thesis uses MATLAB source code based on GMM technique to simulate a power flow of the system. The simulation presents two categories based on a type of distribution system which a result presents a percentage error of source result and PSCAD simulation result from referenced article. In case of balanced 4-bus DC bipolar distribution grid, the result presents a percentage error of validation that equals 0.31%.

in the other case, the percentage error is less than 0.01% with total power loss 95.42 kW and -2.7 % of VUF which the program has satisfactory performance and will be used in the other case study.

The base case simulation (Case I) presents a 48-hours of unbalanced 21-bus DC bipolar distribution system with various dynamic load for using as base case which a simulation result presents a voltage profile, total energy loss, VUF. The simulation can be concluded as follow:

In case of voltage magnitude presents a weak bus location of positive and negative power which a weak bus of positive pole locates at bus 17 is 0.983 p.u. and -0.95 p.u. for negative pole in 15.30 p.m. or timeslot 61 due to unbalance load demand capacity between positive pole and negative pole that the load comprises of unipolar load and bipolar load. In case of highest VUF, the highest VUF locates at bus 18 which have 3.34 % of VUF at 15.30 p.m. due to differential capacity of load demand between positive pole and negative pole at bus 18.

To reduce an unbalance problem of the system, A load balancing method based on PSO is used to solve the problem that was present in Case II or load balancing case simulation. The load balancing method is used to balance a unipolar load demand between positive pole and negative pole by searching an optimal connection type. Which the system with optimal connection type of load can be reduce VUF from 3.34 % to 0.37 % at bus 18 at 15.30 p.m. in case of voltage improvement at bus 17, a load balancing method reduce voltage at positive pole from 0.983 p.u. to 0.967 and increase voltage at negative pole from -0.95 p.u. to -0.968 p.u. with 0.34% of VUF at 15.30 p.m. the case have total energy loss is 471.175 kWh which is 1.73 % of total energy demand of the system or 50.821% of total energy loss of case I.

Third part presents EV charging load demand evaluation by using MCS based on mean and standard deviation of plug-in time and daily travel distance to estimate EV's user behavior which the output of MCS proposed a 48-hrs. EV charging load profile based on 50 of EV quantity distributed on the system with 44.5 kWh of EV battery capacity.

After that, the result of third part is used to integrate with balance system from second subsection that presents an impact of EV charging demand on distribution grid.



Lastly in fourth part, the impact of EV charging demand was solved by load balancing method with EV charging load.

The fourth part comprises of case III and case IV. the case III presents load balancing case with unbalancing probabilistic EV load demand which uses a balanced 21-bus bipolar distribution system as a simulation system integrated with 448-hrs. EV charging demand to simulate impact of uncontrolled EV charging demand on distribution grid. A simulation result of case III presents an impact of EV load demand in form of voltage profile, VUF and energy loss of the system. Firstly, a lowest positive voltage located at 09:15 a.m. of bus 17 which have 0.952 p.u. as a voltage at the moment. Which a reason of the problem at bus 17 is load demand at this moment and 4.5 kW of EV charging load demand during 08:00 p.m. to 10:45 a.m. in the other hand, the lowest negative voltage locates at 08.45 a.m. of bus 17 which have 16 kW of EV charging demand and bipolar load. The voltage decreases from -0.975 p.u. to -0.952 p.u. In case of highest VUF, a highest VUF locates at bus 17 which have 1.326%. a total energy loss is 1,132.83 kWh that increases from case II 661.705 kWh or as 2.44 % of total energy load demand. As a result of higher current flow at each bus and the resulting imbalance state, the EV load demand can have an impact on the overall power loss of the system.

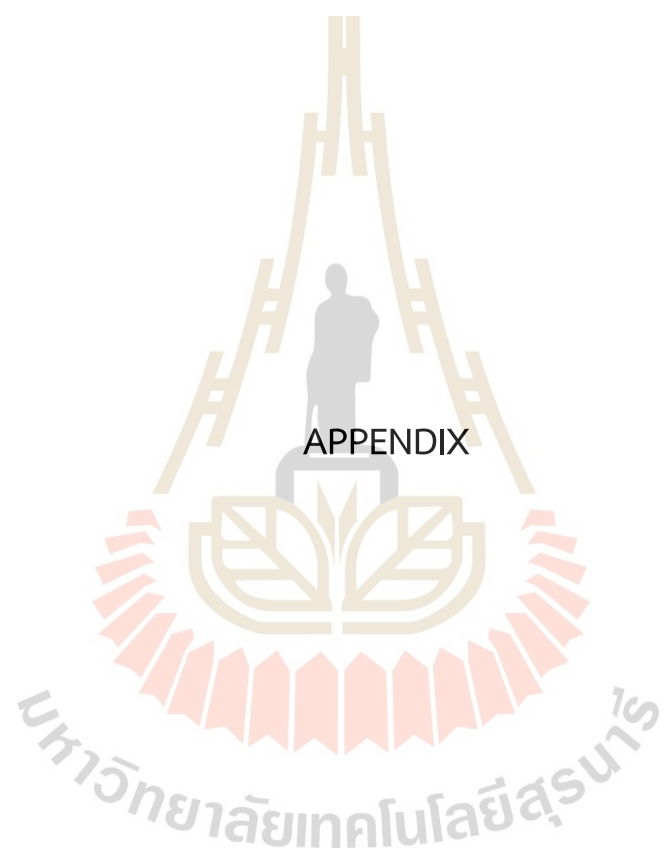
The case IV integrates load balancing method to EV load demand at each bus to reduce impact of uncontrolled EV charging load demand which a simulation result can reduce total energy loss from 1,132.83 kWh to 655.06 kWh or 17.61 % of total energy loss. A highest VUF locates at 17.00 p.m. of bus 17 increase from 1.326 % to 1.523 %.

## 5.1 Future work

The future work is battery integration to load balancing method which can be a huge capacity of battery system or fleet of EV to support load balancing method. An advantage of battery system is high capacity so the battery can act as load to increase load demand or act as source to support load in the network. In the other hand, EV batteries are a movable battery which can be moved to serve power to optimal bus

based on optimization technique for search an optimal position of EV to give a maximize benefit on distribution grid.





APPENDIX

## APPENDIX A

### SIMULATION DATA AND RESULT

#### A.1 Validation simulation

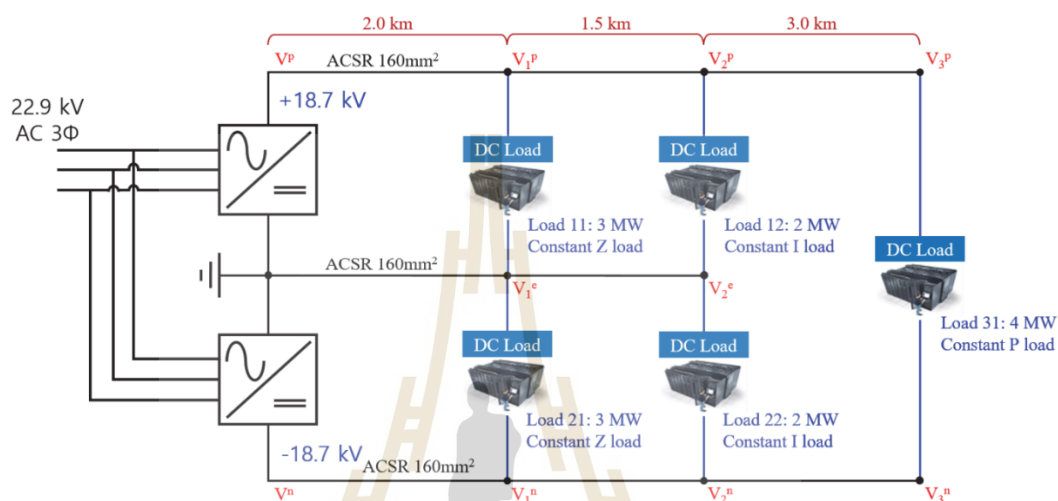


Figure 4.2 4-bus bipolar DC distribution grid

Table A.1 4-bus simulation result

| Bus                              | PSCAD     |           |           | MATLAB    |           |           |
|----------------------------------|-----------|-----------|-----------|-----------|-----------|-----------|
|                                  | $V_+(kV)$ | $V_0(kV)$ | $V_-(kV)$ | $V_+(kV)$ | $V_0(kV)$ | $V_-(kV)$ |
| 1                                | 18.700    | 0         | -18.700   | 18.700    | 0         | -18.700   |
| 2                                | 18.619    | 0         | -18.619   | 18.561    | 0         | -18.561   |
| 3                                | 18.588    | 0         | -18.588   | 18.502    | 0         | -18.502   |
| 4                                | 18.588    | 0         | -18.588   | 18.442    | 0         | -18.442   |
| The average simulation error (%) |           |           |           |           |           | 0.31      |

## A.2 21-bus bipolar DC distribution grid

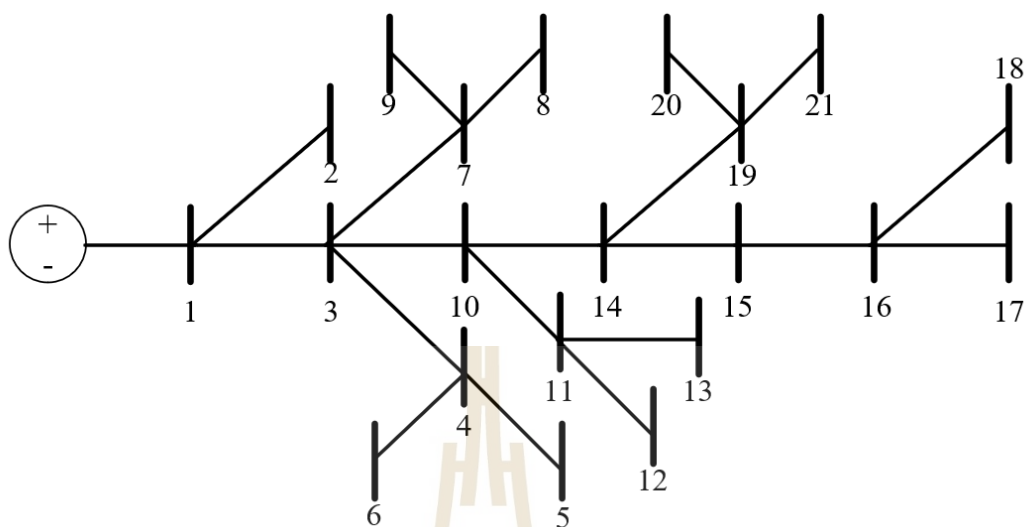


Figure 4.3 21-bus bipolar DC distribution grid

Table A.2 Load data of 21-bus bipolar DC distribution grid for validation simulation

| Bus | P+(kW) | P-(kW) | Pbi(kW) | Bus | P+(kW) | P-(kW) | Pbi(kW) |
|-----|--------|--------|---------|-----|--------|--------|---------|
| 1   | 0      | 0      | 0       | 12  | 68     | 70     | 0       |
| 2   | 70     | 100    | 0       | 13  | 10     | 0      | 75      |
| 3   | 0      | 0      | 0       | 14  | 0      | 0      | 0       |
| 4   | 36     | 40     | 120     | 15  | 22     | 30     | 0       |
| 5   | 4      | 0      | 0       | 16  | 23     | 10     | 0       |
| 6   | 36     | 0      | 0       | 17  | 43     | 0      | 60      |
| 7   | 0      | 0      | 0       | 18  | 34     | 60     | 0       |
| 8   | 32     | 50     | 0       | 19  | 9      | 15     | 0       |
| 9   | 80     | 0      | 100     | 20  | 21     | 10     | 50      |
| 10  | 0      | 10     | 0       | 21  | 21     | 20     | 0       |
| 11  | 45     | 30     | 0       |     |        |        |         |

Table A.3 Bus data of 21-bus bipolar DC distribution grid

| From bus | To bus | Resistance | From bus | To bus | Resistance |
|----------|--------|------------|----------|--------|------------|
| 1        | 2      | 0.053      | 11       | 12     | 0.079      |
| 1        | 3      | 0.054      | 11       | 13     | 0.078      |
| 3        | 4      | 0.054      | 10       | 14     | 0.083      |
| 4        | 5      | 0.063      | 14       | 15     | 0.065      |
| 4        | 6      | 0.051      | 15       | 16     | 0.064      |
| 3        | 7      | 0.037      | 16       | 17     | 0.074      |
| 7        | 8      | 0.079      | 16       | 18     | 0.081      |
| 7        | 9      | 0.072      | 14       | 19     | 0.078      |
| 3        | 10     | 0.053      | 19       | 20     | 0.084      |
| 10       | 11     | 0.038      | 19       | 21     | 0.082      |

Table A.4 Validation result of 21-bus bipolar DC distribution grid

| Bus | PSCAD      |            |            | MATLAB     |            |            |
|-----|------------|------------|------------|------------|------------|------------|
|     | $V_+$ (kV) | $V_0$ (kV) | $V_-$ (kV) | $V_+$ (kV) | $V_0$ (kV) | $V_-$ (kV) |
| 1   | 1,000      | 0          | -1,000     | 1,000      | 0          | -1,000     |
| 2   | 996.28     | -1.62      | -944.66    | 996.28     | -1.62      | -944.66    |
| 3   | 959.52     | 9.22       | -968.74    | 959.52     | 9.22       | -968.74    |
| 4   | 951.76     | 11.37      | -963.14    | 951.76     | 11.37      | -963.14    |
| 5   | 951.50     | 11.64      | -963.14    | 951.50     | 11.64      | -963.14    |
| 6   | 949.80     | 13.33      | -963.14    | 949.80     | 13.33      | -963.14    |
| 7   | 953.12     | 11.77      | -964.89    | 953.12     | 11.77      | -964.89    |
| 8   | 950.43     | 10.39      | -960.82    | 950.43     | 10.39      | -960.82    |
| 9   | 943.11     | 17.80      | -961.11    | 943.11     | 17.10      | -961.11    |
| 10  | 936.57     | 12.49      | -949.06    | 936.57     | 12.49      | -949.06    |
| 11  | 929.93     | 13.62      | -943.55    | 929.93     | 13.62      | -943.55    |

Table A.4 Validation result of 21-bus bipolar DC distribution grid (Continued)

| Bus                   | PSCAD               |                     |                     | MATLAB              |                     |                     |
|-----------------------|---------------------|---------------------|---------------------|---------------------|---------------------|---------------------|
|                       | V <sub>+</sub> (kV) | V <sub>0</sub> (kV) | V <sub>-</sub> (kV) | V <sub>+</sub> (kV) | V <sub>0</sub> (kV) | V <sub>-</sub> (kV) |
| 12                    | 924.02              | 13.71               | -937.73             | 924.02              | 13.71               | -937.73             |
| 13                    | 925.94              | 14.48               | -940.41             | 925.94              | 14.48               | -940.41             |
| 14                    | 915.16              | 15.99               | -931.15             | 915.16              | 15.99               | -931.15             |
| 15                    | 903.90              | 18.11               | -922.02             | 903.90              | 18.11               | -922.02             |
| 16                    | 894.41              | 20.66               | -915.07             | 894.41              | 20.66               | -915.66             |
| 17                    | 888.26              | 24.34               | -912.60             | 888.26              | 24.34               | -912.60             |
| 18                    | 891.25              | 18.58               | -909.83             | 891.25              | 18.58               | -909.83             |
| 19                    | 908.55              | 16.74               | -925.29             | 908.55              | 16.74               | -925.29             |
| 20                    | 904.26              | 17.83               | -922.09             | 904.26              | 17.83               | -922.09             |
| 21                    | 906.62              | 16.98               | -923.54             | 906.61              | 16.93               | -923.54             |
| Validation error (%)  |                     |                     |                     |                     | <0.01%              |                     |
| Total power loss (kW) |                     |                     |                     |                     | 95.42               |                     |
| Maximum VUF (%)       |                     |                     |                     |                     | -2.7<br>(At bus 17) |                     |

### A.3 Base case simulation

Table A.5 Load connection type of base case system

| Bus | P <sub>+</sub> (kW) | P <sub>-</sub> (kW)      | P <sub>bi</sub> (kW) |
|-----|---------------------|--------------------------|----------------------|
| 1   | -                   | -                        | -                    |
| 2   | Load 2(A) Load 3(B) | -                        | -                    |
| 3   | -                   | Load 1(A) Load 5(B)      | Load 4               |
| 4   | -                   | Load 2(A)                | -                    |
| 5   | -                   | Load 2(A)                | -                    |
| 6   | -                   | Load 2(A)                | -                    |
| 7   | -                   | -                        | -                    |
| 8   | Load 1 (A)          | Load 2 (B)               | -                    |
| 9   | Load 2 (A)          | -                        | Load 4               |
| 10  | -                   | Load 2 (B)               | -                    |
| 11  | -                   | Load 1 (A)<br>Load 2 (B) | -                    |
| 12  | -                   | Load 4 (A)<br>Load 5 (B) | -                    |
| 13  | -                   | -                        | -                    |
| 14  | -                   | -                        | -                    |
| 15  | Load 5 (A)          | Load 1 (B)               | -                    |
| 16  | Load 5 (A)          | Load 3 (B)               | -                    |
| 17  | -                   | Load 5 (A)               | Load 6               |
| 18  | -                   | Load 2 (A) Load 5 (B)    | -                    |
| 19  | -                   | Load 1 (A) Load 2 (B)    | -                    |
| 20  | -                   | Load 1 (A) Load 3 (B)    | Load 6               |
| 21  | -                   | Load 1 (A) Load 2 (B)    | -                    |



## APPENDIX B

### PUBLICATIONS

#### List of Publication

##### INTERNATIONAL CONFERENCE PAPER

Sakulphaisan, G., & Chayakulkheeree, K. (2022). Improve a voltage unbalance index of bipolar DC distribution grid by using particle swarm optimization based on load balancing method. *2022 International Electrical Engineering Congress (iEECON)*. <https://doi.org/10.1109/ieecon53204.2022.9741675>

##### INTERNATIONAL JOURNAL PAPER

Sakulphaisan, G., & Chayakulkheeree, K. (2023). Loss minimization for bipolar DC distribution grid considering probabilistic EV charging load using load balancing method. *IEEE Access*, 11, 66995–67012. <https://doi.org/10.1109/access.2023.3289160>

# Improve a Voltage Unbalance Index of Bipolar DC Distribution Grid By using Particle Swarm Optimization Based on Load Balancing Method

Guntinan Sakulphaisan  
 School of Electrical Engineering  
 Institute of Engineering  
 Suranaree University of Technology  
 Nakhon Ratchasima, Thailand  
 B5611850@gmail.com

Keerati Chayakulkheeree  
 School of Electrical Engineering  
 Institute of Engineering  
 Suranaree University of Technology  
 Nakhon Ratchasima, Thailand  
 keerati.ch@sut.ac.th

**Abstract**— This paper presents a bipolar DC distribution grid power flow model and load balancing method by using particle swarm optimization (PSO) to reduce power loss due to neutral current and voltage unbalance factor (VUF) due to unbalance load at each bus. The objective function leads to reducing neutral current by transferring load at each bus to balance a load at each pole by considering the various condition. The results lead to conclude that the load balancing method can be reduced neutral current, reduce power loss and improve the VUF of a modified IEEE 69 bus system.

**Keywords**—load transfer, voltage unbalance factor, bipolar DC distribution grid

## I. INTRODUCTION

Nowadays, The DC distribution system are being implemented in many distribution system as parts of the AC power system. The concept of AC voltage function is transmission electric power from a power plant to load area and convert to suitable DC distribution voltage to feed a group of loads. An issue of bipolar DC system is load unbalance that can be increased power loss of the entire system and increase the temperature of the neutral line. The low voltage DC (LVDC) distribution system can be benefit in the remote rural areas that the distribution system is inaccessible together. The LVDC distribution system is gaining popularity these days. When compare effective of the DC and AC distribution systems, the efficiency of the LVDC distribution system to supply electronic loads is higher than the AC distribution system due to the elimination of conversion stages [1].

In present, a DC distribution system can be built in a unipolar or bipolar configuration. A bipolar LVDC distribution system is a two-phase system with three wires, whereas a unipolar LVDC distribution system has just one voltage level and two wires. the advantage of the DC bipolar architecture is the flexible selection of multiple DC voltage levels for efficient operation more than unipolar architecture [2]. The voltage unbalance problem can be occurred by unequal loads at the positive and negative poles of the bipolar DC distribution system. However, when the system becomes unbalanced, the neutral current is flowing at the neutral cable this causes power loss in the neutral line and increases the temperature at the neutral cable. [3].

So, paper proposes the method of the load balancing method to reduce the neutral current in the neutral wire of bipolar DC distribution grid with ZIP Load which uses VUF and neutral current as an index by optimizing load connection type with particle swarm optimization (PSO).

In this paper, the power flow method for DC distribution grid in illustrated in section II, Section III addresses the PSO based load balancing method. Then, the simulation results are provided in section IV. Lastly, the conclusion is given.

## II. POWER FLOW CALCULATION OF DC DISTRIBUTION GRID WITH ZIP LOAD MODEL

### A. Bipolar DC Distribution Grid

The bipolar system is made up of three lines: positive conductor, negative conductor, and neutral conductor so the voltage level of the bipolar distribution network can be three levels as follows:  $+V_{DC}$ ,  $-V_{DC}$ , and  $2V_{DC}$ . The voltage levels depend on a connection type of loads such as unipolar connection and bipolar connection. A unipolar connection means a connection of load between a positive pole or negative pole to a neutral pole which voltage of a unipolar connection is equal to  $V_{DC}$  or  $-V_{DC}$  depending on the type of pole. A bipolar connection is a load connection between a positive pole to a negative pole in which the load's voltage is  $2V_{DC}$ . The electricity can still be supplied by the other two wires when one of the DC poles has a fault. As a result, the system's reliability, availability, and power quality are better than that of a unipolar DC network. Due to the asymmetric distribution of loads, this may result in system imbalance. Which a bipolar distribution network as shown in Fig 1 and Fig 2 [4].

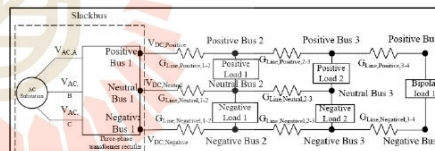


Figure 1 Bipolar DC distribution grid

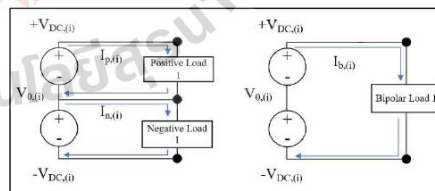


Figure 2 Load current calculation of load

The 2022 International Electrical Engineering Congress (iEECON2022), March 9 - 11, 2022, Khon Kaen, THAILAND

978-1-6654-0206-4/22/\$31.00 ©2022 IEEE

Authorized licensed use limited to: Suranaree University of Technology provided by UniNet. Downloaded on July 04, 2023 at 03:17:31 UTC from IEEE Xplore. Restrictions apply.

2022 International Electrical Engineering Congress (iEECON) | 978-1-6654-0206-4/22/\$31.00 ©2022 IEEE | DOI: 10.1109/iEECON53204.2022.9741675

Figure 1 is a bipolar distribution system that the slack bus comprises of AC substation and 3-phase transformer rectifier which voltage at the slack bus is  $V_{DC}$ ,  $V_{neutral}$  ( $V_0$ ), and  $-V_{DC}$ . The transmission line resistances and loads of this system are represented by dependent current source with the load current of ZIP load model. This paper proposes the method called G-Matrix Method (GMM) for DC load flow analysis as shown in Eqs(1)-(5). To propose a power flow model, the network component comprises two components, mainly the source and load nodes. The slack bus represents index '1'. The index 'n' is the load nodes that start at index 2 to index n. The conductance between node index  $i$  to index  $j$  is the element  $g_{ij}$  in [G]. A bipolar DC network consists of 3 cables. So,  $G_{+/-}$  represents cable conductance of each polarity from node  $i$  to node  $j$ .  $V_{+/-}$  is the voltage at positive neutral and negative at node  $i$  to  $j$  while  $I_{p/n/b}$  represents output current at node  $i$ .  $I_p$ ,  $I_n$  represent current of positive load or negative load which the positive load draw current from a positive node and return to substation via neutral pole and the negative load draws current from neutral pole and returns to substation via the negative pole.  $I_b$  represents a bipolar load that draws current from the positive pole and returns via the negative pole. For every single line modeling nodal analysis Eqs (1) – (3) represent the relationship between unipolar and bipolar load current without transmission loss and the node current analysis at each bus as shown in Fig. 2.

$$I_{p,(i)} = \frac{P_{positive,(i)}}{V_{+, (i)} - V_{0,(i)}} \quad (1)$$

$$I_{n,(i)} = \frac{P_{negative,(i)}}{V_{0,(i)} - (-V_{-, (i)})} \quad (2)$$

$$I_{b,(i)} = \frac{P_{bipolar,(i)}}{V_{+, (i)} - (-V_{-, (i)})} \quad (3)$$

So, the power flow model of the bipolar DC distribution grid can be expressed as Eq (4)-(5).

$$[I] = [G][V] \quad (4)$$

$$\begin{bmatrix} I_p \\ I_n \\ I_b \end{bmatrix} = \begin{bmatrix} G_{pp} & 0 & 0 \\ 0 & G_{nn} & 0 \\ 0 & 0 & G_{bb} \end{bmatrix} \begin{bmatrix} V_p \\ V_n \\ V_b \end{bmatrix} \quad (5)$$

Which integrates the power flow model with the gauss's iteration method. The procedure can be expressed in Fig 3.

#### B. ZIP Load Model of DC Grid

Static models express active and reactive power as functions of bus voltage magnitudes and frequency at an instant given time. The ZIP model uses a polynomial equation that includes constant impedance (Z), current (I), and power (P) components to express the relationship between voltage magnitude and power [5]. The ZIP model is a load model that is generally used in both steady-state and dynamic simulation of DC power systems. This model includes constant impedance (Z), current (I), and power (P) components to describe the relationship between voltage magnitude and power in a polynomial equation. Static load models are suitable for representing load that varies almost instantaneously with changes in the voltage at the load bus when considering the DC network. The detail of the ZIP model can be expressed by Eq (6) when  $C_Z$ ,  $C_I$ ,  $C_P$ ,  $P_0$ ,  $V_0$  and

$V$  are impedance constant factor, current constant factor, power constant factor, rated power, nominal voltage, and load voltage, respectively,

$$P_{ZIP} = P_0 \left[ C_Z \left( \frac{V}{V_0} \right)^2 + C_I \left( \frac{V}{V_0} \right) + C_P \right] \quad (6)$$

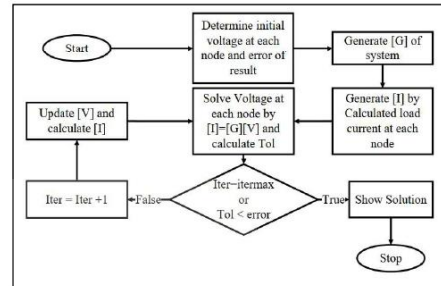


Figure 3 DC power flow calculation procedure

### III. LOAD BALANCING METHOD AND PARTICLE SWARM OPTIMIZATION

#### A. The Problem of Unbalance Loads

In a bipolar LVDC distribution system with unbalanced loads, the positive pole's load capacity is not equal to the negative pole's load capacity. The line current at a positive pole isn't equal to a negative pole which leads to voltage drop in the transmission line by line resistance. In an unbalancing load condition, the neutral current is non-equal which occurs power loss on the neutral wire. Various methods have been used to reduce voltage unbalance in LVDC such as the voltage balancer method that uses voltage balancer to control the voltage of DC/DC converter at PCC. The other method is load transfer by using transfer switch from DC/DC convert at each load bus that used to reduce unbalance load in bipolar DC distribution grid by using static load transfer switch for transfer load to another pole during unbalance condition.

A similar method is the load balancing method which uses in the planning procedure. A load-balancing method is used to find a connection type of load at each bus by using a neutral current as an indicator.

#### B. Particle Swarm Optimization based on Load Balancing Method

The PSO is an optimization method that was developed by Eberhart and Kennedy in 1995. The PSO uses the foraging behavior of a flock of birds to solve an engineering problem by simulating the velocity and distance of a flock of birds to the best result or food location [6]. The PSO is used to search load connection type by using neutral current as an objective function which can be expressed as Eq. (7). The objective condition consists of 2 major variables: branch current's capacity and Voltage Unbalance Factor index (VUF) which can be expressed as Eqs. (8) – (11).

$$\text{Min } I_{Neutral} = \sum_{j=1}^{n-1} I_0(i, j) \quad (7)$$

$$I_+(i, j) < I_{+,m}(i, j) \quad (8)$$

$$I_0(i, j) < I_{0,m}(i, j) \quad (9)$$

$$I_-(i, j) < I_{-,m}(i, j) \quad (10)$$

$$\%VUF < 3\% \quad (11)$$

Where  $I_{Neutral}$  is a sum of neutral current of system,  $I_+(i, j)$ ,  $I_0(i, j)$ , and  $I_-(i, j)$  are positive current, neutral current, and negative current at each bus which  $i$  index,  $j$  index, and  $n$  index are beginning bus, ending bus and total bus, respectively.  $I_{+,m}(i, j)$ ,  $I_{0,m}(i, j)$  and  $I_{-,m}(i, j)$  are maximum current capacity of positive bus, neutral bus and negative bus at each bus  $i$  to bus  $j$ . Which the procedure of load balancing with PSO optimization is shown in Fig 3.

#### C. Voltage Unbalance Factor (VUF)

The VUF is an index that is used to measure voltage differences at the positive pole and negative pole in the system. The high VUF can be led to power loss and heat on the neutral wire. In the worst case, the neutral wire can be burned down. The electrical standard association such as NEMA or ANSI recommends the limitation of VUF within 3%. The VUF can be calculated by using Eq. (12) as follows [7].

$$\%VUF = \frac{|V_{(+),i} - V_{(-),i}|}{\frac{V_{(+),i} + V_{(-),i}}{2}} \times 100\% \quad (12)$$

Where  $V_{(+),i}$  and  $V_{(-),i}$  are positive and negative voltage at bus  $i$ .

### IV. SIMULATION RESULT

#### A. Source Code Validation

The authors in [2] use the PSCAD program to find the voltage solution of bipolar DC microgrid. to validate a program of this paper that writes and run-on the MATLAB program. This subsection presents a comparison of the proposed GMM with PSCAD to validate the result of the program by using a bipolar DC microgrid as shown in Fig. 4.

TABLE I. VALIDATION CASE SIMULATION RESULT

| Bus                                 | PSCAD         |               |               | GMM           |               |               |
|-------------------------------------|---------------|---------------|---------------|---------------|---------------|---------------|
|                                     | $V_+$<br>(kV) | $V_0$<br>(kV) | $V_-$<br>(kV) | $V_+$<br>(kV) | $V_0$<br>(kV) | $V_-$<br>(kV) |
| 1                                   | 18.700        | 0             | -18.700       | 18.700        | 0             | -18.870       |
| 2                                   | 18.619        | 0             | -18.619       | 18.561        | 0             | -18.561       |
| 3                                   | 18.588        | 0             | -18.588       | 18.502        | 0             | -18.502       |
| 4                                   | 18.588        | 0             | -18.588       | 18.442        | 0             | -18.442       |
| The average error of simulation (%) |               |               |               |               |               | 0.31          |

TABLE I. shows a simulation result validation of source code that has 0.31 % of average error. The reason for error may be comprised of line resistance and iteration method which don't exactly determine in the reference research paper.

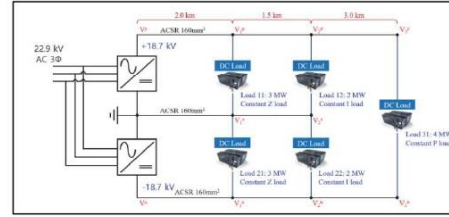


Figure 4 simulation model of PSCAD program

#### B. Base Case

This section simulates bipolar DC microgrid to calculate neutral current, power loss, and VUF of the entire system. The simulation system uses a modified IEEE-69 bus with P constant load type by using the program in subsection A of section IV which the base voltage and base power are 3000 V<sub>DC</sub> and 100 kW. Respectively. The line resistance of this simulation refers to the line resistance of the IEEE-69 bus system and load at each bus as shown in TABLE II. The simulation results as shown in TABLE II that show a load connection type, neutral current, power loss, and maximum VUF of an entire existing system.

Where  $P_{L+}$  and  $P_{L-}$  represent positive load power or positive connection and negative load power or negative connection, respectively. A simulation result shows a load unbalances problem which can observe at the neutral voltage of the whole system. This problem is caused by a load unbalance capacity of connection type at each node which leads to increased neutral current and power loss in the neutral conductor. So, the unbalance problem can estimate by using neutral current flow at each branch of the system with VUF and maximum current capacity at each bus of the system. From the problem, the load balancing method can be used to solve this problem by using the optimization method.

TABLE II. BASE CASE SIMULATION RESULT

| bus              | $P_{L+}$<br>(kW) | $P_L$<br>(kW) | bus             | $P_{L+}$<br>(kW) | $P_L$<br>(kW) | bus             | $P_{L+}$<br>(kW) | $P_L$<br>(kW) |
|------------------|------------------|---------------|-----------------|------------------|---------------|-----------------|------------------|---------------|
| 1                | 0.00             | 0.00          | 24              | 2.80             | 2.00          | 47              | 0.00             | 0.00          |
| 2                | 0.00             | 0.00          | 25              | 0.00             | 0.00          | 48              | 7.90             | 5.64          |
| 3                | 0.00             | 0.00          | 26              | 1.40             | 1.00          | 49              | 38.47            | 27.45         |
| 4                | 0.00             | 0.00          | 27              | 1.40             | 1.00          | 50              | 38.47            | 27.45         |
| 5                | 0.00             | 0.00          | 28              | 2.60             | 1.86          | 51              | 4.05             | 2.83          |
| 6                | 0.26             | 0.22          | 29              | 2.60             | 1.86          | 52              | 0.36             | 0.27          |
| 7                | 4.04             | 3.00          | 30              | 0.00             | 0.00          | 53              | 0.43             | 0.35          |
| 8                | 7.50             | 5.40          | 31              | 0.00             | 0.00          | 54              | 2.64             | 1.90          |
| 9                | 3.00             | 2.20          | 32              | 0.00             | 0.00          | 55              | 2.40             | 1.72          |
| 10               | 2.80             | 1.90          | 33              | 1.40             | 1.00          | 56              | 0.00             | 0.00          |
| 11               | 14.50            | 10.40         | 34              | 1.95             | 1.40          | 57              | 0.00             | 0.00          |
| 12               | 14.50            | 10.40         | 35              | 0.60             | 0.40          | 58              | 0.00             | 0.00          |
| 13               | 0.80             | 0.50          | 36              | 2.60             | 1.85          | 59              | 10.00            | 7.20          |
| 14               | 0.80             | 0.55          | 37              | 2.60             | 1.85          | 60              | 0.00             | 0.00          |
| 15               | 0.00             | 0.00          | 38              | 0.00             | 0.00          | 61              | 124.40           | 88.80         |
| 16               | 4.55             | 3.00          | 39              | 2.40             | 1.70          | 62              | 3.20             | 2.30          |
| 17               | 6.00             | 3.50          | 40              | 2.40             | 1.70          | 63              | 0.00             | 0.00          |
| 18               | 6.00             | 3.50          | 41              | 0.12             | 0.10          | 64              | 22.70            | 16.20         |
| 19               | 0.00             | 0.00          | 42              | 0.00             | 0.00          | 65              | 5.90             | 4.20          |
| 20               | 0.10             | 0.06          | 43              | 0.60             | 0.43          | 66              | 1.80             | 1.30          |
| 21               | 11.40            | 8.10          | 44              | 0.00             | 0.00          | 67              | 1.80             | 1.30          |
| 22               | 0.50             | 0.35          | 45              | 3.92             | 2.63          | 68              | 2.80             | 2.00          |
| 23               | 0.00             | 0.00          | 46              | 3.92             | 2.63          | 69              | 2.80             | 2.00          |
| $I_{Neutral}(A)$ | 713.77           |               | Maximum VUF (%) | 6.15             |               | Power Loss (kW) | 49.54            |               |

C. Load Balancing Case

This subsection proposes a load balancing method to balance the positive and negative load at each bus to reduce neutral current, power loss, and VUF of bipolar DC microgrid by using PSO to search optimal connection type of load at each bus. The result of this method is shown in TABLE III and the comparison of base case and load balancing case as shown in TABLE III and TABLE IV. The PSO convergence characteristic is shown in Fig 5.

TABLE III. LOAD BALANCING CASE SIMULATION RESULT

| bus              | $P_r$ (kW) | $P_s$ (kW) | bus             | $P_r$ (kW) | $P_s$ (kW) | bus             | $P_r$ (kW) | $P_s$ (kW) |
|------------------|------------|------------|-----------------|------------|------------|-----------------|------------|------------|
| 1                | 0.00       | 0.00       | 24              | 2.80       | 2.00       | 47              | 0.00       | 0.00       |
| 2                | 0.00       | 0.00       | 25              | 0.00       | 0.00       | 48              | 5.64       | 7.90       |
| 3                | 0.00       | 0.00       | 26              | 1.00       | 1.40       | 49              | 38.47      | 27.45      |
| 4                | 0.00       | 0.00       | 27              | 1.40       | 1.00       | 50              | 27.45      | 38.47      |
| 5                | 0.00       | 0.00       | 28              | 4.46       | -          | 51              | 2.83       | 4.05       |
| 6                | 0.22       | 0.26       | 29              | 1.86       | 2.60       | 52              | 0.36       | 0.27       |
| 7                | 3.00       | 4.04       | 30              | 0.00       | 0.00       | 53              | 0.78       | -          |
| 8                | 5.40       | 7.50       | 31              | 0.00       | 0.00       | 54              | 4.5        | -          |
| 9                | 3.00       | 2.20       | 32              | 0.00       | 0.00       | 55              | -          | 4.12       |
| 10               | 1.90       | 2.80       | 33              | 2.40       | -          | 56              | 0.00       | 0.00       |
| 11               | 14.50      | 10.40      | 34              | 1.40       | 1.95       | 57              | 0.00       | 0.00       |
| 12               | 10.40      | 14.50      | 35              | 0.40       | 0.60       | 58              | 0.00       | 0.00       |
| 13               | 1.30       | -          | 36              | 2.60       | 1.85       | 59              | -          | 17.20      |
| 14               | 0.55       | 0.80       | 37              | -          | 4.45       | 60              | 0.00       | 0.00       |
| 15               | 0.00       | 0.00       | 38              | 0.00       | 0.00       | 61              | 124.40     | 88.80      |
| 16               | 4.55       | 3.00       | 39              | 4.10       | -          | 62              | 2.30       | 3.20       |
| 17               | -          | 9.50       | 40              | 2.40       | 1.70       | 63              | 0.00       | 0.00       |
| 18               | 9.50       | -          | 41              | -          | 0.22       | 64              | 16.20      | 22.70      |
| 19               | 0.00       | 0.00       | 42              | 0.00       | 0.00       | 65              | -          | 10.10      |
| 20               | 0.16       | -          | 43              | -          | 1.03       | 66              | 3.10       | -          |
| 21               | 8.10       | 11.40      | 44              | 0.00       | 0.00       | 67              | -          | 3.10       |
| 22               | -          | 0.85       | 45              | 3.92       | 2.63       | 68              | 2.00       | 2.80       |
| 23               | 0.00       | 0.00       | 46              | 2.63       | 3.92       | 69              | 2.80       | 2.00       |
| $I_{Neutral}(A)$ | 76.40      |            | Maximum VUF (%) | 0.32       |            | Power Loss (kW) | 40.40      |            |

TABLE IV. A COMPARISON OF SIMULATION RESULT

| Index             | Base Case | Load Balancing Case | % Reduction |
|-------------------|-----------|---------------------|-------------|
| $I_{Neutral}$ (A) | 713.77    | 76.40               | 89.29       |
| Maximum VUF (%)   | 6.15      | 0.32                | 94.79       |
| Power loss (kW)   | 49.54     | 40.40               | 18.44       |

TABLE III shows a load capacity at each bus of modified IEEE-69 bus which is a result of the load balancing method by using PSO.

The convergence of PSO shows an objective function value or sum of neutral current of PSO at each iteration. A comparison shows the efficiency of the load balancing method which can reduce neutral current up to 89.29 % or reduce power loss up to 18.44 % and improve VUF up to 94.79 %

TABLE III shows a load capacity at each bus of modified IEEE-69 bus which is a result of the load balancing method by using PSO.

The convergence of PSO shows an objective function value or sum of neutral current of PSO at each iteration. A comparison shows the efficiency of the load balancing method which can reduce neutral current up to 89.29 % or reduce power loss up to 18.44 % and improve VUF up to 94.79 %

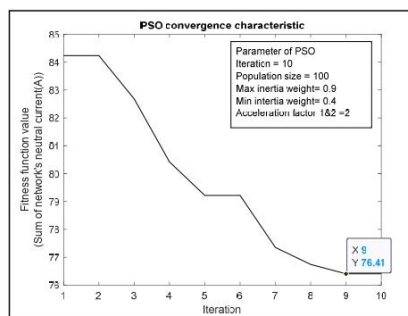


Figure 5 convergence characteristic

V. CONCLUSION

This paper presents a power flow model of bipolar DC power distribution system and load balancing method that is used to determine the load connection strategy. The load balancing method uses the sum of neutral current, VUF, power loss and considers current capacity at each branch as an objective function and various conditions which was solved by using PSO. The load balancing method can be reduced neutral current up to 89.29 % or reduce power loss up to 18.44 % and improve VUF up to 94.79 %.

In the future, this work will integrate with distributed generation to plan and design DC nano grids such as university, community mail, etc. to reduce peak-power during peak hours and reduce transmission power loss in nano grid.

ACKNOWLEDGMENT

This work was supported by the School of Electrical Engineering Institute of Engineering, Suranaree University of Technology.

REFERENCES

- [1] Fleischer, K. R., & Munnings, R. S. (n.d.). Power Systems Analysis for direct current (DC) distribution systems. *Proceedings of Industrial and Commercial Power Systems Conference*. <https://doi.org/10.1109/icps.1994.303571>
- [2] Kim J, Cho J, Kim H, Cho Y, & Lee H (2020). Voltage Balancing for Bipolar DC Distribution Grids: A Power Flow based Binary Integer Multi-Objective Optimization Approach. *KEPCO Journal on Electric Power and Energy*, 4(4), 419–425. <https://doi.org/10.18770>
- [3] Byeon, G., Yoon, T., Oh, S., & Jang, G. (2013). Energy Management Strategy of the DC distribution system in buildings using the EV service model. *IEEE Transactions on Power Electronics*, 28(4), 1544–1554. <https://doi.org/10.1109/tpel.2012.2210911>
- [4] Chew, B. S., Xu, Y., & Wu, Q. (2019). Voltage balancing for bipolar DC distribution grids: A power flow based binary integer multi-objective optimization approach. *IEEE Transactions on Power Systems*, 34(1), 28–39. <https://doi.org/10.1109/tpwrs.2018.2866817>
- [5] Zhou, X. S., Liang, H., & Ma, Y. J. (2013). Review of Electric Load Modeling Research. *Advanced Materials Research*, 811, 627–630. <https://doi.org/10.4028/www.scientific.net/amr.811.627>
- [6] Almadieh, M., Tavakoli, H., Teshnehlab, M., & Aliyari, M. (2009). Novel binary particle swarm optimization. *Particle Swarm Optimization*. <https://doi.org/10.5772/6738>
- [7] Lin, T., & Domijan, A. (2005). On power quality indices and real time measurement. *IEEE Transactions on Power Delivery*, 20(4), 2552–2562. <https://doi.org/10.1109/tpwrd.2005.85233>

Received 30 April 2023, accepted 28 May 2023, date of publication 23 June 2023, date of current version 7 July 2023.

Digital Object Identifier 10.1109/ACCESS.2023.3289160

## RESEARCH ARTICLE

# Loss Minimization for Bipolar DC Distribution Grid Considering Probabilistic EV Charging Load Using Load Balancing Method

GUNTINAN SAKULPHAISAN<sup>✉</sup>, (Graduate Student Member, IEEE),  
AND KEERATI CHAYAKULKHEEREE<sup>✉</sup>, (Senior Member, IEEE)

School of Electrical Engineering, Institute of Engineering, Suranaree University of Technology, Nakhon Ratchasima 30000, Thailand

Corresponding author: Keerati Chayakulkheeree (keerati.ch@sut.ac.th)

This work was supported by the Suranaree University of Technology.

**ABSTRACT** This paper proposes a novel method for power loss minimization and voltage unbalance mitigation in bipolar DC distribution grid (DCDG) considering probabilistic electric vehicle (EV) charging load. In the proposed method, a power flow analysis for the bipolar DCDG is performed by G-matrix and Gauss's iteration methods. The Monte Carlo Simulation (MCS) is used to evaluate the impact of EV charging load demand in probabilistic manner. To reduce the impact of the voltage unbalance problem and minimize power loss of the system, particle swarm optimization (PSO) is employed to search for an optimal load connection type that can minimize voltage unbalance factor (VUF) and total power loss. The proposed method was tested with 21-bus DC bipolar system with several cases to verify the potential of the method. The results shown that the proposed method can successfully minimize total power loss and reduce the VUF of the system with probabilistic EV charging load consideration. Therefore, the proposed methodology can be useful for enhancing DCDG operation and mitigating the impact of EV charging.

**INDEX TERMS** EV charging load, load balancing method, dc power flow, bipolar DC distribution grid.

## I. INTRODUCTION

In 1883, a DC distribution system was proposed by Edison for lighting system [1]. Nowadays, the increment of distribution energy resource (DERs) penetration stimulates the interest of DC distribution grid (DCDG). Examples of DCDG are data center and telecommunication systems, which use 48 V<sub>dc</sub> [2]. As widely known, DCDG has many advantages over AC distribution system. Meanwhile, DCDG has many limitations such as difficulties on high-range voltage levels changing and large DC power generation. A load level increasing in DCDG will cause of voltage drop and high-power loss so the system with high voltage level usually provides better system efficiency and reliability. A voltage level step up or step down of DC voltage need DC – DC converter that have low voltage changing ratio when compare with AC distribution system. The AC distribution system uses transformer to change

voltage level which have high voltage changing ratio. For the reason, the AC distribution system technology development becomes popular than DC distribution technology from the past to the present. Three key benefits of home DC power systems over AC systems are as follow: 1. high efficiency, 2. high power quality and 3. not require a synchronization.

Most of present households' appliance use DC power for their internal circuit. Therefore, the household appliances in DC distribution are not require AC – DC converter. In case of electric vehicles (EVs) charging pile, the power loss of power converter stage can be reduced.

In DC systems, the majority of the power quality concerns, that are prevalent in the AC power system, can be easier prevented. Home equipment powered by DC are not experience frequency variation and rarely facing for voltage swell and voltage sag. Additionally, compared to AC microgrids, the cooperative control of PV, wind turbines, and ESS in the DC system is simpler due to the DC power system does not need synchronization feature for distributed generation [3].

The associate editor coordinating the review of this manuscript and approving it for publication was S. K. Panda<sup>✉</sup>.

This work is licensed under a Creative Commons Attribution-NonCommercial-NoDerivatives 4.0 License.  
For more information, see <https://creativecommons.org/licenses/by-nc-nd/4.0/>

Moreover, a distribution system is facing an emerging high penetration of electric vehicles (EVs) that can extremely increase in load demand leading to effects on stability and security of distribution system [4]. Aforementioned, a load management strategy such as load leveling, load filling or load shifting can reduce an impact of load charging demand by transfer load demand from peak-hours to off-peak hours. On the other hands, a battery of EV can be acted as moveable energy storage device that can charge electricity from grid during off-peak hours and then discharge to grid during peak-hours [5]. Generally, a peak charging time of EV is in the evening and lessen charging load in the morning. A charging load demand evaluation was present in [6] based on Monte Carlo to model a large scale of EV charging demand. The load demand evaluation can be used to limit charging power at charging station via operator or used to manage charging power level of smart charging station for manage load charging demand based on charger connecting time and disconnection time [7], [8], [9].

This paper, therefore, proposes the load balancing method for power loss minimization in bipolar DCDG, considering probabilistic EV charging load. In the proposed method, the particle swarm optimization (PSO) is used to determine the optimal connection for the load at each bus. Meanwhile, the Monte Carlo Simulation (MCS) is used to represent the probabilistic EV charging load in the system.

Aforementioned, the paper was separated into six sections as follow: Section I is the introduction on a DCDG and the influence of EV on distribution system. Next, Section II addresses the overview of voltage level in DCDG including characteristics of unipolar and bipolar DC distribution system. The bus topology of DCDG is illustrated in Section III. Section IV presents bipolar DC power flow calculation. After that, Section V presents a load balancing method which is used to obtain the optimal connection type of load in bipolar DCDG with EV charging station to minimize the power loss of the system. The probabilistic EV charging load model is addressed in Section VI. Section VII presents a simulation result on 21-bus bipolar DC distribution system which comprises of five study cases. Lastly, conclusion is given in section VIII

## II. OVERVIEW OF DCDG

The DCDG voltage level is one of main challenges for DCDG voltage standardization. The difference voltage level offer opportunity for a group of users to choose suitable voltage for loads such as residential, commercial and industrial load [10]. Fortunately, the power electronic technology development can bring a new opportunity for DC power distribution.

In case of residential nano grid, A 48 V<sub>DC</sub> is preferred to interface renewable energy resource to load. However a limitation of 48 VDC is a transmission radius limit in distribution system with multiple households [11].

The primary problem of DC power distribution is voltage level selection of the distribution system. Many standards such as IEC 60038 or IEEE Standard 1709-2010 design to

cover field of automotive, marine, computer electronic and aerospace power system that have a specific DC low voltage range, but do not cover a field of distribution system. The medium voltage and low voltage DC (LVDC) distribution voltage guidelines are being developed by China which the desired value of DC voltage level for low voltage distribution 1000V,600V, 440V, 400V, 336V, 240V and 220V [12].

Meanwhile, the voltage level of the LVDC distribution system testbed used by the CIRED workshop is  $\pm 750$ V. Therefore, 750V is a one of popular choices for the residential DC power systems [13]. A highest LVDC is 1.5 kV for distribution system that is a 750 V bipolar distribution grid that offer two voltage level options for residential load that comprise of  $\pm 750$  V and  $\pm 1.5$  kV with DC converter as an interface to match the voltage levels for households' loads [14].

## III. BUS TOPOLOGY OF DCDG

A DCDG comprises of 1.) DC bus 2.) AC/DC converter, and 3.) load. Normally, a DC bus is used to connect to main grid via AC/DC converter to convert AC voltage to DC voltage and serve power to the load. To compare a loss characteristic of AC distribution system with DCDG, DCDG is a good solution to reduce power loss by reduce amount of power conversion. The system efficiency, cost, and system size are the advantage of DCDG. Additionally, DCDG has high stability owing to the absence of reactive power and is more suitable for distributed energy resources (DERs) integration [15]. Moreover, DCDG can transmit power with two configurations which are unipolar and bipolar systems, that offer difference system abilities such as available voltage level, reliability and power quality.

### A. DC UNIPOLAR BUS TOPOLOGY

A DC unipolar system bus topology like a single-phase AC power system that has only two wires for distribute power to load. In case of DC unipolar bus, the wires are called positive wire and negative wire which a source and loads are connected between the wires, as shown in FIGURE 1. The energy is transferred through the DC bus with single voltage level. So, the DC bus voltage level choosing is important in this system. The system capability depends on voltage level which the high voltage level can increase power transmission system capability, but the DC-DC converter is needed reduce the user voltage level for safety uses. The suitable voltage level selection can avoid large number of DC – DC converter deployment. This topology is practical for off-grid homes in isolated rural locations without utility grid infrastructure. DC unipolar system is simple to implement with symmetry between the pole. On the other hand, a single fault can be led to shut down the system and does not offer different voltage levels option to the users [16], [17].

### B. DC BIPOLAR BUS TOPOLOGY

A DC bipolar bus topology has some advantage over DC unipolar bus topology. Its structure is similar to a three-phase

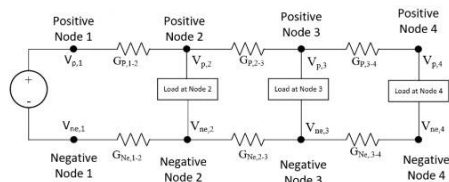


FIGURE 1. Typical DC unipolar bus topology.

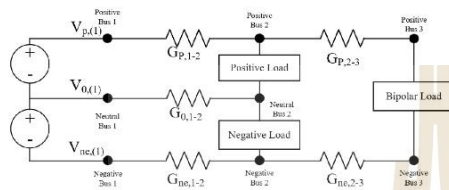


FIGURE 2. Typical DC bipolar bus topology.

AC power system with three wires for transferring energy to load. The wires are called positive line, negative line and neutral line, as shown in FIGURE 2. The topology offers three voltage levels option which consisted of  $+V_{DC}$ ,  $-V_{DC}$  and  $2V_{DC}$ . Under a fault condition, the load at fault bus in bipolar DC bus topology can be transfer to other pole at same bus. Therefore, the reliability, power quality and availability of the system during fault condition are better than unipolar DC bus topology. A difference voltage levels option offers a flexibility to consumer, but can result in the system unbalance condition. The unbalance condition can increase neutral current flow and lead to increase in overall system power loss. So, the system requires a voltage balancer or load balance strategy to prevent unbalance condition [18].

**IV. BIPOLAR DC POWERFLOW CALCULATION**

FIGURE 3 represents the components of bipolar DC power system which comprises of DC substation, transmission line and load (positive load, negative load and bipolar load). This paper uses the method called G-Matrix Method (GMM) for DC load flow analysis [19]. To calculate a power flow model, the network component comprises of two type of bus which are source and load buses. The source bus is replaced by slack bus which represent by index '1' and load bus starts at index '2' to index 'n'. The conductance of every transmission line between bus is donated by  $G_{ij}$  which index 'i' to index 'j' are starting bus and ending bus of conductance in [G]. A bipolar DC network have three cables. So, in [G] have to consists of  $G_{+}/0/-$  that represents cable conductance of positive neutral and negative cable from bus i to bus j.  $V_{+}/0/-$  is a positive, neutral and negative voltage at bus i while  $I_{p}/n/b$  represent load current at each pole.  $I_p$  and  $I_n$  are called unipolar load that draw load current from positive pole or negative pole and return to substation via neutral pole.  $I_b$  represent a bipolar

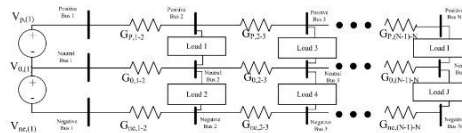


FIGURE 3. Component of DC power system.

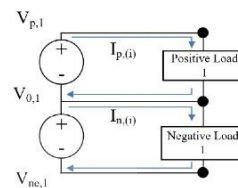


FIGURE 4. Unipolar connection in bipolar DC bus topology.

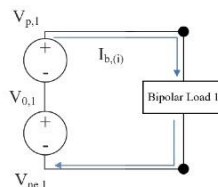


FIGURE 5. Current flow in Bipolar connection of bipolar DC bus topology.

load that draws load current from positive pole and return to substation via negative pole. So, the single line diagram is modeled by nodal analysis that represent the relationship of unipolar and bipolar load current. The direction of loads currents is shown in FIGURE 4 and FIGURE 5.

A load voltage drop can be calculated by consider the difference of voltage between connection pole as,

$$V_{p,i} = V_{+,i} - V_{0,i} \text{ and} \tag{1}$$

$$V_{n,i} = V_{0,i} - V_{-,i}. \tag{2}$$

where  $V_{p,i}$  represents voltage drop of unipolar load at bus i when refer positive pole and neutral pole.  $V_{+,i}$ ,  $V_{-,i}$  and  $V_{0,i}$  represent voltage at positive pole, voltage at negative pole and neutral pole at bus i, respectively. Therefore,  $V_{+,i}$  and  $V_{-,i}$  represent voltage drop of unipolar load at bus i when refer to the neutral pole and negative pole. The sign of  $V_{-,i}$  must be negative to present a direction of current flow from neutral pole to negative pole that represent a current must flow from high voltage to low voltage.

The voltage drops at each bus from Equations (1)-(2) are used to calculate currents at each bus by using Equations (3)-(4) as,

$$I_{p,i} = \frac{P_{p,i}}{V_{p,i}} \text{ and} \tag{3}$$

$$I_{n,i} = \frac{P_{n,i}}{V_{n,i}}. \tag{4}$$



where  $I_{p,i}$  and  $I_{n,i}$  represent a positive pole load and negative pole load at bus  $i$  and  $P_{p,i}$  and  $P_{n,i}$  represent unipolar connection load at bus  $i$  that refer to positive and negative load connections.

In case of bipolar load connection, the load connects between positive pole and negative pole, as shown in FIGURE 5. The load nominal voltage is therefore,  $2V_{DC}$ . The bipolar load voltage drop can be calculated by Equation (5),

$$V_{b,i} = V_{+,i} - V_{-,i}. \quad (5)$$

where  $V_{b,i}$ ,  $V_{+,i}$  and  $V_{-,i}$  are bipolar load voltage drop, positive voltage pole and negative voltage pole. So, the bipolar load current can be calculated by Equation (6),

$$I_{b,i} = \frac{P_{b,i}}{V_{b,i}}. \quad (6)$$

where  $I_{b,i}$  is the bipolar load current at bus  $i$ .  $P_{b,i}$  and  $V_{b,i}$  are bipolar load capacity at bus  $i$  and bipolar load voltage drop at bus  $i$ , respectively. The substation can be replaced as a slack bus which can be assumed the nominal voltages at 1 p.u., 0 p.u., and  $-1$  p.u., for positive bus, neutral bus and negative bus, respectively. The transmission lines are modeled by conductance between buses. So, the power flow equation of system can be calculated by,

$$[I] = [G][V], \quad (7)$$

or

$$\begin{bmatrix} I_p \\ I_0 \\ I_n \end{bmatrix} = \begin{bmatrix} G_p & 0 & 0 \\ 0 & G_0 & 0 \\ 0 & 0 & G_n \end{bmatrix} \begin{bmatrix} V_p \\ V_0 \\ V_n \end{bmatrix}, \quad (8)$$

where

$$V_p = [V_{p,1} \ V_{p,2} \ \dots \ V_{p,N}]^T, \quad (9)$$

$$V_0 = [V_{0,1} \ V_{0,2} \ \dots \ V_{0,N}]^T, \quad (10)$$

$$V_n = [V_{n,1} \ V_{n,2} \ \dots \ V_{n,N}]^T, \quad (11)$$

$$I_p = [I_{p,1}+I_{b,1} \ I_{p,2}+I_{b,2} \ \dots \ I_{p,N}+I_{b,N}]^T, \quad (12)$$

$$I_0 = [I_{0,1} \ I_{0,2} \ \dots \ I_{0,N}]^T, \quad (13)$$

$$I_n = [I_{n,1}+I_{b,1} \ I_{n,2}+I_{b,2} \ \dots \ I_{n,N}+I_{b,N}]^T. \quad (14)$$

$$G_p = \begin{bmatrix} \sum_{i \leftrightarrow 1} G_{p,1i} & -G_{p,12} & \dots & -G_{p,1N} \\ -G_{p,21} & \sum_{i \leftrightarrow 2} G_{p,2i} & -G_{p,23} & -G_{p,2N} \\ \vdots & \vdots & \ddots & \vdots \\ -G_{p,N1} & -G_{p,N2} & \dots & \sum_{i \leftrightarrow N} G_{p,NN} \end{bmatrix}, \quad (15)$$

$$G_0 = \begin{bmatrix} \sum_{i \leftrightarrow 1} G_{0,1i} & -G_{0,12} & \dots & -G_{0,1N} \\ -G_{0,21} & \sum_{i \leftrightarrow 2} G_{0,2i} & -G_{0,23} & -G_{0,2N} \\ \vdots & \vdots & \ddots & \vdots \\ -G_{0,N1} & -G_{0,N2} & \dots & \sum_{i \leftrightarrow N} G_{0,NN} \end{bmatrix}, \quad (16)$$

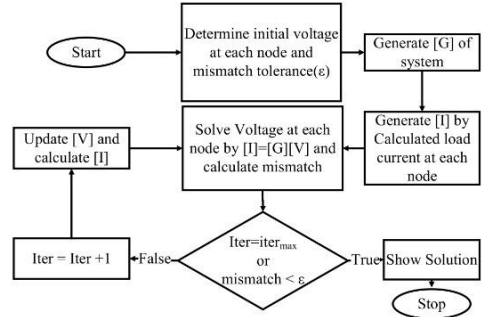


FIGURE 6. Bipolar DC power flow procedure.

$$G_{ne} = \begin{bmatrix} \sum_{i \leftrightarrow 1} G_{ne,1i} & -G_{ne,12} & \dots & -G_{ne,1N} \\ -G_{ne,21} & \sum_{i \leftrightarrow 2} G_{ne,2i} & -G_{ne,23} & -G_{ne,2N} \\ \vdots & \vdots & \ddots & \vdots \\ -G_{ne,N1} & -G_{ne,N2} & \dots & \sum_{i \leftrightarrow N} G_{ne,NN} \end{bmatrix}. \quad (17)$$

where  $[G]$ ,  $[I]$  and  $[V]$  represent conductance matrix, current matrix and voltage matrix of network, respectively. The symbol “ $i \leftrightarrow j$ ” donates “ $i$  connected to  $j$ ”. So, the power flow calculation can be calculated by replace Equation (9)-Equation (17) in Equation (8) to calculate voltage profile, current flow between buses. The computational procedure is shown in FIGURE 6.

## V. PARTICLE SWARM OPTIMIZATION BASED LOAD BALANCING METHOD

In DCDG, the voltage drop between two nodes is depended on the current flow through their interconnecting cables. In the other word, voltage at each bus in DCDG is depended on the distributed load in the grid [20]. So, the main problem of bipolar DCDG is the load unbalance condition, due to the load can be connected to both positive or negative pole, as shown in FIGURE 3. Generally, load unbalance problem is caused by unplanned households’ and EV charging loads [21]. This problem increases current flow in neutral wire, leading to increase in overall system power loss. There are several ways to reduce voltage imbalance in LVDC, For example, the voltage balancer, that controls the voltage of the DC/DC converter at point of common coupling (PCC) to compensate voltage drop at each bus. A demand response or load balancing with electrical price is one of alternative methods to reduce load unbalance by using an energy price to control load demand characteristic of DC bipolar distribution grid and reduce power difference between poles [22].

In this paper, particle swarm optimization (PSO) in [23] is used to search an optimal load connection and EV charging load. The objective function (OF) is to minimize total energy

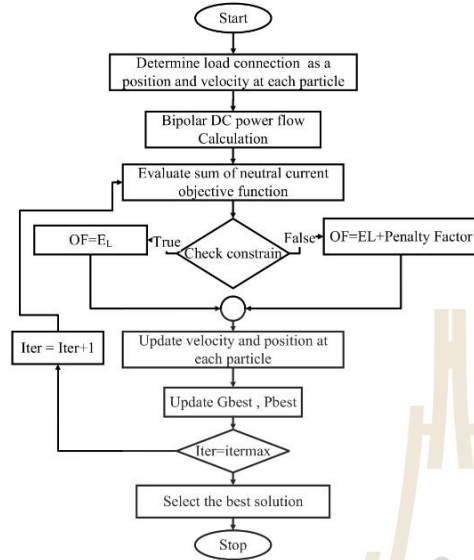


FIGURE 7. PSO based load balancing method procedure.

loss as,

$$\text{Minimize } E_L = \sum_{t=1}^{48} [P_{L,p}(t) + P_{L,0}(t) + P_{L,n}(t)], \quad (18)$$

where

$$P_{L,p} = \sum_{i=1}^{n-1} I_{p,(i,i+1)}^2 G_{p(i,i+1)}, \quad (19)$$

$$P_{L,0} = \sum_{i=1}^{n-1} I_{0,(i,i+1)}^2 G_{0(i,i+1)}, \quad (20)$$

$$P_{L,n} = \sum_{i=1}^{n-1} I_{n,(i,i+1)}^2 G_{n(i,i+1)}, \quad (21)$$

subject to the constraints

$$V_{p \min,i} \leq V_{p,i} \leq V_{p \max,i}, \quad (22)$$

$$V_{0 \min,i} \leq V_{0,i} \leq V_{0 \max,i}, \quad (23)$$

$$V_{p \min,i} \leq V_{p,i} \leq V_{n \max,i}, \text{ and} \quad (24)$$

$$\%VUF < \%VUF_{\max} \quad (25)$$

where subscript  $p$ ,  $0$  and  $n$  represent positive pole, negative pole, and neutral pole, respectively. The computational procedure is shown in FIGURE 7.

## VI. PROBABILISTIC EV CHARGING LOAD BASED ON MONTE CARLO SIMULATION

In this paper, the MCS method is used to simulate various factor that affect to EV charging load characteristic, such as

charging plug-in time and plug-out time, initial state of charge (SOC), daily travel distance, charging duration and charging type. In the home-charging pattern, the EV owners will plug their car when arrive home after work and remove the plug for travel to work. A probabilistic distribution function (PDF) that represent the charging behavior of EV owner can be expressed as,

$$f_c(t_c) = \begin{cases} \frac{1}{\sqrt{2\pi}\sigma_c} \exp\left(-\frac{(t_c + 24 - \mu_c)^2}{2\sigma_c^2}\right), & 0 < t_c \leq \mu_c - 12 \\ \frac{1}{\sqrt{2\pi}\sigma_c} \exp\left(-\frac{(t_c - \mu_c)^2}{2\sigma_c^2}\right), & \mu_c - 12 < t_c \leq 24 \end{cases}, \quad (26)$$

where  $t_c$ ,  $\sigma_c$  and  $\mu_c$  are EV plug-in time, plug-in standard deviation and mean of plug-in time, respectively. The standard deviation and mean of plug-in time are used to generate the sampling probabilistic plug-in time behavior of EV owners.

The PDF that represents the daily travel distance of EV in each day be calculated by,

$$f_d(d) = \frac{1}{\sqrt{2\pi}\sigma_d} \exp\left(-\frac{(d - \mu_d)^2}{2\sigma_d^2}\right), 0 \leq d \leq D \quad (27)$$

where  $d$  is the daily travel distance of the EV.  $D$  is the maximum travel distance at the EV.  $\sigma_c$ , and  $\mu_c$  are the standard deviation and mean of the EV travel distance, respectively.

After calculate the daily travel distance, the result is used to calculate the remaining SOC of EV before charging which can be calculated by,

$$SOC_i = 1 - \frac{d_i}{D_i \times \eta_i}. \quad (28)$$

where subscript  $i$  denotes the parameters of the  $i^{th}$  EV. Whereas,  $\eta_i$ , represents efficiency of the  $i^{th}$  EV.

In the daily scheduling process, the scheduling time is divided into 96 time slot which the length of time slot is 15 minutes. So, the arrival time and departure time of each EV can be calculated by,

$$T_{c,i} = \frac{t_{c,i}}{\Delta T}, \quad (29)$$

$$T_{d,i} = \frac{t_{d,i}}{\Delta T}, \text{ and} \quad (30)$$

$$T_{r,i} = T_{c,i} - T_{d,i}. \quad (31)$$

When  $t_{c,i}$ ,  $t_{d,i}$ , and  $\Delta T$  are plug-in time, plug-off time and duration of time slot, respectively.  $T_{c,i}$ ,  $T_{d,i}$  and  $T_{r,i}$  are plug-in time, plug-off time and remaining time based on time slot, respectively.

To calculate charging level index or charging urgency indicator, the arrival time slot and departure time slot are used to

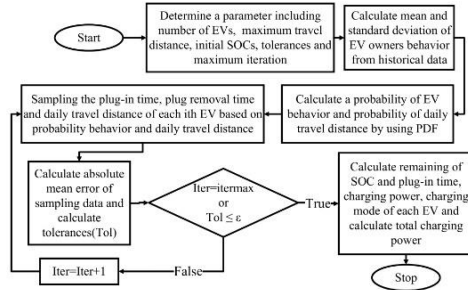


FIGURE 8. MCS based probabilistic EV charging.

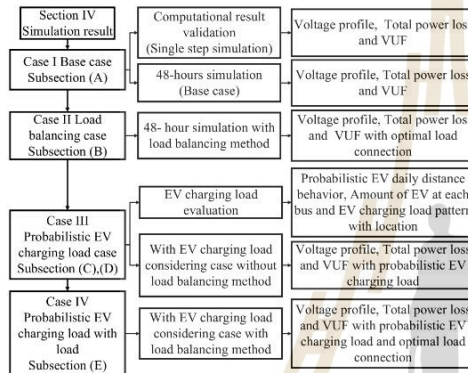


FIGURE 9. Simulation category overview.

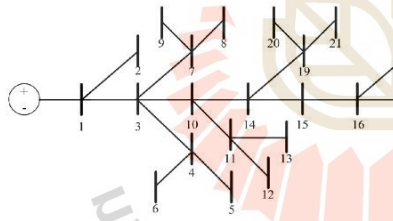


FIGURE 10. IEEE 21 bus case study system.

calculate indicator to manage the charging power level. In this study, the charging urgency indicator is referred to [36] as

$$CUI_i = (T_{r,i} \times \Delta T) \times P_{EV,i}^{slow} \times \eta_{EV} - (SOC_i^{\min} - SOC_i^{\text{con}}) \times Cap_{EV,i}^{\text{batt}} \quad (32)$$

When  $CUI_i$  is charging urgency indicator which is used to choose the charging level of each EV.  $P_{EV,i}^{slow}$ ,  $SOC_i^{\min}$ ,  $SOC_i^{\text{con}}$ , and  $Cap_{EV,i}^{\text{batt}}$  are the slow charging power of EVs, the

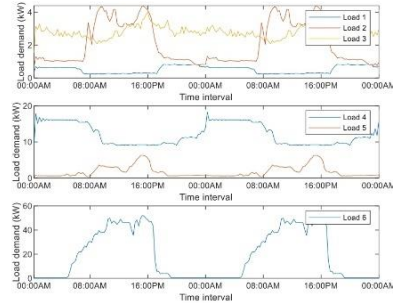


FIGURE 11. 48 hrs. load profile.

TABLE 1. IEEE 21 bus system data.

| From bus | To bus | Resistance |
|----------|--------|------------|
| 1        | 2      | 0.053      |
| 1        | 3      | 0.054      |
| 3        | 4      | 0.054      |
| 4        | 5      | 0.063      |
| 4        | 6      | 0.051      |
| 3        | 7      | 0.037      |
| 7        | 8      | 0.079      |
| 7        | 9      | 0.072      |
| 3        | 10     | 0.053      |
| 10       | 11     | 0.038      |
| 11       | 12     | 0.079      |
| 11       | 13     | 0.078      |
| 10       | 14     | 0.083      |
| 14       | 15     | 0.065      |
| 15       | 16     | 0.064      |
| 16       | 17     | 0.074      |
| 16       | 18     | 0.081      |
| 14       | 19     | 0.078      |
| 19       | 20     | 0.084      |
| 19       | 21     | 0.082      |

minimum SOC required for the  $i^{\text{th}}$  EV after charging, the SOC level of the  $i^{\text{th}}$  EV when connected to charger, and the battery capacity of the  $i^{\text{th}}$  EV, respectively. If  $CUI_i$  is higher than 0, the charging level is slow charging level. In the other hand, the  $CUI_i$  is less than 0, the charging level is fast charging level. The procedure of probabilistic EV load model based on MCS is shown in FIGURE 8.

In FIGURE 8, the EV owner behavior comprises of daily travel distance, charging time and unplugging time are presented. The EV owners data is used to calculate mean, standard deviation and PDF to present the likelihood of EV owners' activities.

## VII. SIMULATION RESULT

The simulation study can be separated into 4 cases including,

- Case I : Base case,
- Case II : Load balancing case,
- Case III : Probabilistic EV charging load case, and

TABLE 2. IEEE 21 load data for validation simulation.

| Bus | Positive Pole Load (kW) | Negative Pole Load (kW) | Bipolar Load (kW) |
|-----|-------------------------|-------------------------|-------------------|
| 1   | 0                       | 0                       | 0                 |
| 2   | 70                      | 100                     | 0                 |
| 32  | 0                       | 0                       | 0                 |
| 4   | 36                      | 40                      | 120               |
| 5   | 4                       | 0                       | 0                 |
| 6   | 36                      | 0                       | 0                 |
| 7   | 0                       | 0                       | 0                 |
| 8   | 32                      | 50                      | 0                 |
| 9   | 80                      | 0                       | 100               |
| 10  | 0                       | 10                      | 0                 |
| 11  | 45                      | 30                      | 0                 |
| 12  | 68                      | 70                      | 0                 |
| 13  | 10                      | 0                       | 75                |
| 14  | 0                       | 0                       | 0                 |
| 15  | 22                      | 30                      | 0                 |
| 16  | 23                      | 10                      | 0                 |
| 17  | 43                      | 0                       | 60                |
| 18  | 34                      | 60                      | 0                 |
| 19  | 9                       | 15                      | 0                 |
| 20  | 21                      | 10                      | 50                |
| 21  | 21                      | 20                      | 0                 |

TABLE 3. Load Connection type of base case.

| Bus | Positive pole Load      | Negative Pole Load        | Bipolar Load |
|-----|-------------------------|---------------------------|--------------|
| 1   | -                       | -                         | -            |
| 2   | Load 2(A),<br>Load 3(B) | -                         | -            |
| 3   | -                       | -                         | -            |
| 4   | -                       | Load 1(A),<br>Load 5(B)   | Load 4       |
| 5   | -                       | Load 2(A)                 | -            |
| 6   | -                       | Load 2(A)                 | -            |
| 7   | -                       | -                         | -            |
| 8   | Load 1 (A)              | Load 2(B)                 | -            |
| 9   | Load 2 (A)              | -                         | Load 4       |
| 10  | -                       | Load 3 (B)                | -            |
| 11  | -                       | Load 1 (A),<br>Load 2 (B) | -            |
| 12  | -                       | Load 4 (A),<br>Load 5 (B) | -            |
| 13  | -                       | -                         | Load 6       |
| 14  | -                       | -                         | -            |
| 15  | Load 5 (A)              | Load 1 (B)                | -            |
| 16  | Load 5 (A)              | Load 3 (B)                | -            |
| 17  | -                       | Load 5 (A)                | Load 6       |
| 18  | -                       | Load 2 (A),<br>Load 5 (B) | -            |
| 19  | -                       | Load 1 (A),<br>Load 2(B)  | -            |
| 20  | -                       | Load 1 (A),<br>Load 3(B)  | Load 6       |
| 21  | -                       | Load 1 (A),<br>Load 2(B)  | -            |

Case IV : Probabilistic EV charging load with load balancing case.

The simulation study comprises of two categories as follow: 1) single step simulation 2) 48-hours simulation. A single step simulation is used to validate computational result and illustrate the load affect to voltage profile via *VUF* and evaluate power loss of the system. A 48-hours simulation

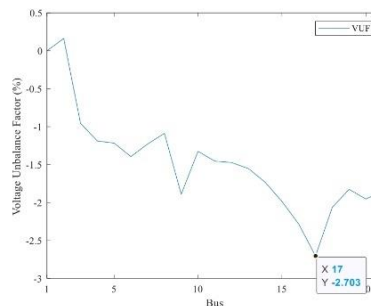


FIGURE 12. Voltage unbalance factor at each bus of base case result.

TABLE 4. Base case simulation result.

| Bus                   | Voltage (V) (simulation) |       |         | Voltage (V) (reference) |       |         |
|-----------------------|--------------------------|-------|---------|-------------------------|-------|---------|
|                       | V+                       | V0    | V-      | V+                      | V0    | V-      |
| 1                     | 1000                     | 0     | -1,000  | 1,000                   | 0     | -1,000  |
| 2                     | 996.28                   | -1.62 | -994.66 | 996.28                  | -1.62 | -994.66 |
| 3                     | 959.52                   | 9.22  | -968.74 | 959.52                  | 9.22  | -968.74 |
| 4                     | 951.76                   | 11.37 | -963.14 | 951.76                  | 11.37 | -963.14 |
| 5                     | 951.50                   | 11.64 | -963.14 | 951.50                  | 11.64 | -963.14 |
| 6                     | 949.80                   | 13.33 | -963.14 | 949.80                  | 13.33 | -963.14 |
| 7                     | 953.12                   | 11.77 | -964.89 | 953.12                  | 11.77 | -964.89 |
| 8                     | 950.43                   | 10.39 | -960.82 | 950.43                  | 10.39 | -960.82 |
| 9                     | 943.11                   | 17.80 | -961.11 | 943.11                  | 17.10 | -961.11 |
| 10                    | 936.57                   | 12.49 | -949.06 | 936.57                  | 12.49 | -949.06 |
| 11                    | 929.93                   | 13.62 | -943.55 | 929.93                  | 13.62 | -943.55 |
| 12                    | 924.02                   | 13.71 | -937.73 | 924.02                  | 13.71 | -937.73 |
| 13                    | 925.94                   | 14.48 | -940.41 | 925.94                  | 14.48 | -940.41 |
| 14                    | 915.16                   | 15.99 | -931.15 | 915.16                  | 15.99 | -931.15 |
| 15                    | 903.90                   | 18.11 | -922.02 | 903.90                  | 18.11 | -922.02 |
| 16                    | 894.41                   | 20.66 | -915.07 | 894.41                  | 20.66 | -915.66 |
| 17                    | 888.26                   | 24.34 | -912.60 | 888.26                  | 24.34 | -912.60 |
| 18                    | 891.25                   | 18.58 | -909.83 | 891.25                  | 18.58 | -909.83 |
| 19                    | 908.55                   | 16.74 | -925.29 | 908.55                  | 16.74 | -925.29 |
| 20                    | 904.26                   | 17.83 | -922.09 | 904.26                  | 17.83 | -922.09 |
| 21                    | 906.62                   | 16.98 | -923.54 | 906.61                  | 16.93 | -923.54 |
| Validation error (%)  |                          |       |         | <0.01 %                 |       |         |
| Total power loss (kW) |                          |       |         | 95.42                   |       |         |
| Maximum VUF (%)       |                          |       |         | -2.7 (At bus 17)        |       |         |

is used to simulate ability of load balancing method in cases with and without EV charging load based on MCS. The simulation study overview is shown in FIGURE 9.

The IEEE 21-bus system is used as test system. The system topology is showed in FIGURE 10 and the parameters of the system are shown in TABLE 1 to TABLE 3. In case of 48 hours simulation, the system load profile data are shown in FIGURE 10 with load types in TABLE 3.

A. BASECASE

This subsection presents the result of power flow solving of bipolar DCDG to validate a simulation result with reference [37] and used to compare with other cases for evaluate

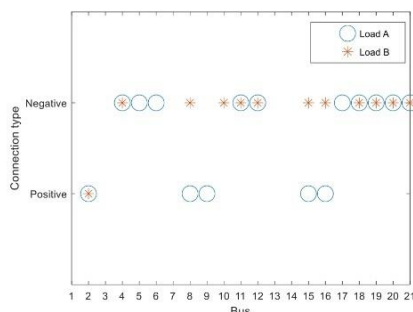


FIGURE 13. Load connection type of base case.

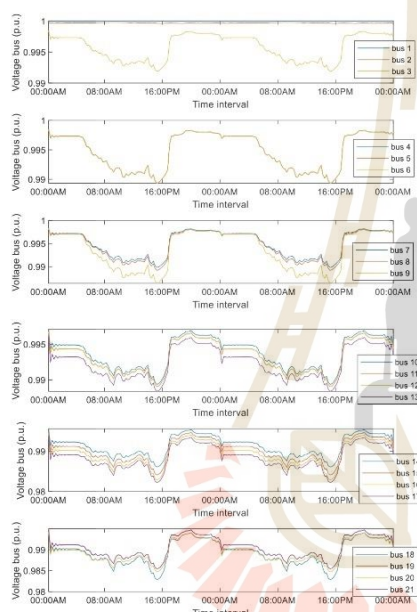


FIGURE 14. Positive voltage profile of base case.

the performance of the proposed method. The simulation result is shown in TABLE 4. FIGURE 12 presents the *VUFs* of the system at all buses.

In TABLE 4, the simulation results including the base case voltage unbalance factor, voltage profile and total loss are addressed. The positive *VUF* is due to load at negative pole is higher than that of in positive pole in each bus. In the other hand, the negative *VUF* is due to positive pole load higher than that of in negative pole. The simulation resulted in the highest *VUF* of -2.7% at bus 17, and total power loss is 95.42 kW with mismatch error less than 0.01 %. FIGURE 13

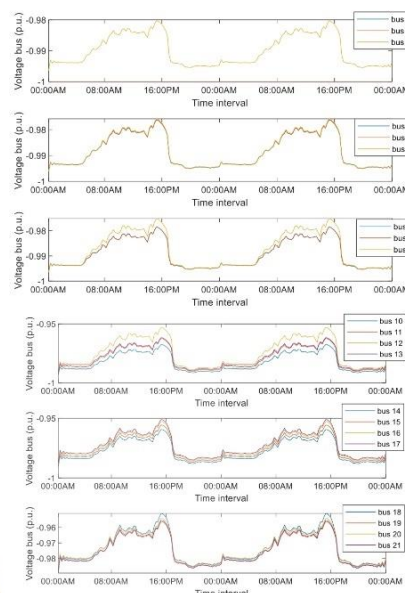


FIGURE 15. (a) Positive voltage profile of base case. (b) Negative voltage profile of base case(cont).

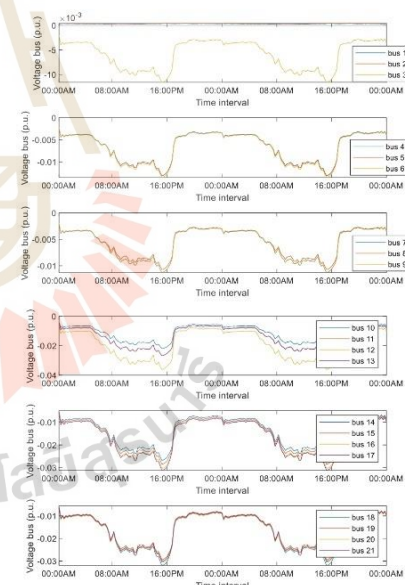


FIGURE 16. Neutral voltage profile of base case.

presents connection type of load A and load B to positive load and negative load, as referred to TABLE 3.

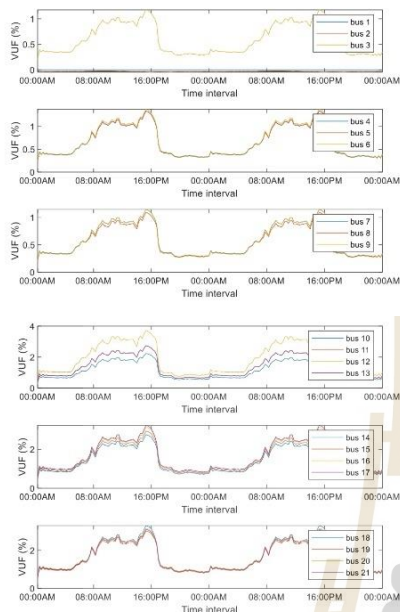


FIGURE 17. 48 hours VUF of base case.

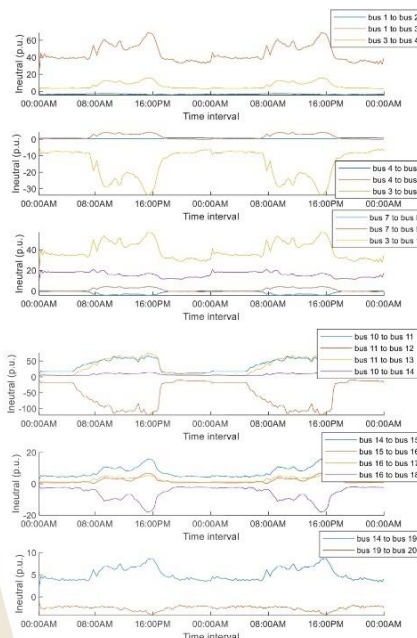


FIGURE 19. Neutral current flow of base case.

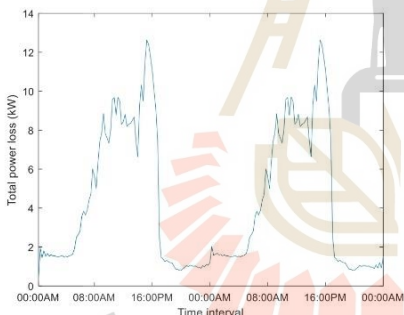


FIGURE 18. Total power loss of base case.

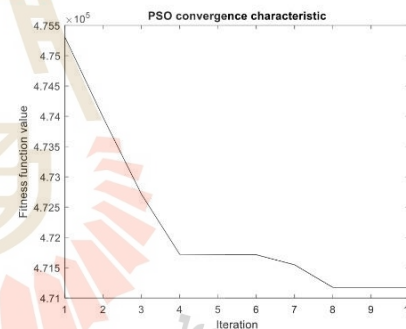


FIGURE 20. PSO convergence characteristic.

FIGURES 14-15 present the positive and negative voltage profile of base case scenario with the load profile in FIGURE 12. The lowest voltage at bus 17 for positive voltage and bus 18 for negative voltage at 15.30 p.m. (timeslot 61). In this case, the load demand at bus 17 includes 6.34 kW at negative pole and 9.26 kW with bipolar connection. Bus 18 was resulted in the lowest negative voltage magnitude. The cause of problem is due to total load demand on negative pole that comprises of 2 load demand, as shown in TABLE 3. The simulation results show that the negative voltage at this

bus is -0.950 p.u. and 0.983 p.u. for positive voltage, with 3.34 % of VUF.

FIGURE 17 presents the VUF of the system for 48 hours. the neutral voltage profiles of base case are shown in FIGURE 16. The magnitude of neutral voltage changes in according to VUF at each bus. The neutral voltage in FIGURE 17 is influenced by unbalance load demand at each pole.

FIGURE 18 present the power loss of the system that is varied by the load demand at each time interval. The highest power loss take place at 15.30 p.m. (time slot 61).

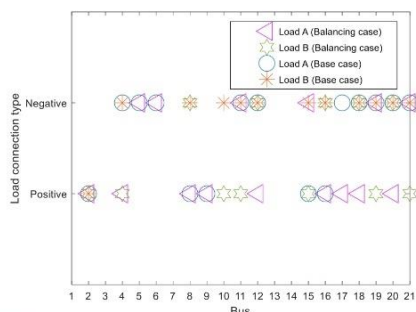


FIGURE 21. Load connection type comparisons of base case and load balancing case.

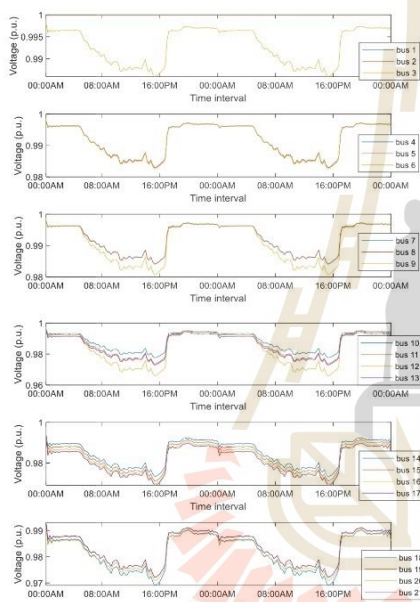


FIGURE 22. Positive voltage profile of load balancing case.

At 15.30 p.m. the load demand at bus 18 connected at the negative pole only, leading to unbalance voltage at the bus and the total daily loss of entire system is equal to 958.100 kWh. FIGURE 19 present a neutral power flow between buses. The highest neutral current flow take place between bus 1 and bus 3 at 15.30 p.m.

**B. LOAD BALANCING CASE (CASE II)**

This subsection presents a simulation result of load balancing method with the objective of minimizing power loss of the system using PSO. The proposed concept is for planning phase to find the best connection type of every load that

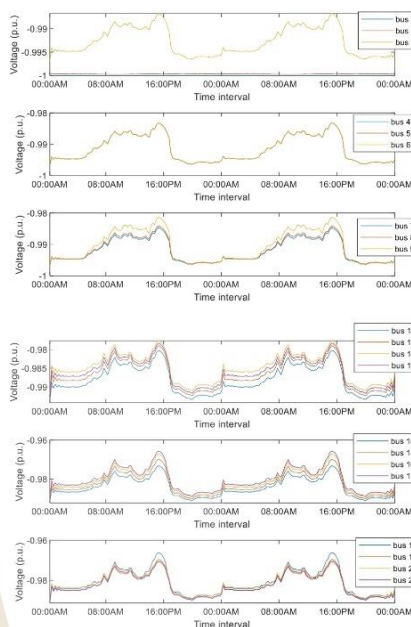


FIGURE 23. Negative voltage profile of load balancing case.

TABLE 5. Particle swarm optimization method parameter.

| Variable                     | Value                              |
|------------------------------|------------------------------------|
| Lower bound                  | 1<br>(Replace positive connection) |
| Upper bound                  | 2<br>(Replace positive connection) |
| Number of variables          | 42                                 |
| Maximum inertia weight       | 0.9                                |
| Minimum inertia weight       | 0.4                                |
| Acceleration factor 1        | 2                                  |
| Acceleration factor 2        | 2                                  |
| Population size              | 500                                |
| Maximum number of iterations | 10                                 |
| Maximum number of runs       | 5                                  |

minimize system power loss and VUF. The PSO parameters are shown in TABLE 5. The simulation results including PSO convergence characteristic, load type, power loss and voltage profile are shown in FIGURES 20-25. Note that, the maximum VUF limit constraint used is 3%.

FIGURE 20 presents a convergence of optimization method which the best fitness function value is 471,200 at iteration 8. The result of optimal load connection types is shown in FIGURE 21. The voltage profile and VUF are shown in FIGURES 22-25.

FIGURE 21 compares the load connection type of balancing case and base case. The objective of load balancing is to

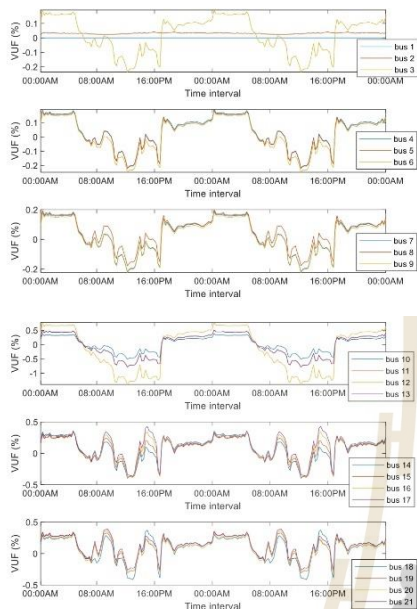


FIGURE 24. Voltage unbalance factor (VUF) of load balancing case.

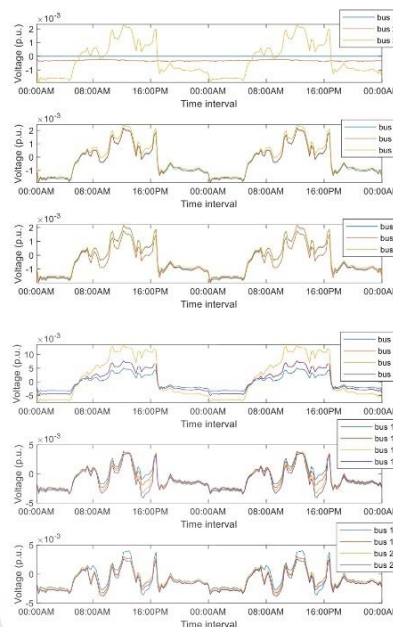


FIGURE 25. Neutral voltage profile of load balancing case.

TABLE 6. Monte carlo simulation condition.

| Data  | Condition                        |
|---|----------------------------------|
| Number of EV                                | 50                               |
| Charger bus                                 | [1,21]                           |
| Initial of battery SOC                      | 100 %                            |
| Charger plug-in time                        | Depend on sampling data from PDF |
| Charger removes time                        | 08.00 AM every day               |
| Iteration                                   | 10,000                           |
| Tolerance                                   | $10^{-5}$                        |
| Standard deviation of plug-in time          | 18                               |
| Mean of plug-in time                        | 3.3                              |
| Standard deviation of daily travel distance | 94.42                            |
| Mean of daily travel distance               | 40                               |
| Maximum travel distance                     | 400 km                           |
| Charging power (slow charging)              | 1.9 kW                           |
| Charging power (fast charging)              | 16 kW                            |
| Charging efficiency                         | 90 %                             |
| Battery Capacity                            | 80 kWh                           |

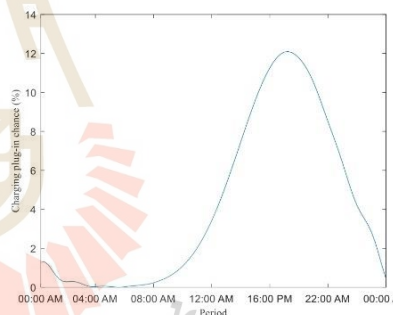


FIGURE 26. Plug-in time of home charger.

reduce the power loss of entire system by change load connection types that reduce between difference of the positive load demand and negative load demand. So, the neutral current of each bus and the system power loss are decreased.

FIGURE 22-25 presents the voltage profile of positive and negative poles. The simulation result shown that the optimal load connection can reduce the voltage drop of positive and negative pole of each bus. In positive pole, the lowest voltage magnitudes at bus 17 were improved to 0.967 p.u. for

positive pole and -0.966 p.u. for negative pole and the VUF was reduced by 0.124% with the neutral voltage reduction to  $1.27 \times 10^{-3}$  p.u. In case of lowest voltage of negative pole that located at bus 18, a magnitude of positive pole and negative pole voltage were improved to 0.967 p.u. and -0.968 p.u., respectively. The neutral voltage at bus 18 equal to  $-0.356 \times 10^{-6}$  p.u. and the VUF of this bus is -0.006 %, which is changed in according to the difference of positive and negative voltage buses. So, the VUF improvement can reduce the neutral current flow of entire system that can



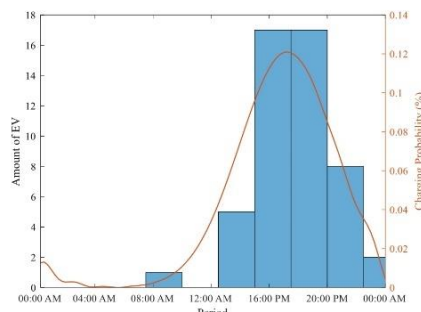


FIGURE 27. Total Plug-in time of home charger.

TABLE 7. MCS result on amount of EV at time interval.

| Time interval     | Amount of EV | Time interval     | Amount of EV |
|-------------------|--------------|-------------------|--------------|
| 07:30 AM-10:00 AM | 1            | 17:30 PM-20:00 PM | 17           |
| 12:30 PM-15:00 PM | 5            | 20:00 PM-22:30 PM | 8            |
| 15:00PM-17:30 PM  | 17           | 22:30 PM-00:00 AM | 2            |

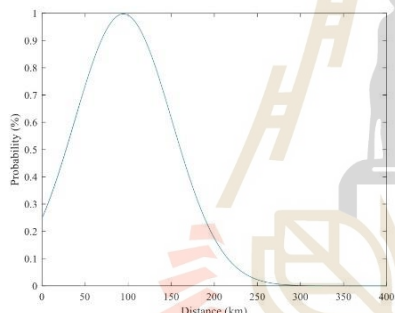


FIGURE 28. Probabilistic daily distance travel of EV.

reduce the power loss of the system by 50.821 % (from 958.100 kWh to 471.175 kWh), for this case.

**C. PROBABILISTIC EV CHARGING MODELING**

This subsection presents the MCS procedure for EV charging load which include probability of plug-in time and daily travel distance for random a sampling EV owner behavior. After that, the sampling data is used to calculate charging time and load demand. The condition of MCS simulation is given in TABLE 6

FIGURE 26 represents an EV charging behavior of home charger. Then, the total probabilistic plug-in time of EV owners' behavior can be obtained as shown in FIGURE 27 and TABLE 7.

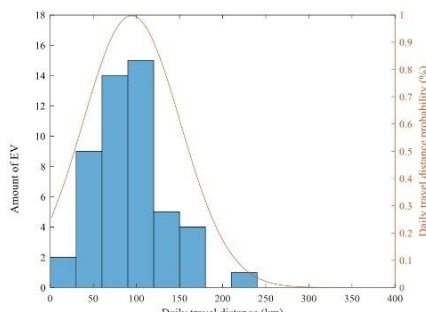


FIGURE 29. Probabilistic of daily distance travel.

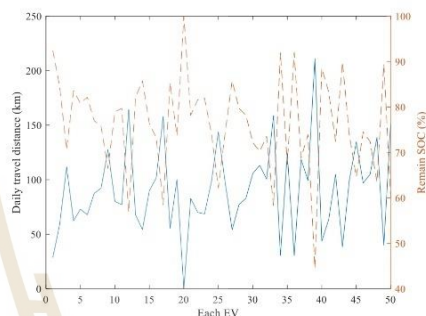


FIGURE 30. Remain SOC of each EV and daily distance travel.

TABLE 8. MCS result on total probabilistic daily distance of EVs.

| Daily travel distance (km) | Amount of EV | Daily travel distance (km) | Amount of EV |
|----------------------------|--------------|----------------------------|--------------|
| 0-30                       | 2            | 121-150                    | 5            |
| 31-60                      | 9            | 151-180                    | 4            |
| 61-90                      | 14           | 181-210                    | 0            |
| 91-120                     | 15           | 211-240                    | 1            |

FIGURE 27 presents the sampling data of EV charging at the times interval based on charging probability in TABLE 7. Consequently, the probability of daily distance travel that present the behavior of EV owners, can be calculated by using Equation 27. The result is shown in FIGURE 28.

FIGURE 28 present probability of daily distance travel of EV owner which varies from 0 km to 283 km. This probability function is used to obtain the daily travel distance for each EV. The result of total probabilistic daily distance travel is shown in FIGURE 29 and TABLE 8

The result in TABLE 8 presents a sampling data of daily distance travel of each EV. The simulation result is used to estimate remain SOC before charging. A number of EVs at

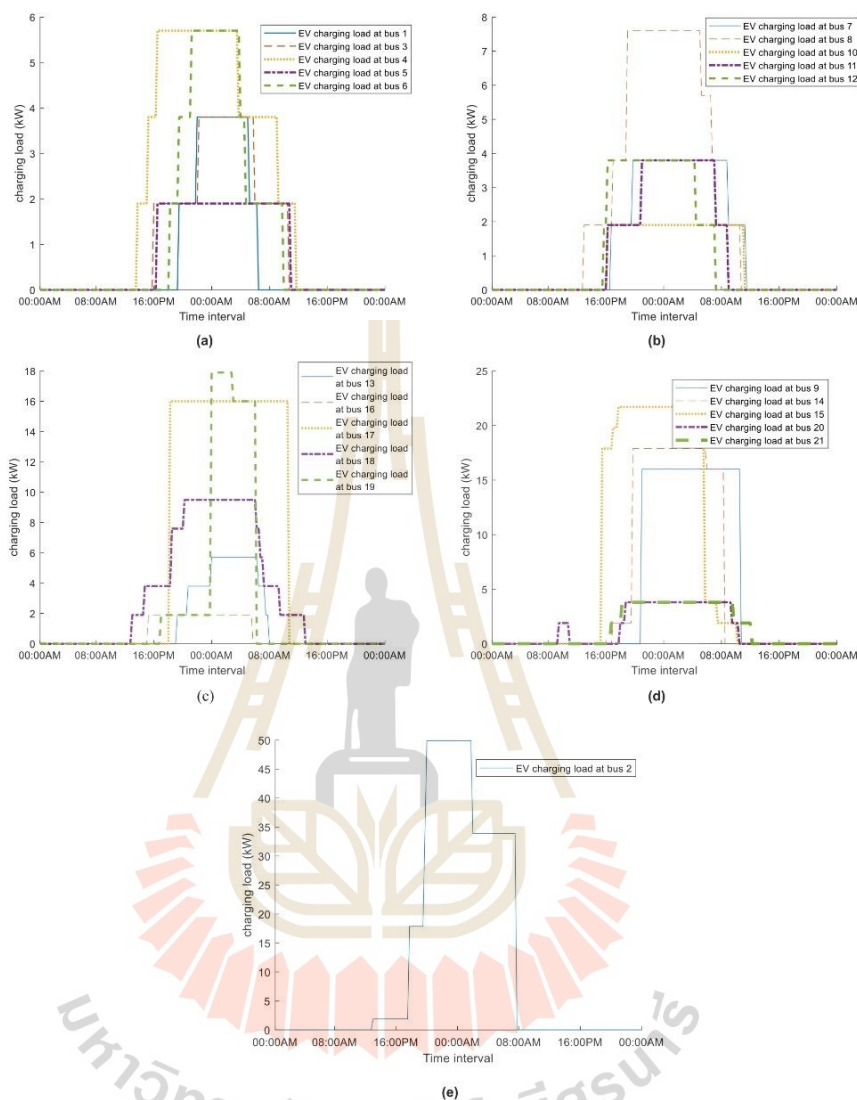


FIGURE 31. (a)-(e) EV home charging load pattern at every bus.

each bus can be random by using information in TABLE 8 and the result is shown in TABLE 9. Aforementioned, the result of remain SOC<sub>s</sub> and EV charging load demand can be shown in FIGURE 30.

FIGURE 30 presents the remaining of EV SOC sampling data based on PDF that related to daily travel distance. The simulation result is used to estimate the charging time of each EV.

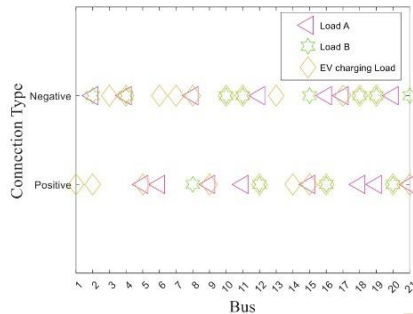


FIGURE 32. Load connection type of bipolar DC distribution grid.

TABLE 9. MCS result on the number of EVs connected at every buses.

| Bus | Numbers of EVs | Bus | Numbers of EVs |
|-----|----------------|-----|----------------|
| 1   | 2              | 12  | 2              |
| 2   | 4              | 13  | 3              |
| 3   | 2              | 14  | 2              |
| 4   | 3              | 15  | 4              |
| 5   | 1              | 16  | 1              |
| 6   | 3              | 17  | 1              |
| 7   | 2              | 18  | 5              |
| 8   | 4              | 19  | 2              |
| 9   | 1              | 20  | 3              |
| 10  | 1              | 21  | 2              |
| 11  | 2              |     |                |

TABLE 10. The comparison of case II and case III.

| Scenario | Highest VUF (%)   | Total Daily Loss (kWh) |
|----------|-------------------|------------------------|
| Case II  | 1.347<br>(Bus 12) | 471.125                |
| Case III | 2.019<br>(Bus 17) | 795.079                |

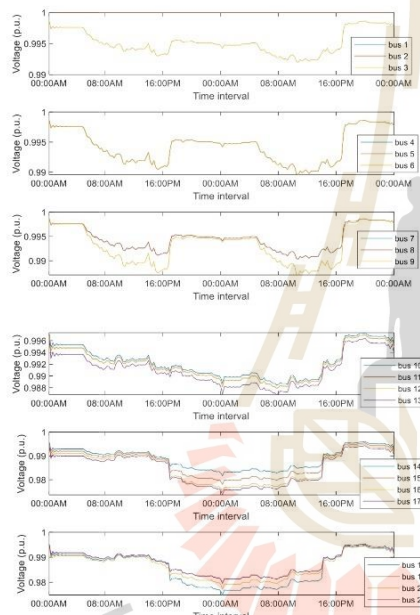


FIGURE 33. Positive voltage profile of case III.

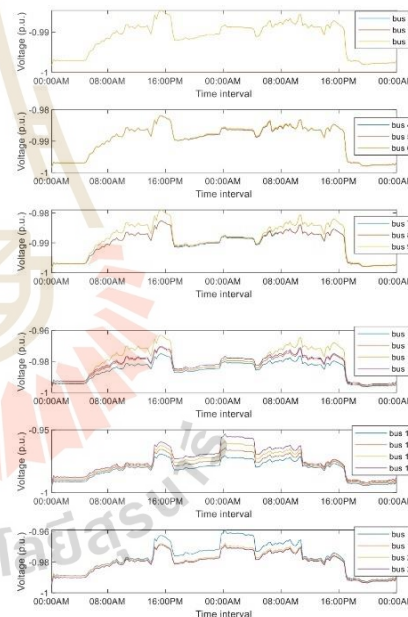


FIGURE 34. Negative voltage profile of case III.

FIGURE 31(a)-(c) present the EV load demand of every bus and amount of EV that charge at each bus in the system. The simulation result is used to calculate voltage profile at each bus and overall power loss in the next subsection.

**D. PROBABILISTIC EV CHARGING LOAD CASE (CASE III)**

This subsection presents the bipolar DCDG load flow with EV charging load integration based on EV load demand pattern from the previous section. The simulation result,

including a voltage profile, power loss and VUF of entire system, are presented in FIGURES 32 –36.

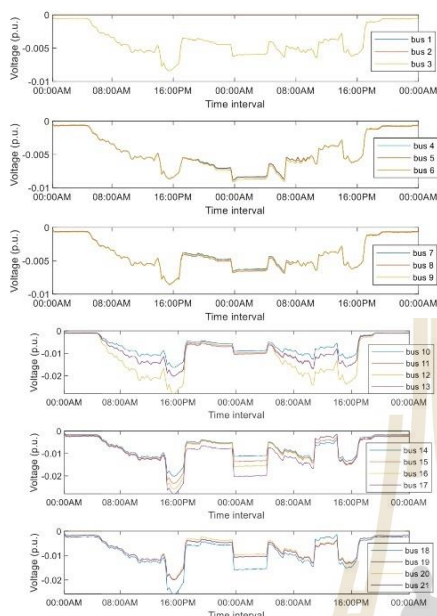


FIGURE 35. Neutral voltage profile of case III.

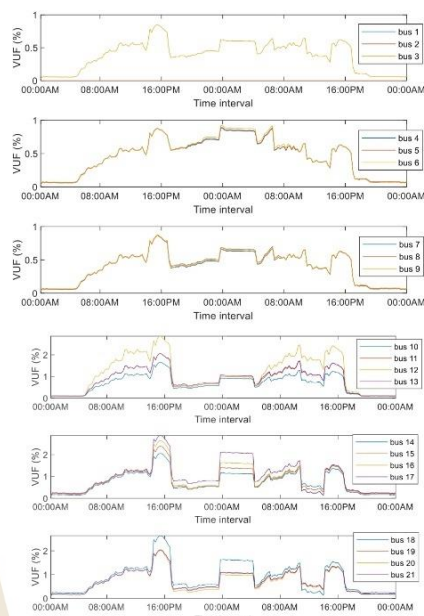


FIGURE 36. Voltage Unbalance Factor of case III.

FIGURE 32 presents a load connection type of load based on load balancing case (Case II) and the probabilistic EV charging load case (Case III).

In this case, the lowest positive and lowest negative voltage magnitudes are at bus 17, in difference time interval. A lowest positive voltage magnitude is 0.962 p.u. at 09.15 a.m. or time slot 133 which caused by existing load and EV charging load. At bus 17, one EV connected to grid via charger with the power rated is 16 kW. The charging duration from 18.00 p.m. to 10.45 a.m. in the next day. So, the voltage drops of bus 17 are caused by the load demand of existing load and EV charging load. In case of negative pole on bus 17, The lowest voltage occurs at 00.15 a.m. or time slot 97, with negative and bipolar loads, without EV charging load. However, the negative voltage bus is reduced from 0.975 p.u. to 0.962 p.u. Therefore, the EV load demand can increase the power loss of entire system due to increasing current flow at each bus and create unbalance condition. The comparison result of Case II and Case III is shown in TABLE 10. From Table 10, it can be seen that the EV charging load can significantly increase the total power loss of the system by 68.76 %

#### E. PROBABILISTIC EV CHARGING LOAD WITH LOAD BALANCING CASE (CASE IV)

This subsection presents a load balancing with probabilistic EV load demand to mitigate the impact of EVs on DCDG

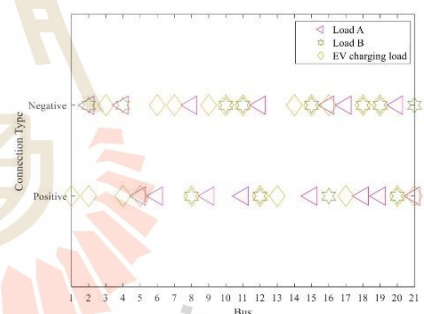


FIGURE 37. Load connection type of bipolar DC distribution grid.

by the proposed method. the optimal load connection types, solved by the proposed method is shown in FIGURE 37.

In the simulation results, the lowest voltage is at bus 17 for both poles. The lowest positive voltage magnitude is 0.948 p.u at bus 17 in 00.15 a.m., or time slot 97 and the lowest negative voltage magnitude is 0.957 p.u. in 09.15 a.m at bus 17, or time slot 133. Therefore, proposed method can reduce the VUF and total power loss of entire system by minimizing the difference of load demand between poles, and the neutral current flow between buses. A comparison of the

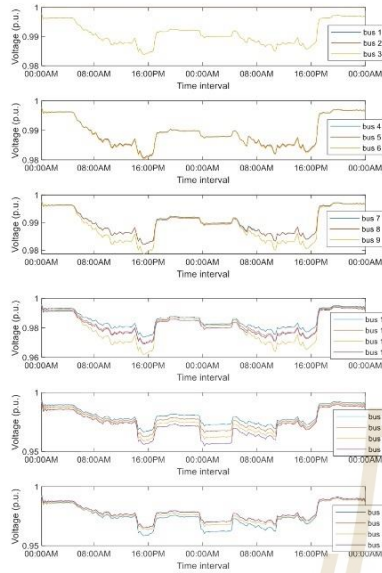


FIGURE 38. Positive voltage profile of case IV.

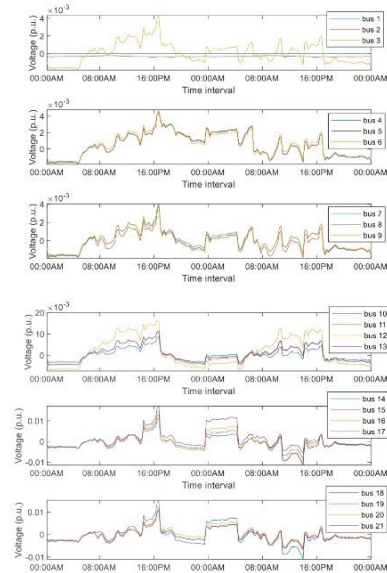


FIGURE 40. Neutral voltage profile of case IV.

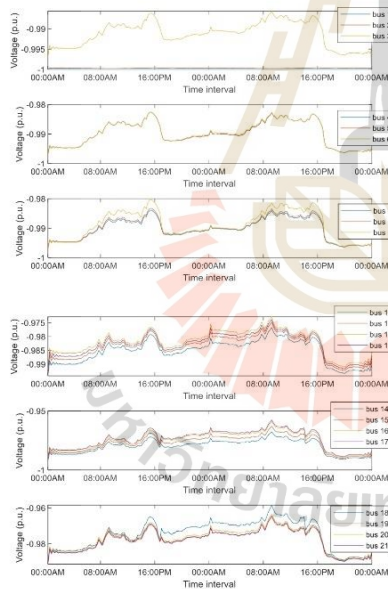


FIGURE 39. Negative voltage profile of case IV.

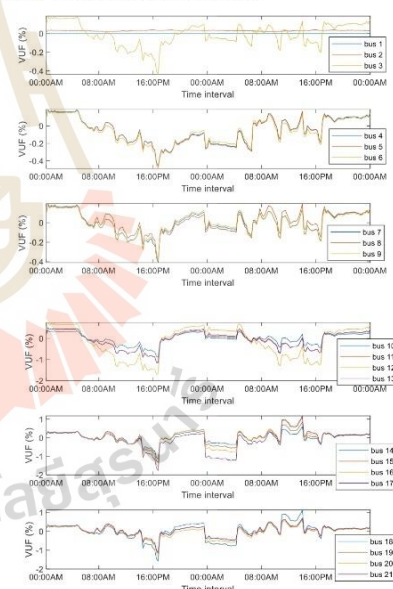


FIGURE 41. Voltage Unbalance Factor of case IV.

simulation results between case III and case IV is shown in TABLE 11. The optimal connection type of the case study

can reduce total daily loss of entire system to 655.060 kWh or by 17.61%

**TABLE 11. The comparison of Case III and Case IV For the highest VUF and total daily loss.**

| Scenario | Highest VUF (%)    | Total daily loss (kWh) |
|----------|--------------------|------------------------|
| Case III | 5.379<br>(Bus 18)  | 795.079                |
| Case IV  | -1.766<br>(bus 17) | 655.060                |

### VIII. CONCLUSION

This paper investigated an impact of EV charging load on bipolar DCDG and proposed a method to improve the DCDG efficiency including mitigate the problem of EV charging load. The study includes the probabilistic model of EV charging load obtained by MCS to evaluate the charging demand during each time interval along the day. A DC power flow for bipolar DCDG, solved by GMM based Gauss's iteration method, is used to determine the voltage profile, VUF, and power loss of entire system. To minimize the total daily loss of DCDG by load balancing method, the optimal load connection type at each bus is searched by using PSO. The achievement of total daily loss minimization also leads to the reduction in VUF. The simulation results showed that the proposed load balancing method can significantly reduce the total daily loss and improve VUF of bipolar DGDC considering probabilistic EV charging load.

### ACKNOWLEDGMENT

The authors would like to express their sincere gratitude to the Suranaree University of Technology (SUT), for providing the necessary support and resources for the completion of this research work. Their financial assistance and facilities have been instrumental in carrying out this study.

### REFERENCES

- [1] T. A. Edison, *System of Electrical Distribution*. NJ, USA: United State Patent Office, 1883.
- [2] V. A. Prabhala, B. P. Baddipadiga, and M. Ferdowsi, "DC distribution systems—An overview," in *Proc. Int. Conf. Renew. Energy Res. Appl. (ICRERA)*, 2014, pp. 307–312.
- [3] V. Nasirian, S. Moayedi, A. Davoudi, and F. L. Lewis, "Distributed cooperative control of DC microgrids," *IEEE Trans. Power Electron.*, vol. 30, no. 4, pp. 2288–2303, Apr. 2015.
- [4] A. G. Anastasiadis, G. P. Kondylis, A. Polyzakis, and G. Vokas, "Effects of increased electric vehicles into a distribution network," *Energy Proc.*, vol. 157, pp. 586–593, Jan. 2019.
- [5] G. A. Putrus, P. Suwanapinkarl, D. Johnston, E. C. Bentley, and M. Narayana, "Impact of electric vehicles on power distribution networks," in *Proc. IEEE Vehicle Power Propuls. Conf.*, Sep. 2009, pp. 827–831.
- [6] Q. Tiantian, "Calculation of electric vehicle charging power based on spatial-temporal activity model," in *Proc. China Int. Conf. Electr. Distrib. (CICED)*, Sep. 2018, pp. 2884–2888.
- [7] C. Camus, C. M. Silva, T. L. Farias, and J. Esteves, "Impact of plug-in hybrid electric vehicles in the Portuguese electric utility system," in *Proc. Int. Conf. Power Eng., Energy Electr. Drives*, Mar. 2009, pp. 285–290.
- [8] S. Schey, D. Scofield, and J. Smart, "A first look at the impact of electric vehicle charging on the electric grid in the EV project," *World Electr. Vehicle J.*, vol. 5, no. 3, pp. 667–678, Sep. 2012.
- [9] P. Morrissey, P. Weldon, and M. O'Mahony, "Future standard and fast charging infrastructure planning: An analysis of electric vehicle charging behaviour," *Energy Policy*, vol. 89, pp. 257–270, Feb. 2016.
- [10] D. Kumar, F. Zare, and A. Ghosh, "DC microgrid technology: System architectures, AC grid interfaces, grounding schemes, power quality, communication networks, applications, and standardizations aspects," *IEEE Access*, vol. 5, pp. 12230–12256, 2017.
- [11] A. de Almeida, P. Moura, and N. Quaresma, "Energy-efficient off-grid systems—Review," *Energy Efficiency*, vol. 13, no. 2, pp. 349–376, Feb. 2020.
- [12] F. Wang, L. Wang, X. Zhang, J. Wang, S. Li, and Y. Liu, "Voltage level study for DC distribution grid based on comprehensive evaluation," in *Proc. IEEE Int. Conf. Power Electron., Comput. Appl. (ICPECA)*, Jan. 2021, pp. 492–496.
- [13] T. Kaipia, P. Nuutinen, A. Pinomaa, A. Lana, J. Partanen, J. Lohjala, and M. Matikainen, "Field test environment for LVDC distribution—Implementation experiences," in *Proc. CIGRE Workshop, Integr. Renewables Distrib. Grid*, May 2012, pp. 1–4.
- [14] E. Rodriguez-Diaz, F. Chen, J. C. Vasquez, J. M. Guerrero, R. Burgos, and D. Boroyevich, "Voltage-level selection of future two-level LVdc distribution grids: A compromise between grid compatibility, safety, and efficiency," *IEEE Electr. Mag.*, vol. 4, no. 2, pp. 20–28, Jun. 2016.
- [15] Y. Yoldaş, A. Önen, S. M. Mueyen, A. V. Vasilakos, and I. Alan, "Enhancing smart grid with microgrids: Challenges and opportunities," *Renew. Sustain. Energy Rev.*, vol. 72, pp. 205–214, May 2017.
- [16] A. Jhunjhunwala, A. Lolla, and P. Kaur, "Solar-DC microgrid for Indian homes: A transforming power scenario," *IEEE Electr. Mag.*, vol. 4, no. 2, pp. 10–19, Jun. 2016.
- [17] J. Karppanen, T. Kaipia, P. Nuutinen, A. Lana, P. Peltoniemi, A. Pinomaa, A. Mattsson, J. Partanen, J. Cho, and J. Kim, "Effect of voltage level selection on earthing and protection of LVDC distribution systems," in *Proc. 11th IET Int. Conf. AC DC Power Transmiss.*, Feb. 2015, pp. 1–8.
- [18] H. Kakigano, Y. Miura, T. Ise, and R. Uchida, "DC voltage control of the DC micro-grid for super high quality distribution," in *Proc. Power Convers. Conf. Nagoya*, Apr. 2007, pp. 518–525.
- [19] G. Sakulphaisan and K. Chayakulkheeree, "Improve a voltage unbalance index of bipolar DC distribution grid by using particle swarm optimization based on load balancing method," in *Proc. Int. Electr. Eng. Congr. (IEECON)*, Mar. 2022, pp. 1–4.
- [20] S. Anand, B. G. Fernandes, and J. Guerrero, "Distributed control to ensure proportional load sharing and improve voltage regulation in low-voltage DC microgrids," *IEEE Trans. Power Electron.*, vol. 28, no. 4, pp. 1900–1913, Apr. 2013.
- [21] I. Sharma, C. Cañizares, and K. Bhattacharya, "Smart charging of PEV's penetrating into residential distribution systems," *IEEE Trans. Smart Grid*, vol. 5, no. 3, pp. 1196–1209, May 2014.
- [22] A. Chiş, J. Rajasekharan, J. Lundén, and V. Koivunen, "Demand response for renewable energy integration and load balancing in smart grid communities," in *Proc. 24th Eur. Signal Process. Conf. (EUSIPCO)*, Aug. 2016, pp. 1423–1427.
- [23] J. Kennedy and R. Eberhart, "Particle swarm optimization," in *Proc. Int. Conf. Neural Netw. (ICNN)*, vol. 4, 1995, pp. 1942–1948.
- [24] R. A. Verzijlbergh, M. O. W. Grond, Z. Lukszo, J. G. Sloopweg, and M. D. Ilic, "Network impacts and cost savings of controlled EV charging," *IEEE Trans. Smart Grid*, vol. 3, no. 3, pp. 1203–1212, Sep. 2012.
- [25] G. Saldaña, J. I. S. Martín, L. Zamora, F. J. Asensio, and O. Onederra, "Electric vehicle into the grid: Charging methodologies aimed at providing ancillary services considering battery degradation," *Energies*, vol. 12, no. 12, p. 2443, Jun. 2019, doi: 10.3390/en12122443.
- [26] M. Gilleran, E. Bonnema, J. Woods, P. Mishra, I. Doebber, C. Hunter, M. Mitchell, and M. Mann, "Impact of electric vehicle charging on the power demand of retail buildings," *Adv. Appl. Energy*, vol. 4, Nov. 2021, Art. no. 100062.
- [27] S. Deilami, A. S. Masoum, P. S. Moses, and M. A. S. Masoum, "Real-time coordination of plug-in electric vehicle charging in smart grids to minimize power losses and improve voltage profile," *IEEE Trans. Smart Grid*, vol. 2, no. 3, pp. 456–467, Sep. 2011.
- [28] N. I. Nimalsiri, C. P. Mediwaththe, E. L. Ratnam, M. Shaw, D. B. Smith, and S. K. Halgamuge, "A survey of algorithms for distributed charging control of electric vehicles in smart grid," *IEEE Trans. Intell. Transp. Syst.*, vol. 21, no. 11, pp. 4497–4515, Nov. 2020.

- [29] S. Alshahrani, M. Khalid, and M. Almuhaini, "Electric vehicles beyond energy storage and modern power networks: Challenges and applications," *IEEE Access*, vol. 7, pp. 99031–99064, 2019.
- [30] A. H. Einaddin and A. S. Yazdankhab, "A novel approach for multi-objective optimal scheduling of large-scale EV fleets in a smart distribution grid considering realistic and stochastic modeling framework," *Int. J. Electr. Power Energy Syst.*, vol. 117, May 2020, Art. no. 105617.
- [31] K. Clement-Nyns, E. Haesen, and J. Driesen, "The impact of charging plug-in hybrid electric vehicles on a residential distribution grid," *IEEE Trans. Power Syst.*, vol. 25, no. 1, pp. 371–380, Feb. 2010.
- [32] E. Sortomme, M. M. Hindi, S. D. J. MacPherson, and S. S. Venkata, "Coordinated charging of plug-in hybrid electric vehicles to minimize distribution system losses," *IEEE Trans. Smart Grid*, vol. 2, no. 1, pp. 198–205, Mar. 2011.
- [33] S. Aghajan-Eshkevari, S. Azad, M. Nazari-Heris, M. T. Ameli, and S. Asadi, "Charging and discharging of electric vehicles in power systems: An updated and detailed review of methods, control structures, objectives, and optimization methodologies," *Sustainability*, vol. 14, no. 4, p. 2137, Feb. 2022, doi: 10.3390/su14042137.
- [34] S. Bahrami and M. Parniani, "Game theoretic based charging strategy for plug-in hybrid electric vehicles," *IEEE Trans. Smart Grid*, vol. 5, no. 5, pp. 2368–2375, Sep. 2014.
- [35] S. S. Amiri, S. Jadid, and H. Saboori, "Multi-objective optimum charging management of electric vehicles through battery swapping stations," *Energy*, vol. 165, pp. 549–562, Dec. 2018.
- [36] K. Zhou, L. Cheng, L. Wen, X. Lu, and T. Ding, "A coordinated charging scheduling method for electric vehicles considering different charging demands," *Energy*, vol. 213, Dec. 2020, Art. no. 118882.
- [37] B. S. H. Chew, Y. Xu, and Q. Wu, "Voltage balancing for bipolar DC distribution grids: A power flow based binary integer multi-objective optimization approach," *IEEE Trans. Power Syst.*, vol. 34, no. 1, pp. 28–39, Jan. 2019.



**GUNTINAN SAKULPHAISAN** (Graduate Student Member, IEEE) was born in Chaiyaphum, Thailand, in 1995. He received the bachelor's and master's degrees in electrical engineering from the Suranaree University of Technology (SUT), in 2017 and 2019, respectively, where he is currently pursuing the Ph.D. degree in electrical engineering. His research interests include electric vehicles (EV), dc grid, and railway electrification.



**KEERATI CHAYAKULKHEEREE** (Senior Member, IEEE) received the B.Eng. degree in EE from KMITL, in 1995, and the M.Eng. and D.Eng. degrees in electric power system management from AIT, in 1999 and 2004, respectively. He is currently an Associate Professor with the School of Electrical Engineering, Institute of Engineering, Suranaree University of Technology, Thailand.

\*\*\*

## BIOGRAPHY

Mr. Guntinan Sakulphaisan was born on April 14, 1995 in Chaiyaphum city, Chaiyaphum province, Thailand. He obtain a Bachelor's degree and Master' degree in electrical engineering from Suranaree university of technology, from 2014 -2017 and 2017 – 2019, respectively. After graduating, he was a lecturer in electrical engineering at Bangkok Thonburi University for 3 and half year (2019-2022). Then, He move to be a lecturer in pathumwan institute of technology until now (2022 - present).

